# GROUNDWATER EXPLOITATION AND ARSENIC OCCURRENCE IN THE MEKONG DELTA AQUIFER SYSTEM

A DISSERTATION
SUBMITTED TO THE DEPARTMENT OF
ENVIRONMENTAL EARTH SYSTEM SCIENCE
AND THE COMMITTEE ON GRADUATE STUDIES
OF STANFORD UNIVERSITY
IN PARTIAL FULFILLMENT OF THE REQUIREMENTS FOR THE
DEGREE OF DOCTOR OF PHILOSOPHY

Laura E. Erban

December 2013



This dissertation is online at: http://purl.stanford.edu/fx861nd2581

I certify that I have read this dissertation and that, in my opinion, it is fully adequate in scope and quality as a dissertation for the degree of Doctor of Philosophy.

**Steven Gorelick, Primary Adviser**

I certify that I have read this dissertation and that, in my opinion, it is fully adequate in scope and quality as a dissertation for the degree of Doctor of Philosophy.

**Scott Fendorf**

I certify that I have read this dissertation and that, in my opinion, it is fully adequate in scope and quality as a dissertation for the degree of Doctor of Philosophy.

**Peter Kitanidis**

Approved for the Stanford University Committee on Graduate Studies.

**Patricia J. Gumport, Vice Provost for Graduate Education**

*This signature page was generated electronically upon submission of this dissertation in electronic format. An original signed hard copy of the signature page is on file in University Archives.*

# Abstract

The Mekong Delta is home to over 20 million people living in Cambodia and Vietnam, many of whom rely on groundwater contaminated with arsenic. Arsenic occurs naturally there, as in many other river basins across South and Southeast Asia, but the extent and spread of contamination is also mediated by human activities. This dissertation is concerned with the consequences of intensive groundwater exploitation for arsenic contamination in the Vietnamese portion of the Mekong Delta, with implications for other similarly-affected regions.

The current distribution of arsenic throughout the Delta's multi-aquifer system is strongly related to large-scale variability in physico-chemical conditions. This work relied upon measurements from more than 40,000 wells extracted from a nationwide arsenic survey and ancillary datasets describing natural properties of the subsurface. Parsimonious sets of explanatory variables describe the probability of well contamination above the WHO drinking water standard (10µg/L). Among shallow aquifers, the exceedance probability is largely predicted by well depth, distance to channels of the Mekong river, distance to the Delta front, and location within different depositional zones within the broader Delta region. These findings are consistent with known, natural contamination generating and remediating processes. Among deeper aquifers, however, widespread arsenic contamination in a cluster of nearly 900 wells in an area >1000 $km^2$ observed in the Mekong Delta is unprecedented based on

surveys in similar Asian systems, and unexplained by presently-accepted mechanisms of arsenic contamination.

Further investigation of the deep well cluster suggests a human influence on this deep contamination. It cannot, however, be explained by pumping-induced vertical transport of arsenic or arsenic-mobilizing solutes, the leading explanation until now. A shallow source is contraindicated by the facts that 1) the group of shallow wells overlying the area of deep contamination has a lower mean arsenic concentration and 2) downward groundwater velocities through the complex stratigraphy, which is marked by thick sequences of confining clays, are extremely low. Yet, pumping is implicated since deep contaminated wells are considerably older than surrounding clean wells in the same aquifers and are found in a region of the aquifer system where pumping rates are elevated. Hydromechanical modeling suggests that these pumping rates induce compaction of interbedded clay layers on the order of 1-3 cm/yr. This estimate is confirmed by direct measurements of land subsidence, the consequence of subsurface compaction, made using satellite-based Interferometric Synthetic Aperture Radar (InSAR). The principal finding of this component of the work is that there is a previously unrecognized mechanism of arsenic contamination: water containing arsenic or arsenic-mobilizing solutes expelled from compacting clays to adjacent aquifers is responsible for contaminating deep wells.

Pumping occurs throughout the Delta, but is uneven over space and among different aquifers. The distribution of wells and their influence on hydraulic heads is understood, owing to Delta-wide monitoring of all major exploited aquifers.

However, the effects of over-exploitation on land subsidence, and potentially arsenic contamination related to it, remain unknown. A final piece of this work extends InSAR analysis to the entire Delta in Vietnam and parts of Cambodia, estimating subsidence rates throughout the region. Subsidence is then related to spatially-explicit effects of groundwater overdraft and variability in compaction of the aquifer-confining bed system. A clear correlation exists between InSAR-based subsidence rates and those determined using a hydrogeologically-based approach. In addition to providing the first estimates of land subsidence that can be used independently for planning and management purposes, these results could be further used as a reconnaissance tool for detecting regions that may potentially be at risk of compaction-induced arsenic contamination.

In summary, this work comprehensively describes the current burden of groundwater arsenic in the Mekong Delta aquifer system, and serves as a baseline for assessing future changes. In the process, it identified a regional-scale human-induced impact on arsenic mobilization and consequent contamination of groundwater. The new contamination mechanism proposed here, based on observations from the Mekong Delta, may also be relevant in similarly-arsenic affected systems throughout South and Southeast Asia. The potential for exacerbation of the arsenic crisis via pumping-induced compaction and other human-mediated mechanisms must be considered as these groundwater systems continue to be developed.

# Acknowledgments

A dissertation is really a group effort, and I have many people to thank for this one. My primary advisor, Steven Gorelick, brought me to Stanford and has guided me along every step of the way. Steve's tireless support, advice and candor have been essential to my success in this work. What's more, the independence Steve allowed me and confidence he had in me throughout the process has been fundamental to my personal and scholarly growth. I am deeply appreciative for Steve's mentorship.

I have learned from many other faculty advisors here too. Scott Fendorf enthusiastically welcomed me to work with his group when I had only the vaguest ideas about what I might do, brought me overseas first chance he got, and refined my knowledge and vision through conversations in the field and on campus. I am so grateful for Scott's guidance. Howard Zebker became a mission-critical mentor when my project took a turn in the direction of his expertise, making resources available to me without reservation, for which I am most thankful. Peter Kitanidis has always asked key questions of me during seminars and meetings that have made me think hard and move forward. Eric Lambin helped me consider other research directions, notably by including me in lab group meetings, and I am enriched by all of our interactions. My heartfelt thanks go out to this group in particular, but also to all of the other outstanding faculty members who have instructed me during my time at

Stanford. I would also like to thank George Hornberger, who taught me my first lessons in hydrogeology and encouraged me to pursue graduate studies in the field.

Intellectual and social support was extended to me by so many inspirational students I have known at Stanford, though I will call out only a few here. All students in the Gorelick and Fendorf labs, and many in the larger department, have cheered and critiqued my work, making it better and easier to do. I benefited enormously from crucial advice, female role-modeling and friendship from Kevan Moffett and Veena Srinivasan. My field work and project development, particularly early phases, were boosted by help from Ben Kocar, Matt Polizzotto, Jason Stuckey, Mike Schaeffer and Jessi Dittmar.

Administrative and financial support also got me through. Thanks go out to the entire administrative staff of Environmental Earth System Science, especially Robin Maslin. I am indebted to many sources of funding from School of Earth Sciences fellowships and McGee research grants, the Stanford Graduate Fellowship, the UPS Fund at Stanford and the National Science Foundation under grant EAR-1313518 to Stanford University. Any opinions, findings, and conclusions or recommendations expressed in this material are those of the author and do not necessarily reflect the views of the National Science Foundation.

I am most fortunate to have two unconditionally loving families. Both let me make the unthinkable move to the West Coast and one let me take their only son with me! My biological family is a huge (literally) source of strength for me. My married family is the best addition I could ask for. I could not have done this dissertation

without their unquestioning belief in it despite all my doubts. To my husband Adam, who has made so many accommodations so that I could study here, all my love and thanks for your companionship.

# Contents

**1 Introduction and research questions ..... 1**

1.1 Motivation ..... 1

1.2 State of prior knowledge ..... 3

1.3 Research question ..... 8

1.4 Structure of the dissertation ..... 8

**2 Arsenic in the multi-aquifer system of the Mekong Delta, Vietnam: analysis of large-scale spatial trends and controlling factors ..... 14**

2.1 Abstract ..... 14

2.2 Introduction ..... 15

2.3 Materials and Methods ..... 17

*2.3.1 Data ..... 17*

*2.3.2 Modeling approach ..... 18*

2.4 Results ..... 21

2.5 Discussion ..... 28

2.6 Supporting Information ..... 35

*2.6.1 Data analysis ..... 35*

*2.6.2 Statistical modeling ..... 44*

**3 Release of arsenic to deep groundwater in the Mekong Delta, Vietnam, linked to pumping-induced land subsidence ..... 51**

3.1 Abstract ..... 51

3.2 Introduction ..... 52

3.3 Results ..... 54

3.4 Materials and Methods ..... 65

3.5 Supporting Information ..... 70

*3.5.1 Data analysis ..... 70*

*3.5.2 Vertical flow calculations ..... 71*

*3.5.3 Simulation of the aquifer - clay confining bed system mechanics ..... 72*

*3.5.4 InSAR-based land subsidence estimates ..... 78*

**4 Pumping-induced regional land subsidence in the Mekong Delta detected using InSAR ..... 85**
4.1 Abstract ..... 85
4.2 Introduction ..... 86
4.3 Background ..... 88
*4.3.1 The aquifer system ..... 88*
*4.3.2 Groundwater exploitation over space and time ..... 89*
*4.3.3 Principles of compaction and subsidence ..... 90*
*4.3.4 Principles of measuring subsidence using InSAR ..... 91*
4.4 Data and methods ..... 92
*4.4.1 Description of SAR acquisitions ..... 92*
*4.4.2 InSAR processing ..... 93*
*4.4.3 Analysis of spatially-explicit drawdown rates ..... 95*
*4.4.4 Estimate of spatially-explicit system storage ..... 96*
*4.4.5 Synthesis ..... 97*
4.5 Results ..... 98
*4.5.1 Spatio-temporal patterns in InSAR signal quality ..... 98*
*4.5.2 Comparison between patterns in InSAR-based subsidence and drawdown ..... 100*
*4.5.3 Comparison between InSAR and hydrogeologically-based subsidence rates ..... 101*
4.6 Discussion ..... 102
*4.6.1 Pumping-induced subsidence in the Mekong Delta ..... 102*
*4.6.2 Considerations ..... 104*
4.7 Conclusions ..... 105
**5 Summary and future directions ..... 110**
5.1 Overview of findings ..... 110
5.2 Guidance for future research ..... 111
*5.2.1 Primary data collection ..... 111*
*5.2.2 Modeling ..... 114*
*5.2.3 InSAR as a reconnaissance tool ..... 116*
5.3 Guidance for water resources management in arsenic-prone regions ..... 117

**Appendix A. Additional transport considerations associated with the compaction-induced arsenic contamination mechanism ..... 121**

A.1 Arsenic concentrations of water sources ..... 122

*A.1.1 Background arsenic concentrations in the aquifer ..... 122*

*A.1.2 Arsenic concentrations in compacting clays ..... 123*

A.2 Attenuation capacity of the aquifer sediments ..... 127

A.3 Capture envelope of the pumping well ..... 128

**Appendix B. InSAR as a reconnaissance tool for detecting areas of potential compaction-induced arsenic contamination in the Mekong Delta ..... 139**

B.1 Generalized region of land subsidence in the Mekong Delta ..... 139

B.2 Correspondence between regions of land subsidence and arsenic incidence ..... 140

B.3 Potential for compaction-induced arsenic in subsiding regions ..... 142

B.4 Considerations for the use of InSAR as an arsenic-detection tool ..... 145

# Figures

**Figure 2.1** Probability of arsenic contamination in wells of the Mekong Delta ..... 21

**Figure 2.2** Trends with distance to river ..... 22

**Figure 2.3** Trends with depth ..... 24

**Figure 2.4** Location map for example cross-sections. ..... 35

**Figure 2.5** Example geologic cross-sections ..... 37

**Figure 2.6** Hydraulic head (m) maps in April, 2005 ..... 38

**Figure 2.7** Locations of total dissolved solids (TDS) measurements and mapped faults ..... 39

**Figure 2.8** Generalized soil types for the Vietnamese region of the Mekong Delta. ..... 40

**Figure 2.9** Maps of arsenic observations by shallow and deep aquifer groups ..... 43

**Figure 2.10** Well age plotted using depth-priority ..... 44

**Figure 2.11** Well counts in concentration:depth space and in TDS: concentration space. ..... 46

**Figure 2.12** Outcome discrimination performance of models. ..... 46

**Figure 3.1** Groundwater arsenic concentrations in the Mekong Delta, Vietnam ..... 55

**Figure 3.2** Physico-chemical characteristics of the focus area ..... 56

**Figure 3.3** Depth profile of groundwater arsenic occurrence in surveys of major affected areas in South and Southeast Asia. ..... 57

**Figure 3.4** InSAR and simulation-based land subsidence. ..... 61

**Figure 3.5** Conceptual model for depth distribution of arsenic in groundwater. ..... 63

**Figure 3.6** Active domain of groundwater flow model ..... 73

**Figure 3.7** Observed and simulated hydraulic heads ..... 74

**Figure 3.8** Well installations over time ..... 75

**Figure 3.9**. Error estimates for InSAR stacks. ..... 80

**Figure 4.1** Location map showing Mekong Delta and surrounding region ..... 88

**Figure 4.2** Drawdown rates during the 2006-2010 period..... 95

**Figure 4.3** Mean amplitude and correlation of InSAR stacks. ..... 99

**Figure 4.4** InSAR-based subsidence rates in the Mekong Delta ..... 100

**Figure 4.5** Maximum drawdown rates among all aquifers at each well nest. ..... 101

**Figure 4.6** Comparison between InSAR and hydrogeologically-based (modeled) subsidence rates. ..... 102

**Figure A1** Evolution in time of the capture envelope of a pumping well below a clay layer undergoing compaction.. ..... 131

**Figure A2** Factors affecting the travel time of solutes to a pumping well. ..... 132

**Figure A3** Simulated temporal concentration trajectories ..... 134

**Figure A4** Arsenic data compared with pumping intensity ..... 135

**Figure B1** Generalized regions of InSAR-based subsidence..... 140

**Figure B2** Generalized area of InSAR-based subsidence with superimposed areas of low arsenic incidence. ..... 141

**Figure B3** Arsenic clusters superimposed on regions of subsidence and generally low arsenic incidence…….…….. 142

# Tables

**Table 2.1** Categories of processes and explanatory variables..... 20

**Table 2.2** Model results ..... 28

**Table 2.3** Summary statistics for arsenic in wells by surface soil type and aquifer. ..... 41

**Table 3.1** Summary statistics for wells in the shallow and deep focus area zones..... 70

**Table 3.2**: Range of parameters used in the calculation of vertical flow between zones of the focus area..... 71

**Table 3.3** Groundwater flow model parameter values..... 76

**Table 3.4** Collection dates of data used in InSAR stacks ..... 79

**Table B1** Summary statistics for arsenic clusters. ..... 143

# 1 Introduction and research questions

## 1.1 Motivation

Arsenic contamination poses a major challenge for the safe use of groundwater in the Mekong Delta. Here, as in many other river basins across South and Southeast Asia, arsenic dissolves out of sediments eroded in the Himalayas and deposited on the densely populated floodplains. More than 20 million people live in the Mekong Delta, shared by Cambodia and Vietnam, many of them tapping groundwater to supplement or replace other sources of water. Chronic consumption of arsenic in groundwater is devastating to human health, causing increased risk of skin and internal cancers, cardiovascular disease and many other adverse conditions in adults and children. Indirect exposure to arsenic through crops irrigated with contaminated groundwater further compounds these health concerns for consumers in the Delta, while foreign export of such crops and products made from them may spread arsenic-related risks around the world.

Despite widespread awareness of the arsenic threat, groundwater exploitation in the Mekong Delta has risen dramatically in recent decades. Post-conflict stability has encouraged socioeconomic growth, in turn driving the expansion of access to wells in more areas and at greater depths. Shallow wells (<150m) are the most abundant, serving mainly low-volume household needs, but deep wells are also widespread and intensively pumped. Deep aquifers have been experiencing widespread overdraft since the mid-1990s throughout large regions (1000s of $km^2$),

prompting concern for the long-term availability and quality of their valuable water reserves. Over-exploitation has caused saline intrusion and land subsidence in this and many other deltaic aquifer systems around the world. In the Mekong Delta, over-extraction has exacerbated already widespread arsenic contamination.

This dissertation is concerned with the consequences of development of groundwater resources on the mobilization of naturally-occurring arsenic contamination in the Mekong Delta, with implications for analogous systems. Arsenic is an abundant crustal impurity that contaminates many aquifer systems around the world. In developed countries, arsenic is readily removed from water supplies before delivery to consumers. However, in the Mekong Delta, as in similarly arsenic-affected river basins throughout Southeast Asia, untreated groundwater is often directly self-supplied by users. Reliance on the Delta's groundwater resources continues to rise, not only among domestic but also agricultural and industrial users, spurred on by growing demand for water in the face of increasingly contaminated and unreliable surface water supplies. In the short term, development in the Delta benefits from groundwater exploitation, but it also introduces large populations to new risks that may manifest over longer time scales. Among these lagged risks is increased exposure to arsenic.

The extent and severity of groundwater arsenic contamination in the Mekong Delta, and similar systems, are determined by natural and human-mediated processes that interact dynamically. Most arsenic found in the Delta is geogenic; inputs from pesticide and defoliant applications are minor by comparison. The Delta's sediments

are laced with arsenic that is only conditionally stable in solid forms. At the Delta scale, the natural balance of arsenic in solid and aqueous phases is controlled by biogeochemical processes and groundwater flow on timescales of millennia to millions of years. Natural processes can be accelerated, however, when humans begin to exploit aquifers, instigating new contamination events over decades. Pumping-induced groundwater flow overwhelms natural hydraulic gradients in low-lying areas. When intensive pumping occurs, solutes necessary for arsenic mobilization are dragged from surface water bodies into the subsurface in greater quantities and at faster rates. Arsenic or arsenic-mobilizing solutes harbored in interbedded clays are squeezed into adjacent aquifers during pumping-induced compaction (Chapter 3).

The consequences for arsenic contamination of human activities that affect subsurface conditions are difficult to predict. The processes that we know act to release, sequester, dilute and retard arsenic act in site-specific and scale-dependent ways. At the regional scale, it may be possible to understand the net effects of these competing processes by studying how past human interventions in the subsurface have already influenced groundwater arsenic contamination outcomes. Full consideration of these outcomes is essential if the Mekong Delta aquifer system, and similarly arsenic-affected basins throughout Southeast Asia, is to be managed for safe, long-term human use.

### 1.2 State of prior knowledge

Beginning in the early 1980s, discoveries of mass poisonings in West Bengal, India and neighboring Bangladesh were linked to protracted consumption of

groundwater containing high levels of arsenic (Das et al., 1995; Saha, 1995; Chakraborty and Saha, 1987). The arsenic hazard is common to numerous aquifer systems around the world. However, in the 1970s, when many of the wells responsible for these poisonings were installed, the dissolution processes operative in South and Southeast Asia were not yet recognized (Smith et al., 2000). The human health crisis prompted considerable efforts aimed at determining the causes of groundwater arsenic contamination. Since the first discoveries, elevated arsenic levels in significant numbers of wells have been found in sedimentary aquifers throughout the region (Berg et al., 2001; Chitrakar and Neku, 2001; Feldman and Rosenboom, 2001).

Decades of investigation since have revealed the natural processes that release solid-phase arsenic to groundwater across South and Southeast Asia. Himalayan-draining rivers broadly deposit arsenic-rich sediments during annual floods. Below the floodplains, the microbially-mediated reductive dissolution of iron(hydr)oxides bearing arsenic is predominantly responsible for groundwater contamination. Given sufficient organic carbon and deprived of oxygen, respiring subsurface microbes utilize alternate electron acceptors, including iron and arsenic itself. Arsenic-binding minerals are dissolved in the process, releasing arsenic to the aqueous phase. The dissolved arsenic pool in an anoxic subsurface remains high in the absence of sufficient sulfate, which can be reduced to form sparingly soluble sulfide minerals that can sequester arsenic (Buschmann and Berg, 2009; Lowers et al., 2007; Kirk et al., 2004, O'Day et al., 2004), and if other physico-chemical mechanisms cannot provide natural remediation.

Arsenic-mobilizing conditions are met in the region's floodplains. The tropical climate sustains high rates of primary productivity, carbon fixation and burial, particularly in oxbow lakes and other wetlands that flank the rivers. These abundant, perennial surface water bodies create hotspots of arsenic release and transport to underlying aquifers (Benner et al., 2008; Polizzotto et al., 2008). In the Mekong Delta, high concentration contaminant plumes are often found within a <5km lateral and 100m vertical buffer of the main river reaches, likely caught in river stage-driven local flow cells. Gradients for groundwater flow induced by seasonally-oscillatory surface water bodies weaken with distance from them. In areas far from the major river reaches, natural hydraulic gradients may be insufficient to transport significant volumes of arsenic-laden water from surficial clay to underlying aquifers. Arsenic mobilization can also occur throughout the reduced subsurface of the floodplains where the requisite suite of biogeochemical conditions are present.

Once mobile, the spread and influence of dissolved arsenic is further controlled by a set of physico-chemical processes that operate along groundwater flow paths. At the regional scale, mixing, dilution and flushing counteract dissolution as groundwater flows from recharge to discharge zones. Sorption along the flow path may similarly lessen dissolved arsenic occurrence in aquifers where minerals are oxidized, as in the much-cited Pleistocene sands of Bangladesh (Radloff et al., 2011; Stollenwerk et al., 2007; Swartz et al., 2004). In the vertical dimension, dissolved arsenic profiles show signs of natural purging of weakly bound arsenic over geologic timescales. High concentrations in the near-surface fall rapidly to low levels at greater depths where sediments are older, reactants more recalcitrant, and flushing more complete.

Arsenic in aquifer pore fluids and on solids have received the bulk of attention to date, yet the substantial confining clay layers that characterize these systems are also critical to arsenic mobilization and transport. Confining clays can offer physical protection to clean aquifers by preventing downward flow from contaminated shallow aquifers under natural or pumping-induced conditions. However, clay layers, rich in carbon and arsenic-hosting minerals, are also known to release high concentrations of dissolved arsenic in shallow clays that remain high over the course of millennia (Benner et al., 2008; Kocar et al., 2008). These elevated concentrations can persist in clay layers long after burial, when hydraulic gradients for flushing are reduced, maintained by on-going dissolution, along with slow desorption (Tufano et al., 2008) and diffusion from occluded pore spaces. Arsenic diffusion out of these low permeability layers has yet to be addressed in field studies in the Southeast Asian context, but in Cretaceous-age aquitards in Canada, diffusion of arsenic from confining clays into adjacent aquifers appears to continue over the >70 million year timeframe (Yan et al., 2000). Solutes harbored in confining clays may in fact represent the most significant source of contamination at depth, where the more permeable aquifers have been remediated by flushing.

Human activities further contribute to contamination over a variety of scales. At the local scale, naturally arsenic-mobilizing features that behave like wetlands may be recreated by human modifications to the land surface, for example, dual-purpose fish pond latrines or excavations for levee-building that later become man-made ponds. Field-scale studies have demonstrated that irrigation pumping can draw fresh organic carbon from such ponds into the subsurface where it triggers arsenic

mobilization (Lawson et al., 2013; Neumann et al., 2009; Harvey et al., 2002). At the regional scale, intensive groundwater extraction has been linked to contamination of deep aquifers due to migration of solutes from the near-surface or from interbedded compacting clays (Erban et al., 2013; Mukherjee et al., 2011; Winkel et al., 2011). Basin-scale studies have evaluated the potential for various levels of distributed deep pumping to compromise the quality of deep aquifers that are presently safe by drawing in shallow arsenic contamination (Radloff et al., 2011; Burgess et al., 2010; Michael and Voss, 2008).

The effects of human activities on arsenic contamination remain ill-constrained, largely due to differences in site conditions and scale-dependencies of particular studies. Field studies scale poorly to larger areas where less detailed geochemical data and physical characterization are available. Conversely, the limited number of large-scale studies has yet to adequately demonstrate cause and effect. Predictive physical modeling studies make numerous assumptions, perhaps most importantly when assigning pumping rates, while their predictions have not been tested against data. Data-based work on regional-scale, pumping-induced vertical transport (Mukherjee et al., 2011; Winkel et al., 2011) has not been conducted in paired under-used and over-pumped settings. Thus, none of these lines of inquiry directly considers pre- and post- disturbance conditions to properly parse the relative influences of natural and anthropogenic factors. Moreover, since arsenic has rarely been detected in deep wells (>150m), it has long been assumed that contamination is mainly a near-surface problem. As humans increasingly access deeper, older aquifers

more extensively and intensively, the validity of that assumption is called into question.

### 1.3 Research question

This work pursues the unresolved question of how human activities affect the distribution of dissolved arsenic in naturally arsenic-prone aquifer systems at the region to basin scale. The Mekong Delta is chosen as a model system in which to address this question, as socio-political conditions have imposed dramatic differences in land and water use in large areas of the same, continuously arsenic-burdened groundwater system. Here, the undisturbed case can be tested against various levels of subsurface disturbance, to elucidate how the time scales and intensities of human activities affect arsenic contamination.

### 1.4 Structure of the dissertation

The over-arching research topic is addressed in a series of chapters that build on one another.

Chapter 2**, "***Arsenic in the multi-aquifer system of the Mekong Delta, Vietnam: analysis of large-scale spatial trends and controlling factors",* describes the current distribution of arsenic throughout the Delta. A hypothesis-driven approach is used to develop logistic regression models that relate the probability of arsenic in wells exceeding the 10 µg/L World Health Organization drinking water standard to explanatory physico-chemical variables. Parsimonious models illustrate the importance of a fully 3D analysis that allows for consideration of depth dependencies

in both arsenic occurrence and explanatory variables. Much of the variability among wells is captured by these models, facilitating synthesis of the suite of natural and human-induced conditions governing arsenic occurrence in the Mekong Delta.

Chapter 3, *"Release of arsenic to deep groundwater in the Mekong Delta, Vietnam, linked to pumping-induced land subsidence"* follows up on an observation from the previous chapter that a large cluster of high-arsenic deep wells is co-located with an area of particularly intensive groundwater exploitation. An integrated suite of methods including analysis of well data and hydromechanical modeling confirmed by InSAR-based estimates of land subsidence is used to propose that deep contamination in this anomalous region is due to a previously unrecognized mechanism: release of arsenic or arsenic-mobilizing solutes to deep aquifers during pumping-induced compaction of interbedded clays. Chapter 3 was published in *Proceedings of the National Academy of Sciences of the United States of America* as:

> Erban, L. E., Gorelick, S. M., Zebker, H. A, and Fendorf, S. (2013). Release of arsenic to deep groundwater in the Mekong Delta, Vietnam, linked to pumping-induced land subsidence. *Proceedings of the National Academy of Sciences of the United States of America*. doi:10.1073/pnas.1300503110

Chapter 4, "*Pumping-induced regional land subsidence in the Mekong Delta detected using InSAR*" continues the investigation of Chapter 3 by extending analysis of land subsidence to the entire Mekong Delta. Widespread subsidence is observed by InSAR coincident with regions where overdraft in multiple aquifers was indicated by nested monitoring wells. Hydrogeologically-based rates of subsidence determined

at each well nest using mechanistic equations agree well with InSAR-based rates. In addition to providing the first estimates of land subsidence Delta-wide, results illustrate the successful use of InSAR in a landscape that is exceedingly difficult to study by this method.

Chapter 5, "*Summary and future directions*" assesses the findings of the dissertation and proposes directions for future research, given the lessons learned in this work. Additional appendices give further analysis that was ultimately excluded from the chapters, manuscript and supporting materials.

## References


Benner, S. G., Polizzotto, M. L., Kocar, B. D., Ganguly, S., Phan, K., Ouch, K., Sampson, M., and Fendorf, S. (2008). Groundwater flow in an arsenic-contaminated aquifer, Mekong Delta, Cambodia. *Applied Geochemistry*, 23(11), 3072–3087.

Berg, M., Tran, H. C., Nguyen, T. C., Pham, H. V, Schertenleib, R., and Giger, W. (2001). Arsenic contamination of groundwater and drinking water in Vietnam: a human health threat. *Environmental science & technology*, 35(13), 2621–2626.

Burgess, W. G., Hoque, M. A., Michael, H. A., Voss, C. I., Breit, G. N., and Ahmed, K. M. (2010). Vulnerability of deep groundwater in the Bengal Aquifer System to contamination by arsenic. *Nature Geoscience*, 3, 83–87. doi:10.1038/ngeo750.

Buschmann, J., and Berg, M. (2009). Impact of sulfate reduction on the scale of arsenic contamination in groundwater of the Mekong, Bengal and Red River deltas. *Applied Geochemistry*, 24, 1278–1286.

Chakraborty, A.K., and Saha, K. C. (1987). Arsenical dermatosis from tubewell water in West Bengal. *Indian journal of medical research*, 85, 326–334.

Chitrakar, R.L., Neku, A. (2001). The scenario of arsenic in drinking water in Nepal. *SAARC Regional Conference of Environmental Pollution and its Control*. Kathmandu, December 3-4.

Das, D., Chatterjee, A., Mandal, B.K., Samanta, G., Chakraborti, D., and Chanda, B. (1995). Arsenic in ground water in six districts of West Bengal, India: the biggest arsenic calamity in the world. Part 2. Arsenic concentration in drinking water, hair, nails, urine, skin-scale and liver tissue (biopsy) of the affected people. *Analyst*, 120, 917–924.

Erban, L. E., Gorelick, S. M., Zebker, H. A., and Fendorf, S. (2013). Release of arsenic to deep groundwater in the Mekong Delta, Vietnam, linked to pumping-induced land subsidence. *Proceedings of the National Academy of Sciences of the United States of America*. doi:10.1073/pnas.1300503110.

Feldman, P.R. and Rosenboom, J. W. (2001). Cambodia drinking water quality assessment. Phnom Penh, Cambodia. *World Health Organisation of the UN [WHO] in cooperation with Cambodian Ministry of Rural Development and the Ministry of Industry, Mines and Energy*. Phnom Penh.

Harvey, C. F., Swartz, C. H., Badruzzaman, A. B. M., Keon-Blute, N., Yu, W., Ali, M. A., Jay, J., Beckie, R., Niedan, V., Brabander, D., Oates, P. M., Ashfaque, K. N., Islam, S., Hemond, H. F., and Ahmed, M. F. (2002). Arsenic Mobility and Groundwater Extraction in Bangladesh. *Science*, 298(5598), 1602–1606. doi:10.1126/science.1076978.

Kirk, M. F., Holm, T. R., Park, J., Jin, Q., Sanford, R. A., Fouke, B. W., and Bethke, C. M. (2004). Bacterial sulfate reduction limits natural arsenic contamination in groundwater. *Geology*, 32(11), 953–956. doi:10.1130/G20842.1.

Kocar, B. D., Polizzotto, M. L., Benner, S. G., Ying, S. C., Ung, M., Ouch, K., Samreth, S., Suy, B., Phan, K., Sampson, M., and Fendorf, S. (2008). Integrated biogeochemical and hydrologic processes driving arsenic release from shallow sediments to groundwaters of the Mekong delta. *Applied Geochemistry*, 23(11), 3059–3071.

Lawson, M., Polya, D. A, Boyce, A. J., Bryant, C., Mondal, D., Shantz, A., and Ballentine, C. J. (2013). Pond-derived organic carbon driving changes in arsenic hazard found in asian groundwaters. *Environmental science & technology*, 47(13), 7085–94. doi:10.1021/es400114q.

Lowers, H. A., Breit, G. N., Foster, A. L., Whitney, J., Yount, J., Uddin, M. N., and Muneem, A. A. (2007). Arsenic incorporation into authigenic pyrite, Bengal Basin sediment, Bangladesh. *Geochimica et cosmochimica acta*, 71(11), 2699–2717.

Michael, H. A., and Voss, C. I. (2008). Evaluation of the sustainability of deep groundwater as an arsenic-safe resource in the Bengal Basin. *Proceedings of the National Academy of Sciences of the United States of America*, 105(25), 8531–8536.

Mukherjee, A., Fryar, A. E., Scanlon, B. R., Bhattacharya, P., and Bhattacharya, A. (2011). Elevated arsenic in deeper groundwater of the western Bengal basin, India: Extent and controls from regional to local scale. *Applied Geochemistry*, 26(4), 600–613.

Neumann, R. B., Ashfaque, K. N., Badruzzaman, A. B. M., Ashraf Ali, M., Shoemaker, J. K., and Harvey, C. F. (2009). Anthropogenic influences on groundwater arsenic concentrations in Bangladesh. *Nature Geoscience*. doi:10.1038/ngeo685.

O'Day, P. A., Vlassopoulos, D., Root, R., and Rivera, N. (2004). The influence of sulfur and iron on dissolved arsenic concentrations in the shallow subsurface under changing redox conditions. *Proceedings of the National Academy of Sciences of the United States of America*, 101(38), 13703–8. doi:10.1073/pnas.0402775101.

Polizzotto, M. L., Kocar, B. D., Benner, S. G., Sampson, M., and Fendorf, S. (2008). Near-surface wetland sediments as a source of arsenic release to ground water in Asia. *Nature*, 454(7203), 505–508. doi:10.1038/nature07093.

Radloff, K. A., Zheng, Y., Michael, H. A., Stute, M., Bostick, B. C., Mihajlov, I., Bounds, M., Huq, I., Choudhury, M.W., Rahman, P., Schlosser, K.M., Ahmed, K.M., and van Geen, A. (2011). Arsenic migration to deep groundwater in Bangladesh influenced by adsorption and water demand. *Nature Geoscience*, 4(11), 793–798. doi:10.1038/ngeo1283.

Saha, K. (1995). Chronic arsenical dermatoses from tube-well water in West Bengal during 1983-87. *Indian Journal of Dermatology*, 40, 1–12.

Smith, A. H., Lingas, E. O., and Rahman, M. (2000). Contamination of drinking-water by arsenic in Bangladesh: a public health emergency. *Bulletin of the World Health Organization*, 78, 1093–1103.

Stollenwerk, K. G., Breit, G. N., Welch, A. H., Yount, J. C., Whitney, J. W., Foster, A. L., Uddin, M.N., Majumder, R.K., and Ahmed, N. (2007). Arsenic attenuation by oxidized aquifer sediments in Bangladesh. *Science of the Total Environment*, 379(2-3), 133–150.

Swartz, C. H., Blute, N. K., Badruzzman, B., Ali, A., Brabander, D., Jay, J., Besancon, J., Islam, S., Hemond, H.F., and Harvey, C. F. (2004). Mobility of arsenic in a Bangladesh aquifer: Inferences from geochemical profiles, leaching data, and mineralogical characterization. *Geochimica et Cosmochimica Acta*, 68(22), 4539–4557.

Tufano, K. J., Reyes, C., Saltikov, C. W., and Fendorf, S. (2008). Reductive Processes Controlling Arsenic Retention: Revealing the Relative Importance of Iron and Arsenic Reduction. *Environmental Science & Technology*, 42(22), 8283–8289. doi:10.1021/es801059s.

Winkel, L. H., Pham, T. K. T., Vi, M.L., Stengel, C., Amini, M., Nguyen, T. H., Pham, H.V., and Berg, M. (2011). Arsenic pollution of groundwater in Vietnam exacerbated by deep aquifer exploitation for more than a century. *Proceedings of the National Academy of Sciences*, 108(4), 1246–1251.

Yan, X. P., Kerrich, R., and Hendry, M. J. (2000). Distribution of arsenic (III), arsenic (V) and total inorganic arsenic in porewaters from a thick till and clay-rich aquitard sequence, Saskatchewan, Canada. *Geochimica et Cosmochimica Acta*, 64(15), 2637–2648.

# 2 Arsenic in the multi-aquifer system of the Mekong Delta, Vietnam: analysis of large-scale spatial trends and controlling factors

## 2.1 Abstract

Groundwater exploitation is rising in the Mekong Delta, Vietnam, potentially exacerbating arsenic contamination from natural sources. We investigate trends and controls on contamination patterns throughout the Delta's multi-aquifer system as observed in a spatially exhaustive dataset of arsenic measured in >40,000 wells, 10.5% of which exceed the WHO drinking water standard for arsenic (10µg/L). We relate strong trends in the distribution of contamination among well samples to explanatory variables derived from 3D ancillary physico-chemical datasets using logistic regression models. Parsimonious models describe much of the observed variability in arsenic occurrence, which differs considerably between subsets of wells tapping shallow versus deeper aquifer groups. In the shallowest Holocene-Pleistocene aquifers, arsenic occurrence is best described by distance to the Mekong river channels and delta front, depth, and location within fault-bounded zones of the region. The same model, however, fails to explain observations in the deeper group of Pliocene-Miocene aquifers. Among these deeper units, arsenic occurrence is rare except among older wells in near-river, heavily pumped areas. Our analysis is the first to examine both natural and anthropogenically-mediated contributions to the distribution of arsenic throughout the Mekong Delta's multi-aquifer system, with implications for management of similarly affected basins throughout Southeast Asia.

## 2.2 Introduction

In the Mekong Delta, naturally occurring groundwater arsenic poses serious health risks to a large and growing population. The Delta, shared by Cambodia and Vietnam, is home to over 20 million people, many of whom extract groundwater for a variety of domestic, agricultural and industrial purposes. In the densely settled floodplain, arsenic concentrations in these wells have exceeded 100 times the World Health Organization's (WHO) drinking water standard (10μg/L) (Hoang et al., 2010; Polizzotto et al., 2008; Berg et al., 2007). The dissolved arsenic burden tends to be most significant, in terms of both concentration and proportion of affected wells, among wells that are proximate to the main river network and screened in the most shallow, Holocene-Pleistocene age aquifers (typically <150m). Past studies of arsenic contamination patterns in the Vietnamese Delta (Hoang et al., 2010; Nguyen and Itoi, 2009; Berg et al., 2007; Stanger et al, 2005) have focused on this near-river, near-surface portion of the aquifer system. However, deeper (200-500m) Pliocene-Miocene aquifers are also widely contaminated and heavily used. Rising exploitation may exacerbate the groundwater arsenic crisis.

More than a decade of research across the arsenic-affected river basins of Southeast Asia has revealed the fundamental processes leading to groundwater contamination. In these contexts, the dominant release mechanism is the microbially mediated reductive dissolution of abundant Fe-(hydr)oxide host minerals (Dowling et al., 2002; Berg et al., 2001; McArthur et al., 2001; Nickson et al., 2000). Mineral destabilization appears to be most favorable in carbon-rich near-surface (<100m) environments, where high concentrations of dissolved arsenic are mobilized, and this

contaminated water is subsequently transported by natural and pumping-induced groundwater flow in shallow aquifers (Neumann et al., 2009; Polizzotto et al., 2008; van Geen et al., 2003; Harvey et al., 2002). Deeper aquifers (generally >150m) tend to be less contaminated owing to a variety of factors that may include their flushing history (Harvey et al., 2005), adsorption capacity (Radloff et al., 2011; Stollenwerk et al., 2007; Swartz et al., 2004), increased recalcitrance of carbon and host mineral forms (Postma et al., 2007; Harvey et al., 2002), and the physical protection provided by confining clays that may prevent influx of near-surface arsenic or arsenic-mobilizing solutes (McArthur et al., 2008; Michael and Voss, 2008). Deep pumping has been implicated, however, in causing contamination of less naturally burdened deep aquifers, by inducing solute transport from the near-surface or from within interbedded confining clays (Erban et al., 2013; Mukherjee et al., 2011; Winkel et al., 2011). Although in these complex systems, arsenic occurrence is characterized by a high degree of heterogeneity at the local scale (order $10^2$-$10^3$ m), landscape-scale patterns ($10^4$-$10^5$ m) can be amenable to statistical modeling (e.g., Rodriguez-Lado et al., 2013; Amini et al., 2008; Winkel et al., 2008).

Here we analyze an unprecedentedly large and spatially comprehensive dataset of arsenic in wells tapping the seven major exploited Holocene-Miocene age aquifers in the Mekong Delta, Vietnam. Our analysis is the first attempt to explain the 3D patterns of dissolved arsenic throughout the heavily exploited, multi-aquifer system. Arsenic concentration data are drawn from a national survey of wells which includes more than 50,000 measurements in the Delta and adjacent areas lowland (<10m) areas from wells up to 600m deep. We explore trends among these observations using

ancillary hydrogeologic datasets to reconstruct the subsurface environment. Our analysis, based on multiple logistic regression, is aimed at identifying variables related to both natural conditions and recent exploitation of groundwater that best explain the current distribution of arsenic throughout the Delta. Findings serve as a baseline for assessing future changes to arsenic contamination and may support water resources management activities in the Delta.

## 2.3 Materials and Methods

### *2.3.1 Data*

Measurements of arsenic in wells were drawn from a nationwide survey conducted over the period 2002-2008 by the Department of Water Resources Management (DWRM), Vietnam. The subset of wells studied in this work is provided as a supporting dataset that includes arsenic concentration, Global Positioning System (GPS) coordinates, well depth and installation year. Explanation of sample collection and analysis methods is given in the online Supporting Information (SI).

To reconstruct the subsurface environment in which these wells are situated, ancillary data were acquired from several sources. The Department of Water Resources Planning and Investigation for the South (DWRPIS) of Vietnam, located in Ho Chi Minh City, provided 1) stratigraphic cross-sections, 2) maps of regional faults and 3) total dissolved solids (TDS) measurements, mapped to specific to aquifer units in 2004. These data are shown in the SI. The Soils Fertilization Research Institute (SFRI), in Hanoi**,** provided digital soils maps, classified by 26 distinct types, which we

grouped into 4 major types: alluvial, acid sulfate, saline and other (see SI). Additional geographic features, such as the course of the modern Mekong River network, were drawn from the International Water Management Institute's IDIS Mekong Basin Kit (Marchand, 2006). Standard built-in tools in ArcGIS (Version 10) were used to calculate the 'distance to river' and 'distance to the delta front' along an axis of delta-building aligned with the fault-bound Bassac River, a major distributary of the Mekong. The 'distance to delta front' metric increases along this axis with distance from the South China Sea. For additional details on the treatment of these data in advance of statistical modeling data, please see the SI.

Finally, each well was assigned to an aquifer according to its latitude, longitude and well screen elevation, estimated as the well's recorded depth relative to the Shuttle Radar Topography Mission's (STRM) 90m Digital Elevation Model (DEM) and tagged with values for potential explanatory variables (Table 1) according to its classified aquifer and GPS coordinates.

### *2.3.2 Modeling approach*

Our models seek to represent well-supported contamination-mediating processes in three overarching categories, each with associated scientific hypotheses. The first category focuses on contamination-generating mechanisms. The hypothesis for this first category is that arsenic *dissolution* is enhanced in shallow (i.e., modern), near-river areas, relative to other parts of the aquifer system, due to favorable biogeochemical conditions that are in turn mediated by depositional environments (Berg et al., 2008; Kocar et al., 2008; Papacostas et al., 2008; Polizzotto et al., 2008).

The second process-based category is concerned with *remediation* mechanisms. These mechanisms are represented by two hypotheses: 1) *physical* remediation by flushing and dilution acts over time alongside diminishing dissolution rates (Postma et al., 2012; Kocar et al., 2008) to reduce the dissolved arsenic burden of deeper aquifers in rough proportion to aquifer age and 2) *chemical remediation* via sulfide inhibition, during which sulfate reduction produces sulfide minerals that can sequester arsenic, may also lessen the dissolved arsenic pool (e.g., Buschmann and Berg, 2009; Lowers et al., 2007; Kirk et al., 2004; O'Day et al., 2004). Sulfide inhibition may counteract arsenic dissolution in subsurface areas that are either hydrologically connected to acid sulfate soils or were subjected to past marine inundation. The third process-based category deals with human-induced contaminant *transport.* The corresponding hypothesis is that over-exploitation may cause new contamination events by drawing arsenic or arsenic-mobilizing solutes towards supply wells. Contaminant arrival at wells is preceded by a time lag (Erban et al., 2013; Mukherjee et al., 2011; Neumann et al., 2009; Harvey et al., 2002) that could potentially be signified by well age.

To test the relative importance of these hypotheses in describing the spatial distribution of dissolved arsenic in wells in the Mekong Delta, we use a multiple logistic regression framework. Logistic regression models considers the logit or log odds, i.e., the ratio of the probability that an outcome occurs ($P(y=1)$) to the probability that it does not ($(1-P(y=1))$), by assuming linear relationships between the logit and explanatory variables ($X_1 \ldots X_n$). It is formalized as:

$$\ln\left[\frac{P(y=1)}{1-P(y=1)}\right] = \beta_0 X_0 + \beta_1 X_1 + \beta_2 X_2 + \ldots + \beta_n X_n \qquad \textit{Eq. 2.1}$$

where $\beta_0 \ldots \beta_n$ are the regression coefficients. In the logistic framework, the dependent variable is valued as 1 or 0 for an outcome that does or does not occur. Here, the outcome for a well is whether or not its arsenic concentration exceeds the 10 µg/L WHO drinking water standard. The chance of this outcome is hereafter referred to as the exceedance probability.

**TABLE 2.1 Categories of processes and explanatory variables**

| In-text category | Process | *linked to* | Explanatory variables | Data type |
|---|---|---|---|---|
| 1 | Dissolution | | Distance to river system (m) | continuous |
| | | | Fault zone | indicator |
| | | | Distance to delta front (m) | continuous |
| 2 | Remediation | | Soil type | categorical |
| | | | Well depth (m) | continuous |
| | | | Aquifer | ordinal |
| 3 | Transport | | Well age (yrs) | continuous |
| | | | Hydraulic head (m) | continuous |

Arsenic exceedance probability covaries with explanatory variables in ways that change considerably throughout the aquifer system. Distinctly lower overall occurrence is observed in parts of the Delta margins coincident with three fault-bounded zones (see Fig. 2.1) that may signal discontinuities in physico-chemical conditions. This is not to say that fault zone is itself an explanatory variable, but rather that fault zone categorization is needed to better model the data. Bivariate relationships also differ markedly between the group of Holocene-Pleistocene aquifers

and the deeper group of Pliocene-Miocene aquifers (see Fig. 2.3). In order to maintain linear relationships between explanatory variables and the logit for arsenic occurrence, the dataset was further categorized according to these spatial distinctions, using 1) an indicator variable for high and low-occurrence fault zones, and 2) subsets for shallow and deep aquifer groups. Maps for these subsets are provided in the supporting information.

## 2.4 Results

The plan view (2D) probability of arsenic exceeding the WHO drinking water standard of 10 µg/L in the Vietnamese portion of the Mekong Delta is shown in Fig. 2.1. Delta-wide, the percentage of wells exceeding this standard is 10.5%. Whole-Delta aggregation, however, masks evident patterns in the spatial distribution of contaminated wells. Affected wells are concentrated in a high-occurrence (11.4%) area

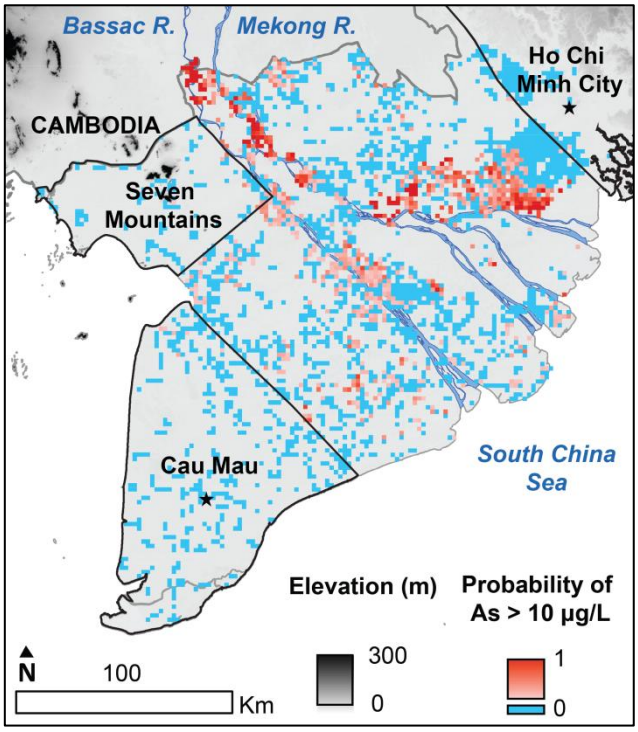


**Figure 2.1** Probability of arsenic contamination above the WHO drinking water standard of 10µg/L among wells in the Mekong Delta. Wells are aggregated over all depths in each 4km$^2$ grid cell. Fault-bounded regions of low arsenic occurrence are indicated with black borders and are labeled by prominent geographic features. The Mekong River and its major distributaries (including the Bassac River) are shown in dark blue.

contiguous with the main river network while large regions of the Delta have much lower occurrence (0.9%). Low-occurrence regions are labeled in Fig 2.1 by their major geographic features.

In addition to large-scale regional differences, arsenic contamination in the Mekong Delta exhibits local 2D spatial trends (in X,Y space, map view). The mean concentration among wells declines sharply with well distance from the main river network in approximately log-linear form (Fig. 2.2, *Top* and SI). The exceedance probability is 25.6% for wells located within 1km of the main river network and falls to <2% among wells at distances greater than 25 km from it (Fig. 2.2, *Bottom*). This trend appears to be related, in part, to a) the correspondence between soil types and proximity to the river network and b) the large representation in the dataset of

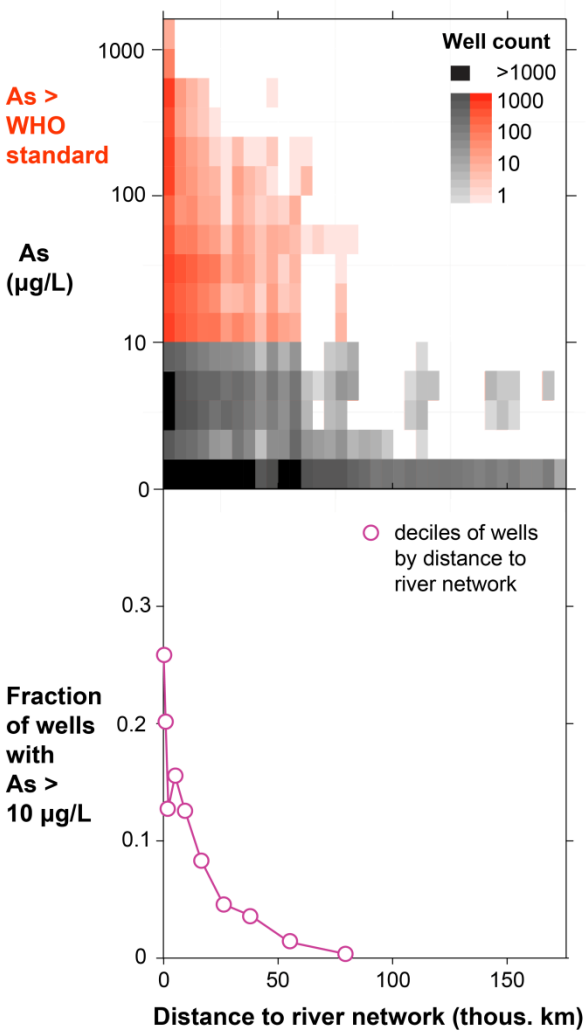


**Figure 2.2 Trends with distance to river. *Top*:** Heat map showing density of wells (well count per pixel) with distance to river network. Red indicates exceedance of the WHO 10µg/L drinking water standard. ***Bottom*:** Fraction of wells with As > 10µg/L in deciles of distance to the Mekong/Bassac River network (colored blue in Fig. 2.1).

shallow wells near the river. Among Holocene wells (4,264 total or 10% of the dataset), both the mean concentration and exceedance probability are appreciably higher for those mapped to alluvial soils (98 µg/L, 34.5 %) relative to saline (11 µg/L, 8.8%) or acid sulfate soils (2 µg/L, 2.1%). These trends are similar, though the spreads among values are reduced, for wells in the Upper Pleistocene aquifer (16,406 total, 38.6% of the dataset), alluvial (30 µg/L, 15%), saline (2.5 µg/L, 3.4%), acid sulfate soils (5.4 µg/L, 5.4%). The differences among soil types for both mean concentration and exceedance probability declines with increasing aquifer age through the Pleistocene aquifers, to values that are similar among types in older units (see SI).

Arsenic contamination also trends strongly with depth (Z) and age of the aquifers. Much like the observed trend with distance to the river network, high concentrations decline with depth in the shallow subsurface. Wells with concentrations exceeding 1,000 µg/L (0.02% of total, max: 1,470 µg/L) are exclusively found within the shallowest Holocene and Pleistocene aquifers. The log-mean arsenic concentration of wells declines linearly through the oldest of the Pleistocene aquifers, increasing again in older, deeper Pliocene-Miocene units (Fig. 2.3 and SI). The exceedance probability follows the same trend; declining consistently from a high of 23.7% in the shallowest Holocene aquifer to a low of 1.8% in the deepest of the Pleistocene units, increasing again to exceed near-surface values in the Miocene aquifer, where 35.7% of wells are contaminated (As > 10µg/L). Considering all wells tapping aquifers that predate the Pleistocene, 20.2% are contaminated, which is nearly twice the proportion in the Delta overall.

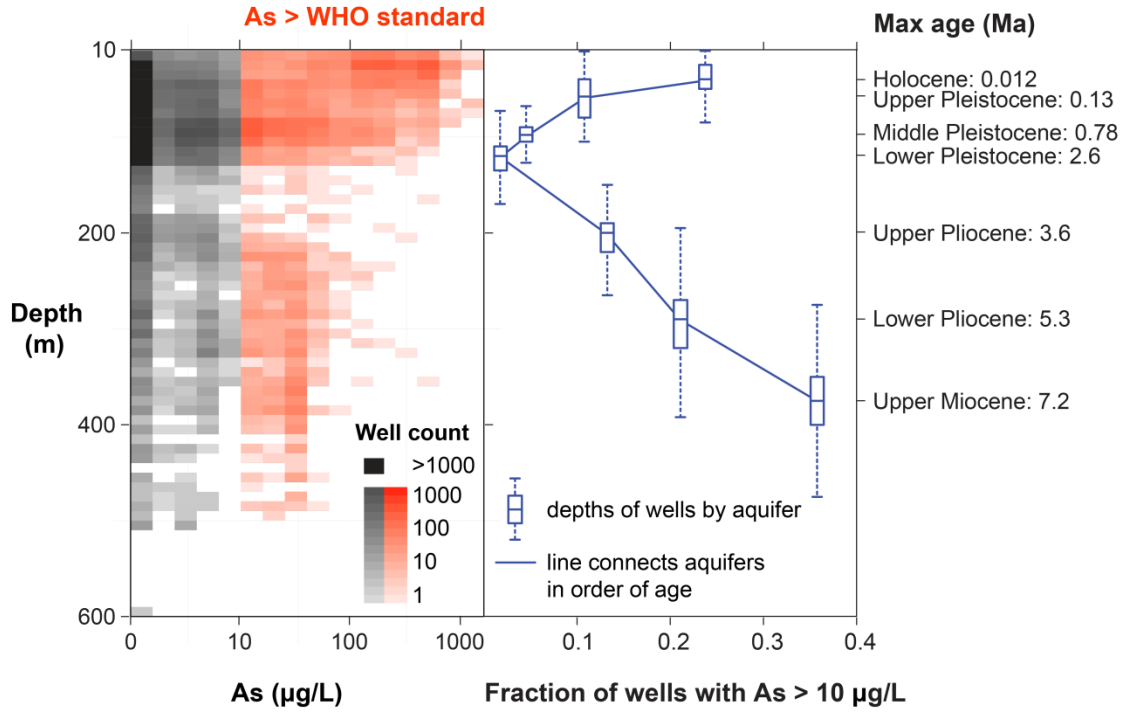


**Figure 2.3 Trends with depth.** ***Left:*** Density of wells with depth. Red indicates exceedance of the WHO 10µg/L drinking water standard. ***Right:*** Fraction of wells with As > 10µg/L by aquifer. Box-plots showing 25%-median-75% ranges of depths of wells classified to each of the seven major aquifers. Outliers (+/- 1.5 IQR outside of boxes) not shown. Significant overlap of box-plot boxes with depth is an indication of the stratigraphic complexity.

Two other contamination trends, less obvious than those related to depth and river distance, are nonetheless apparent. First, an inverse relationship between arsenic concentrations and TDS (max: 20 g/L) is observed in the dataset as a whole (see SI). Second, in a large cluster of nearly 1,400 deep wells, more than half of which are contaminated, well age appears to be a distinguishing feature. In fact, this deep cluster of contaminated wells (see SI) is primarily responsible for the rise in mean concentration and occurrence probability in the group of Pliocene-Miocene aquifers (Fig. 2.3). In addition to the advanced median age of wells in the deep cluster, which is ~10 years older compared to nearby (<10km) wells, they are also located in a part of

the aquifer system where depressed hydraulic heads indicate that intensive exploitation is occurring (see SI). We previously related high arsenic observations in this deep cluster to pumping-induced clay compaction and associated solute expulsion (Erban et al., 2013).

Logistic regressions of the outcome that a well exceeds the 10 μg/L drinking water standard perform well with parsimonious sets of explanatory variables. Model summaries for the subsets of observations classified to shallow and deep aquifer groups are shown in Table 2.2 along with the metrics used to evaluate their performance. For the subset of shallow observations, those in the Holocene-Pleistocene age aquifers, arsenic occurrence is well-described by four explanatory variables: depth, distance to the river network, distance to the delta front and the fault zone indicator. The four chosen variables all evidence clear relationships with the logit and their coefficients have interpretations that are consistent with known contamination-mediating processes (see Discussion). A model including only these variables yields a c-statistic of 0.80 and an overall classification accuracy of 85.7% (Table 2.2). Model performance is lowered upon inclusion of correlated variables, e.g., soil type and distance to delta front, (see SI). Other explanatory variables, notably those that indicate anthropogenic disturbance (i.e., well age, or the time scale for pumping, and hydraulic head), yield marginal increases in the values of performance metrics. These metrics are sensitive, however, when the dataset is large (Raftery, 1995), to explanatory variables with no evident relationship to arsenic occurrence. As such, inclusion of some variables might appear to improve model performance while defying meaningful physical or chemical interpretation. This does

not rule out the possibility that additional explanatory variables are not important, though it cannot be convincingly shown in this case with the available data.

Interestingly, the same set of explanatory variables does not suffice to explain arsenic occurrence among observations in the deep group of Pliocene-Miocene aquifers. For this subset of observations, depth and relative position (location) on the axis of delta-building are no longer statistically significant. Rather, the best model given the available data includes only the distance to river and well age variables. Distance to the modern river is likely correlated with distance to the ancient Mekong system, as offshore sedimentary records suggest the river's overall course has not changed substantially since at least the late Miocene (Li et al., 2013; Murray and Dorobek, 2004). As such, distance to river may indicate a potential for biogeochemical conditions analogous to those responsible for high levels of dissolved arsenic in near-river Holocene clays (Kocar et al., 2008) to be found in the deep confining clays, which were deposited during climatic periods as warm or warmer than at present (Heaney, 1991; Robinson et al., 2008). Well age appears to indicate the time scale for pumping and associated compaction of these clays, where longer time scales are associated with a greater risk of compaction-induced contamination. The deep model has a c-statistic of 0.89 and an overall classification accuracy of 84.0%. The fault zone code indicator is consistent with deep contamination patterns but not additionally useful for explaining them. Inclusion of the hydraulic head variable is complicated by the fact that 1) drawdown is most pronounced in low-occurrence areas in the region's largest urban pumping centers, Ca Mau in the Southwest and Ho Chi Minh City in the Northeast, and 2) outside of the hydraulic

head depressions caused by these cities, the most significant region of co-located drawdown and surveyed wells is where many of the oldest wells are also found (the aforementioned deep cluster). There, the hydraulic head and well age variables likely express some redundant information, since they can be positively correlated in heavily pumped areas. In that region, well age serves as the superior measure in terms model performance, likely because it provides greater specificity to conditions at the individual well than the more coarsely distributed hydraulic head measurements.

For the logistic model, interpretation of the regression coefficients differs from classic linear regression. Exponentiation of the logistic regression coefficient gives the odds ratio, the multiplier for the change in the odds of contamination associated with a unit change in an explanatory variable, holding all others constant. For the shallow model, the odds of well contamination change by a factor of 0.986, or a decline of 14% for every additional 10 meters of depth. Furthermore, a 4.6% decline in odds is predicted for every kilometer in added distance from the Mekong's river channel network. Since the reference case for the fault zone indicator is low-occurrence, a change in location to the high-occurrence zone is, accounting for all other factors, associated with a five-fold increase in odds. Along the axis of delta-building, one kilometer in advancement toward the coast is associated with a decline in odds of 1.1%. For the deep model, every additional kilometer of distance to river channels is associated with a 13% reduction in odds of contamination while for every additional year of well age, an 11% increase is expected.

**TABLE 2.2 Model results**[a]

*Data subset*

| **Shallow** (n = 38049) | | **Deep** (n = 4404) | |
|---|---|---|---|
| **Variable** | **exp(β)** | **Variable** | **exp(β)** |
| Depth (m) | 0.99 | Distance to river (m) | 0.87 |
| Distance to river (m) | 0.95 | Well age (yrs) | 1.11 |
| Distance to delta front (m) | 1.01 | | |
| Fault zone [-] | 5.95 | | |
| **Performance metric** | **value** | **Performance metric** | **value** |
| c-statistic | 0.80 | c-statistic | 0.89 |
| classification accuracy (%) | 85.7 | classification accuracy (%) | 84.0 |

[a] Coefficients are denoted by β as in Eq. 1. All variables have p value for Wald statistic <0.001.

## 2.5 Discussion

Our analysis suggests that the dominant trends in groundwater arsenic in the Mekong Delta are mediated by both natural and anthropogenic factors that vary in influence throughout the complex subsurface. The mean concentration and the probability of well contamination are distinctly different within and among the seven major exploited aquifers. Throughout the 3D aquifer system, the relationships between arsenic occurrence and potential explanatory variables change considerably. Despite this variability, large-scale spatial trends are also evident.

The most striking trends in groundwater arsenic in the Mekong Delta are consistent with known natural processes that promote contamination. Annual flooding of much of the land surface leads to the widespread co-burial of arsenic-rich sediments and labile organic carbon needed to dissolve them in near-river areas with alluvial soils, making these areas more prone to contamination when deposits are young. Over depositional time scales, on-going reductive dissolution exhausts favorable reactant

pools, leaving behind increasingly recalcitrant forms. As sediment depth accumulates, arsenic dissolution rates are diminished (Postma et al., 2012; Kocar et al., 2008). The relative favorability of the dissolution process throughout the aquifer system thus accords with the observed decline in mean arsenic concentration and exceedance probability with increasing distance from the major river channels and depth. Similar patterns have been described in the other arsenic-affected river deltas in Southeast Asia (Fendorf et al., 2010; Winkel et al., 2008).

The distribution of arsenic in the Delta aquifer system is also consistent with processes that naturally inhibit or remediate aquifer contamination. Sequestration of arsenic by sulfide minerals is likely responsible for low occurrence in near-surface aquifers underlying acid sulfate soils. Sulfide sequestration may also affect parts of the subsurface subject to past marine inundation and may be partly responsible for the inverse relationship between arsenic concentrations and TDS, though the available data do not permit investigation of the relationship between TDS and sulfate, or other solutes represented in the TDS measurements that may be important in mediating arsenic occurrence. Dissipation of contamination by advection, dilution and adsorption appears to occur over prolonged time scales. As the aquifer system is built, on-going groundwater flow flushes the original dissolved arsenic burden in each aquifer such that well observations in deeper units show increasingly less correspondence with surface soil types and instead reflect greater degrees of remediation. Flushing likely explains the consistent declines in arsenic concentration and exceedance probability among the four most shallow aquifers, dating from the Holocene to Pleistocene epochs. Contamination in the older, deeper Pliocene-

Miocene aquifers in the Delta appears to have resulted from human influence, as in the area of the deep contaminated well cluster where deep pumping is significant.

The causal relationships between human activities and arsenic occurrence vary throughout the subsurface in ways that are as yet not completely understood. It is known that near-surface contamination events can be stimulated by changes in the belowground availability of arsenic-mobilizing solutes and hydraulic gradients promoting groundwater flow caused by modification of the land surface and shallow pumping (Neumann et al., 2009; Harvey et al., 2002). Determining the contribution of such activities to the shallow contaminant burden would require finer resolution ancillary physico-chemical than that available for this study. Deeper aquifers appear to have naturally lower dissolved arsenic concentrations, making the impact of pumping more apparent. Pumping of the deep subsurface may cause contamination of naturally low-arsenic deep aquifers by inducing downward solute transport through poorly sealed well bores or through the aquifer system itself (Mukherjee et al., 2011; Winkel et al., 2011; Burgess et al., 2010). Over-exploitation may also induce compaction of interbedded confining clays, and expulsion of solutes to adjacent aquifers, leading to new contamination events. New contamination by this process is likely in the deep aquifers of the high-occurrence region where they are heavily exploited (Erban et al., 2013). Nonetheless, the most intense groundwater extraction centers in the Delta, at Ho Chi Minh City and Ca Mau, are found in low-occurrence regions of the Delta. The prolonged pumping in these cities has not led to high arsenic occurrence among local wells, suggesting that the different depositional conditions in these particular regions are ultimately controlling.

The dependency of explanatory variables on depth, often ignored in spatial statistical models of groundwater contamination, is clearly crucial. Depth is directly related to both the time scale for physically-based remediation processes and paleoclimatic conditions under which sediments in a given region of the aquifer system where deposited, which in turn control their capacity for arsenic dissolution or attenuation. Depth dependencies may help explain why distance to river outperforms soil type in the model results. The soil types explanatory variable suffers from at least two depth related limitations: 1) original soil types are not known at depth, and may differ considerably from surface types owing to dramatic changes in paleoclimate, sea level and river course, and 2) chemical constituents inherited from surface soils become increasingly recalcitrant with time, diminishing the differences in contamination even between known soil types. Distance to river, which is correlated with soil type, appears to capture more of the variance in unknown subsurface conditions. Ideally, better characterization of the origin and chemical properties of subsurface deposits would allow for improved consideration of depth dependencies, which should be considered in statistical models of groundwater arsenic.

Logistic regressions help overcome the difficulties of modeling the extreme local-scale heterogeneity among arsenic concentrations by framing contamination in probabilistic terms. The logistic models presented here describe arsenic contamination by targeting the relative importance of the major explanatory variables for which data is available. Careful variable selection is necessary to avoid over-fitting and uninterpretable results stemming from the multicollinearity among explanatory variables and the high sensitivity of these data-rich models to misleading inputs.

Limitations of this analysis are rooted in the associations between available data and the scales of the processes they represent. Regional-scale reconstruction of the subsurface stratigraphy from the sparse well logs cannot discern local variability in conditions. Supplemental information from TDS and hydraulic head data helps to compensate, however, these measurements were made at many fewer locations than the wells surveyed for arsenic. Additional physico-chemical indicators not measured in the arsenic survey and not otherwise available could potentially explain the high degree of heterogeneity among wells at sub-kilometer scales, and would make arsenic concentrations more amenable to standard regression modeling.

In conclusion, we have used a comprehensive, fully 3D approach to investigate the conditions leading to arsenic contamination in the Mekong Delta's multi-aquifer system. Throughout it, the probability of well contamination above the 10 µg/L WHO drinking water standard varies considerably while exhibiting large-scale spatial trends. We enhance our examination of these trends by modeling the individual observations, without aggregating the data over space or depth, and relating them to available explanatory variables through parsimonious models. Our models describe a suite of natural and human-induced conditions influencing the current distribution of groundwater arsenic system-wide. Among shallow wells, arsenic occurrence appears to be well-explained by variables associated with natural arsenic-mediating processes, though human activities may be important at finer scales than our investigation permits. Importantly, however, the shallow model is inadequate to explain arsenic occurrence in the deepest, most heavily-exploited Pliocene-Miocene age aquifers. In

these deeper aquifers, contaminated wells are instead primarily found where over-exploitation is evident in naturally arsenic-prone regions.

The implications for management of groundwater resources in the Mekong Delta, and in other similarly arsenic-affected regions, are profound. Shallow wells installed to provide water for direct human consumption cannot be sited in the population-dense, near-river regions without proper monitoring or planning for water treatment that includes arsenic removal. Deep wells tapping accessible and productive deep aquifers offer an attractive alternative to other water supply options. However, over-exploitation of deep aquifers by wells that may initially have low arsenic occurrence may induce new contamination events over just a few decades. In addition, excessive pumping in deltaic aquifers systems can also cause land subsidence and saline intrusion. For all of these reasons, groundwater pumping should be limited to areas in which all other sources are inadequate, and restricted to low-volume uses. Water resources management efforts aimed at maximizing human welfare should consider all available sources, treated to appropriate standards, including harvested rainfall, surface water, shallow and deep groundwater. Optimal allocation of these supplies will depend on the quantity and quality required by each purpose of use such that exposure to a variety of risks, including those due to arsenic, is minimized.

**Acknowledgments**

We thank multiple Vietnamese governmental agencies for providing source data, namely the DWRM, DWRPIS and SFRI, and P. Switzer for helpful modeling advice. We gratefully acknowledge funding from by the UPS Endowment Fund, Stanford School of Earth Science McGee Grant, Stanford Graduate Fellowship and the Global Freshwater Initiative of the Woods Institute for the Environment at Stanford. This work is being supported by the National Science Foundation under grant EAR-1313518 to Stanford University. Any opinions, findings, and conclusions or recommendations expressed in this material are those of the authors and do not necessarily reflect the views of the National Science Foundation.

## 2.6 Supporting Information

### *2.6.1 Data analysis*

The Vietnamese Department of Water Resources Management's (DWRM) nationwide survey (2002-2008) of arsenic in wells provides the basis for this study, along with several ancillary data sources. Well samples were collected following procedures specified in the national standard TCVN 4556-88. They were analyzed by hydride-generation atomic absorption spectroscopy (ISO 11969:1996) in certified laboratories (Vietnam Laboratory Accreditation Scheme, VILAS). Along with measured arsenic concentration, the survey reported the GPS coordinates, depth and year of installation for each well. DWRM further provided aquifer-specific hydraulic head maps for April, 2005 (April is the end of the dry season, when heads are lowest). Wells in the DWRM arsenic survey were excluded from further consideration if they had 1) no recorded installation year, 2) no recorded depth or very shallow depth (≤10m, potentially open wells that may be exposed to surface conditions) or 3) could not be classified to an unconsolidated layer in the basin. These exclusions reduced the

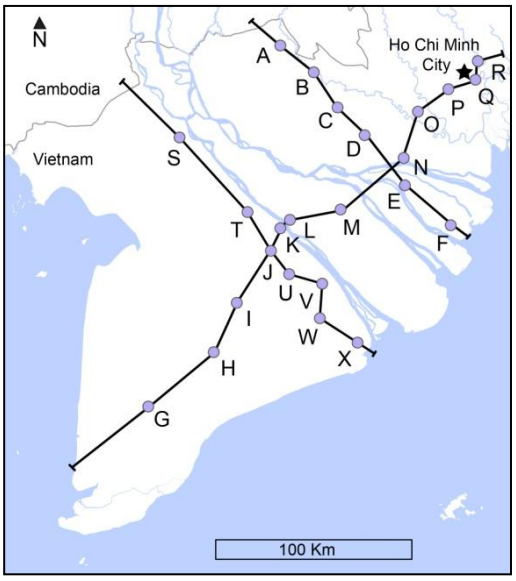


**Figure 2.4** Location map for example cross-sections.

sample size from 52,858 total wells that were surveyed in the Delta and surrounding lowland (<10m) areas to 42,453 used in the following analyses.

Wells in the analysis subset were classified to aquifers using a reconstruction of 3D subsurface layering based on interpretation of well-logs and geologic cross-sections. Seven major aquifers and confining units, ranging in age from the Holocene and Miocene, are distinguished in Delta cross-sections. The Miocene aquifer terminates at bedrock throughout much of the basin, but extends to unknown depths in a deep trough underlying the central Delta. Units predating the Miocene are spatially limited, minimally exploited and not adequately mapped. A few of the deepest wells in the dataset were classified to the Miocene aquifer though they may in fact be screened in these older units.

Example cross-sections provided in Fig. 2.5 illustrate the aquifer classification scheme along with the changing thicknesses and depths of hydrogeologic units over large scales (10's of km) and interruptions by faults. Faults are mapped below in plan view in Fig. 2.7.

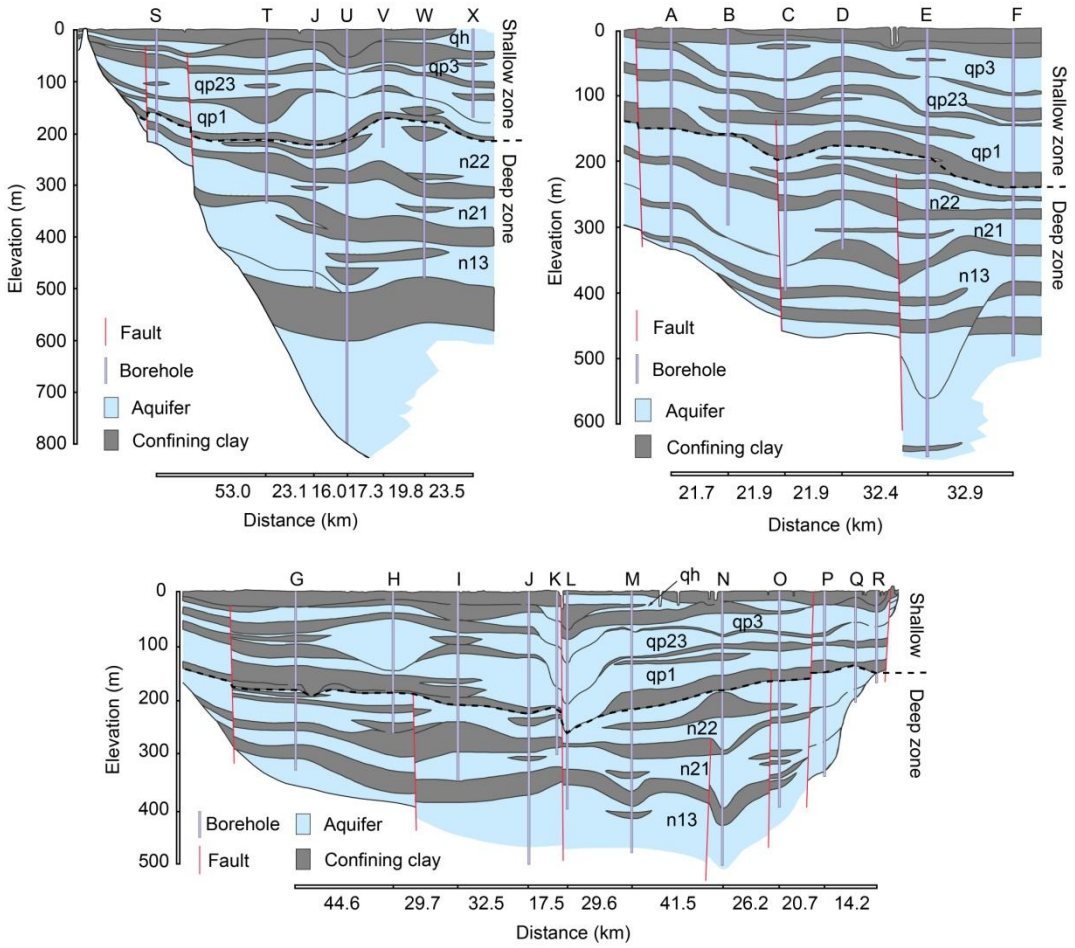


**Figure 2.5** Example geologic cross-sections spanning the Mekong Delta with labeled aquifers: qh = Holocene, qp3 = Upper Pleistocene, qp23 = Middle Pleistocene, qp1 = Lower Pleistocene, n22 = Upper Pliocene, n21 = Lower Pliocene, n13 = Miocene.

Measurements from DWRM–surveyed wells were linked, according to their classified aquifer and 2D GPS coordinates, with ancillary data. Hydraulic head maps for all available aquifers from April 2005, end of the dry season, are shown in Fig. 2.6. The spatial patterns in drawdown described in the manuscript are evident, with major pumping centers indicated at Ca Mau, Ho Chi Minh and along a near-diagonal axis between them.

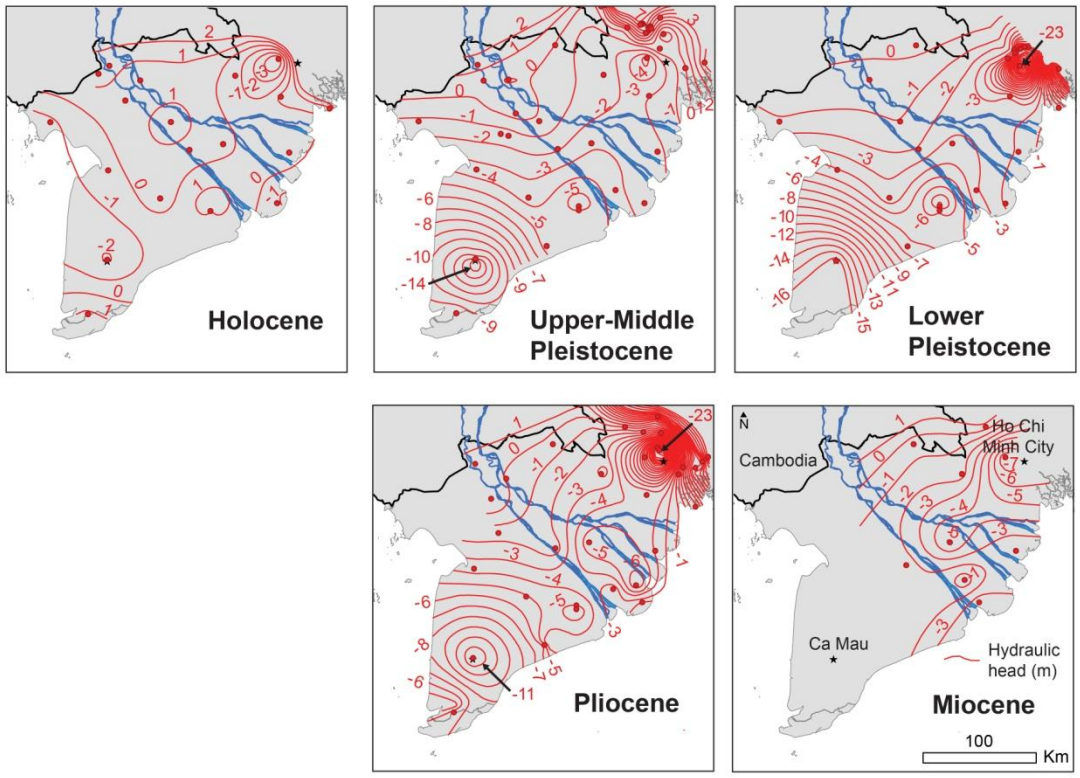


**Figure 2.6** Hydraulic head (m) maps in April, 2005 in all aquifers for which data are available. Measurement locations are indicated with red dots. All contour intervals are 1m. In locations of dense contour spacing, not all are labeled, the minimum contour is indicated by the labeled arrows. "Pliocene" heads were used for both Upper and Lower Pliocene aquifers. The Miocene aquifer is not monitored within the Ca Mau peninsula.

For each of the mapped aquifers, TDS measurements (from 2004) were interpolated to form continuous coverage over the Mekong Delta region (1 $km^2$ resolution). The locations and values of mapped TDS measurements (any underlying aquifer) are shown in Fig. 2.7 (left). Values above the WHO palatability guideline of 1 g/L can be found nearly anywhere in the Delta at some depth, owing to its exceedingly complex depositional history, and likely influences the depth distribution of wells. Fig. 2.7 (right) shows the locations of mapped faults. Those used to distinguish regions of low arsenic occurrence (As >10µg/L) are marked.

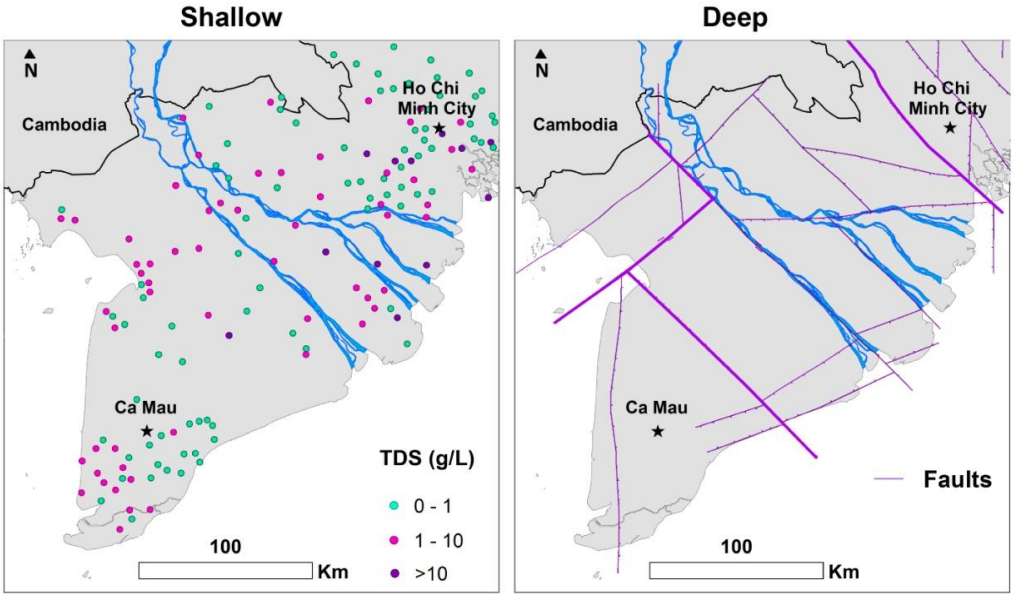


**Figure 2.7** *Left.* Locations of total dissolved solids (TDS) measurements, all aquifers. WHO palatability guideline is 1 g/L. Patterns of TDS are highly complex in the 3D subsurface; in most locations elevated values can be found at some depth. *Right.* Locations of mapped faults with those used to delineate low-arsenic regions indicated with heavier line weight.

Wells in the arsenic survey were also associated, according to their 2D spatial coordinates (no depth consideration), with the surface soils types mapped in Fig. 2.8. Original mapped surface soil classifications (27 total) were grouped into 4 major types, resulting in the noted percent of the total mapped Delta area (37,855 $km^2$): alluvial (27.6%), saline (21.4%), acid sulfate (45.5%) and other (5.5%).

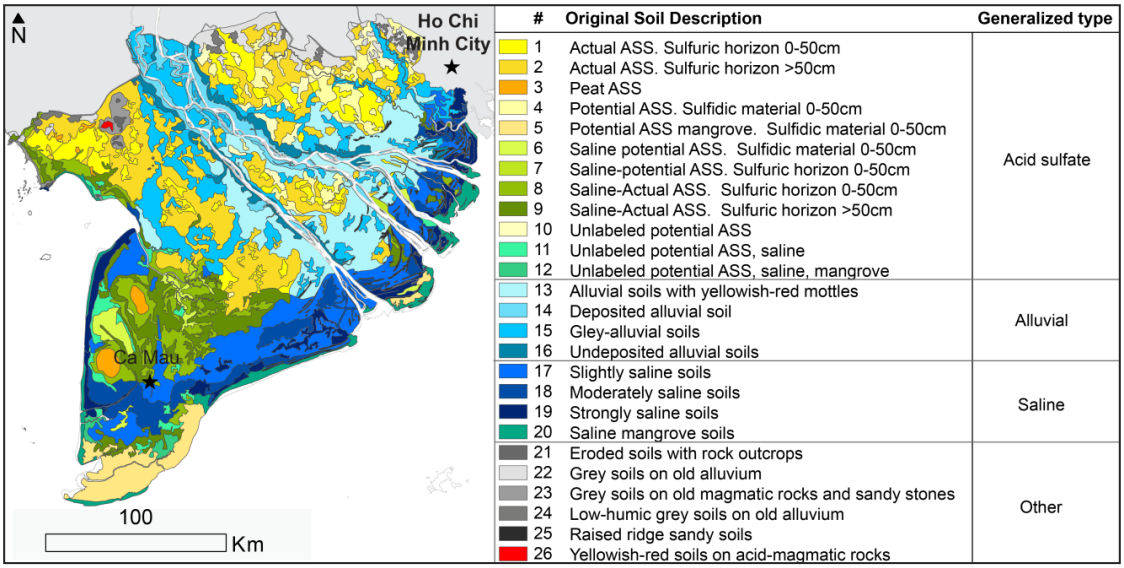


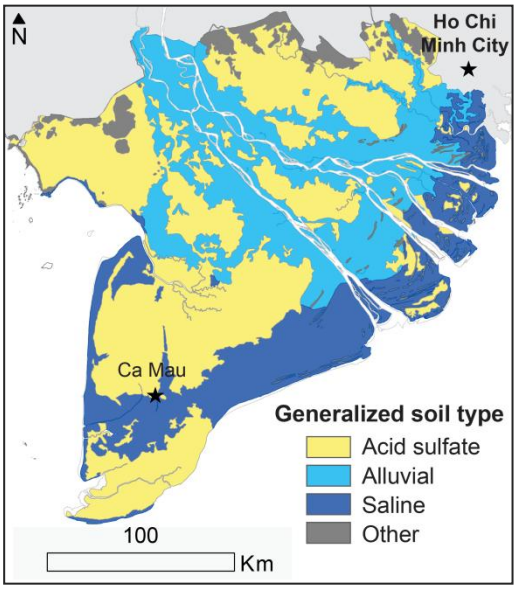


**Figure 2.8** Generalized soil types for the Vietnamese region of the Mekong Delta.

The relevance of surface soils type for distinguishing contamination outcomes (mean concentration of wells or exceedance probability) is questionable for depths other than in the very near-surface. Table 2.3 documents large spreads in outcomes between soil types are observed among Holocene wells that diminish in sequentially

older aquifers. Values for these outcomes are similar across soil types for the Middle-Lower Pleistocene aquifers, suggesting surface soil types are irrelevant at this point in the vertical profile. Values for deeper units are shown for completeness.

| Aquifer | Soil type (mean concentration / exceedance probability) | | | | |
|---|---|---|---|---|---|
| | Alluvial | Saline | Sulfidic | Other | Difference: Alluvial-Sulfidic |
| Holocene | 98 / 0.35 | 11 / 0.09 | 2 / 0.02 | 4 / 0.06 | 96 / 0.32 |
| Upper Pleistocene | 30 / 0.15 | 2 / 0.03 | 5 / 0.05 | 5 / 0.06 | 25 / 0.10 |
| Middle Pleistocene | 5 / 0.06 | 2 / 0.02 | 5 / 0.05 | 4 / 0.04 | 1 / 0.01 |
| Lower Pleistocene | 10 / 0.07 | 0 / 0.00 | 1 / 0.03 | 0 / 0.00 | 8 / 0.05 |
| Upper Pliocene | 6 / 0.17 | 2 / 0.02 | 3 / 0.06 | 14 / 0.43 | 4 / 0.10 |
| Lower Pliocene | 10 / 0.28 | 1 / 0.02 | 3 / 0.10 | 11 / 0.26 | 7 / 0.18 |
| Miocene | 15 / 0.50 | 11 / 0.39 | 5 / 0.19 | 7 / 0.17 | 9 / 0.31 |

**Table 2.3** Summary statistics for arsenic in wells by surface soil type and aquifer.

A subset of wells with depths >10m in the DWRM survey was selected for statistical modeling to ensure that only tube wells, as opposed to open wells, were considered. The wells excluded on the basis of shallow depth (6,141 total) should not, however, lead to bias in our analysis. Excluded shallow wells are found throughout the Delta, except in Ca Mau, where the Holocene aquifer generally has high TDS; they are generally well-distributed. Excluded shallow wells have exceedance probabilities of 10.1% in the high-occurrence region and 1.8% in the low occurrence region, compared with 11.4% and 0.9% for included wells in the same regions, respectively, as reported in the main text.

Finally, wells measured in the DWRM arsenic survey were divided into two groups for modeling purposes: a shallow group of wells classified to Holocene-Pleistocene aquifers and a deep group of wells classified to Pliocene-Miocene

aquifers. We illustrate these shallow and deep subsets in Fig. 2.9. To provide some sense of relative well depth and also allow high concentration observations to be visible in data dense areas, two sets of these maps are provided. In the first set (top row), wells are plotted by depth: the maps appear as they would if the aquifer system were translucent and viewed from above, with shallower wells plotting on top of the deeper wells in a given area. In the second set of maps (bottom row), plotting priority is assigned according to arsenic concentration, with highest observations at the top. The second set is consistent with the method used for plotting Fig. 2.1 of the main text, in which the entire dataset is plotted with the concentration-based priority.

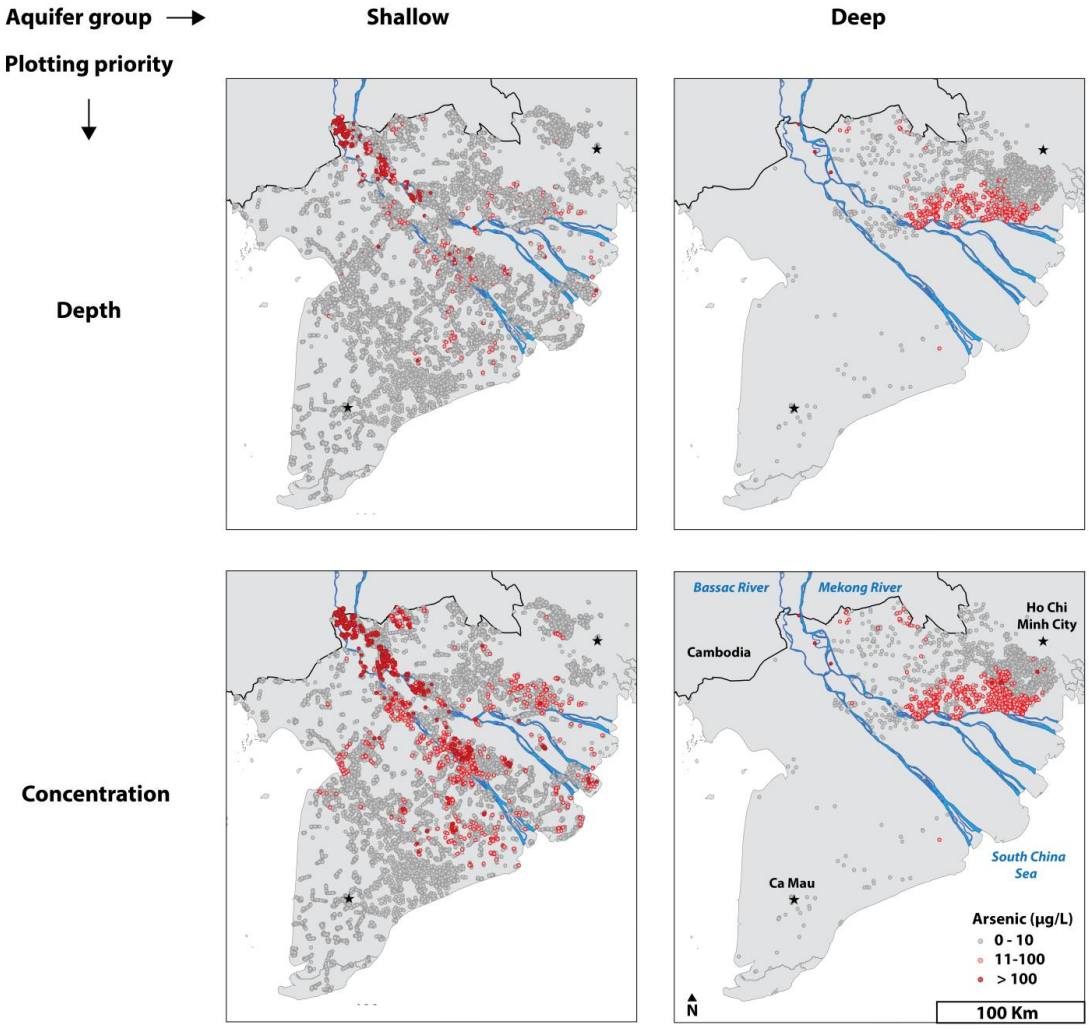


**Figure 2.9** Maps of arsenic observations by shallow and deep aquifer groups with depth and concentration-based plotting priorities (see text for explanation).

The importance of well age and its relationship to observed arsenic contamination in the shallow and deep subsets of wells was also discussed in the manuscript. Fig. 2.10 shows depth-priority maps of well age, with older wells drawn using larger symbols.

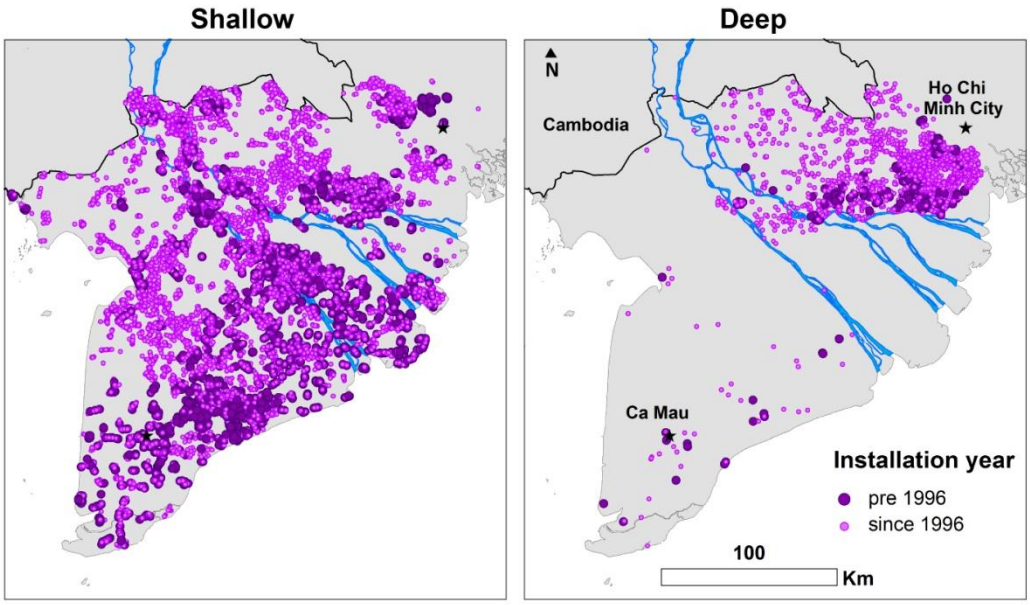


**Figure 2.10** Well age plotted using depth-priority (shallowest observations plot on top) and larger symbols for older wells for the shallow (left) and deep (right) groups of observations.

### *2.6.2 Statistical modeling*

Logistic regression, which models the probability of a binary outcome, is commonly chosen for modeling natural contamination events for two major reasons 1) observations often have extremely heterogeneous values over short spatial lags and display high heteroscedasticity that undermines standard linear regression, and 2) regulatory standards are typically based on a threshold, such that exceedance or non-exceedance of that threshold can be represented as a binary outcome.

In advance of fitting the regression models, we first individually examined the bivariate relationships between each explanatory, or independent, variable associated with a hypothesis (see Table 1) and the logit, or log odds of a well being contaminated, the dependent variable in logistic regression modeling. To calculate the logit, we used deciles of the data across each explanatory variable. We selected only

those explanatory variables and interactions among them that showed linear relationships with the logit or, in the case of the categorical soil type variable, showed effects consistent with known contamination-mediating mechanisms. This approach is preferred to automated stepwise procedures, especially in cases of very large-n datasets such as ours where statistical significance is not a meaningful measure; small, uninterpretable effects often have extremely high significance (Raftery, 1995). Second, after the first cull of explanatory variables, Bayesian Model Averaging (BMA) was used to select a model. Briefly, BMA provides an estimate of the probability that a chosen model is the true one, given all other possible choices with a selected set of variables. The BMA package for R was used to expeditiously probe the full space of variable combinations and select the most likely of numerous possible models (Raftery et al., 2012).

The most noteworthy bivariate relationships between arsenic contamination in wells and explanatory variables were illustrated in the manuscript and above supplement. Here we further show the mean arsenic concentration by aquifer in Fig. 2.11 (*left*) and the inverse relationship between concentration and TDS in Fig. 2.11 (*right*).

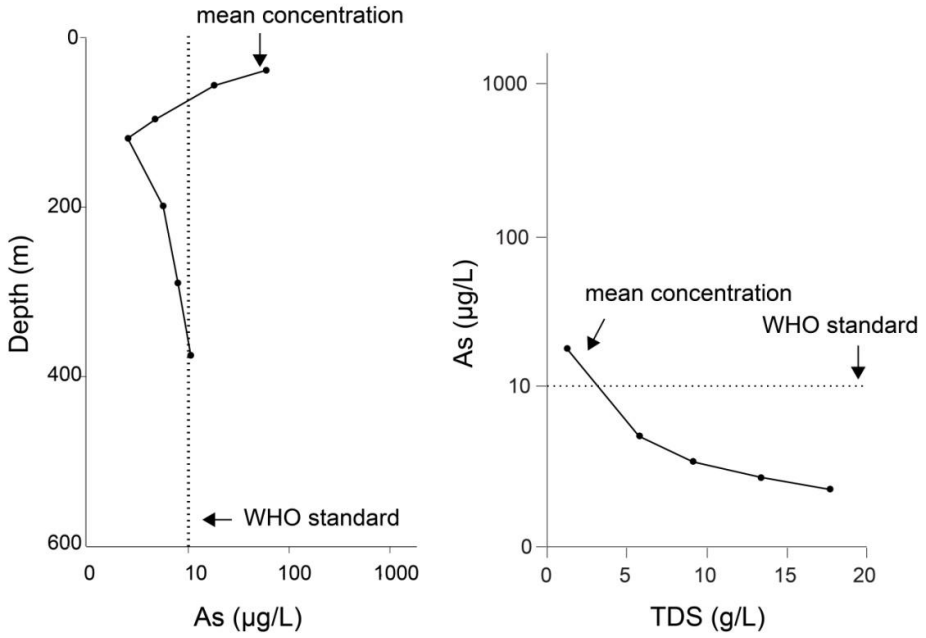


**Figure 2.11** *Left:* Well counts in concentration:depth space with superimposed mean concentration of wells by aquifer. *Right:* Well counts in TDS: concentration space, with superimposed mean concentration binned by increments of 5 TDS units.

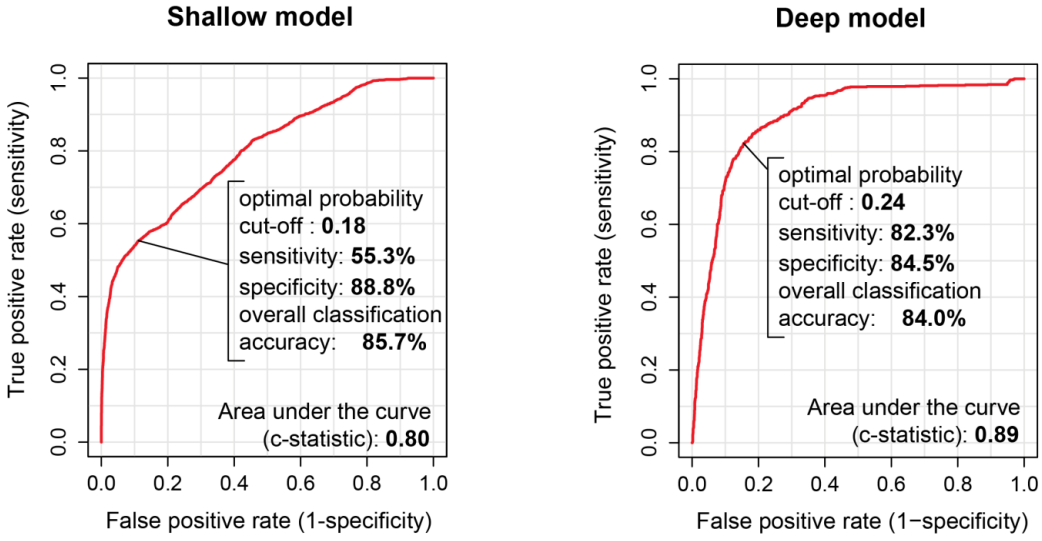


**Figure 2.12** Outcome discrimination performance of models.

## References


Amini, M., Abbaspour, K. C., Berg, M., Winkel, L., Hug, S. J., Hoehn, E., Yang, H., and Johnson, C. A. (2008). Statistical modeling of global geogenic arsenic contamination in groundwater. *Environmental science & technology*, 42(10), 3669–3675.

Berg, M., Stengel, C., Pham, T. K. T., Pham, H. V., Sampson, M. L., Leng, M., Samreth, S., and Fredericks, D. (2007). Magnitude of arsenic pollution in the Mekong and Red River Deltas—Cambodia and Vietnam. *Science of the Total Environment*, 372, 413–425.

Berg, M., Tran, H. C., Nguyen, T. C., Pham, H. V., Schertenleib, R., and Giger, W. (2001). Arsenic contamination of groundwater and drinking water in Vietnam: a human health threat. *Environmental science & technology*, 35, 2621–2626.

Berg, M., Pham, T. K. T., Stengel, C., Buschmann, J., Pham, H. V., Nguyen, V. D., Giger, W., and Stüben, D. (2008). Hydrological and sedimentary controls leading to arsenic contamination of groundwater in the Hanoi area, Vietnam: The impact of iron-arsenic ratios, peat, river bank deposits, and excessive groundwater abstraction. *Chemical Geology*, 249, 91–112.

Burgess, W. G., Hoque, M. A., Michael, H. A., Voss, C. I., Breit, G. N., and Ahmed, K. M. (2010). Vulnerability of deep groundwater in the Bengal Aquifer System to contamination by arsenic. *Nature Geoscience*, 3, 83–87.

Buschmann, J., and Berg, M. (2009) Impact of sulfate reduction on the scale of arsenic contamination in groundwater of the Mekong, Bengal and Red River deltas. *Applied Geochemistry*, 24, 1278-1286.

Dowling, C. B., Poreda, R. J., Basu, A. R., Peters, S. L., and Aggarwal, P. K. (2002). Geochemical study of arsenic release mechanisms in the Bengal Basin groundwater. *Water Resources Research*, 38, DOI 10.1029/2001WR000968.

Erban, L. E., Gorelick, S. M., Zebker, H. A, and Fendorf, S. (2013). Release of arsenic to deep groundwater in the Mekong Delta, Vietnam, linked to pumping-induced land subsidence. *Proceedings of the National Academy of Sciences of the United States of America*, DOI 10.1073/pnas.1300503110.

Fendorf, S., Michael, H. A., and van Geen, A. (2010). Spatial and Temporal Variations of Groundwater Arsenic in South and Southeast Asia. *Science*, 328, 1123–1127.

Harvey, C. F., Swartz, C. H., Badruzzaman, A. B., Keon-Blute, N., Yu, W., Ali, M. A., Jay, J., Beckie, R., Niedan, V., Brabander, D., Oates, P. M., Ashfaque, K. N., Islam, S., Hemond, H. F., and Ahmed, M. F. (2005). Groundwater arsenic contamination on the Ganges Delta: biogeochemistry, hydrology, human perturbations, and human suffering on a large scale. *Comptes rendus-Geoscience*, 337, 285–296.

Harvey, C. F., Swartz, C. H., Badruzzaman, A. B. M., Keon-Blute, N., Yu, W. Ali, M. A., Jay, J., Beckie, R., Niedan, V., Brabander, D., Oates, P. M., Ashfaque, K. N., Islam, S., Hemond, H. F., and Ahmed, M. F. (2002). Arsenic Mobility and Groundwater Extraction in Bangladesh. *Science*, 298, 1602–1606.

Heaney, L. R. (1991). A synopsis of climatic and vegetational change in Southeast Asia. *Climatic Change*, 19(1), 53–61.

Hoang, T. H., Bang, S., Kim, K. W., Nguyen, M. H., and Dang, D. M. (2010). Arsenic in groundwater and sediment in the Mekong River delta, Vietnam. *Environmental Pollution*, 158, 2648–2658.

Hosmer, D. W., and Lemeshow, S. Applied Logistic Regression, John Wiley & Sons: New York, 2000.

Kirk, M. F., Holm, T. R., Park, J., Jin, Q., Sanford, R. A., Fouke, B. W., and Bethke, C. M. (2004) Bacterial sulfate reduction limits natural arsenic contamination in groundwater. *Geology*, 32, 953–956.

Kocar, B. D., Polizzotto, M. L., Benner, S. G., Ying, S. C., Ung, M., Ouch, K., Samreth, S., Suy, B., Phan, K., Sampson, M., and Fendorf, S. Integrated biogeochemical and hydrologic processes driving arsenic release from shallow sediments to groundwaters of the Mekong delta. Appl. Geochemistry 2008, 23, 3059–3071.

Li, L., Clift, P. D., and Nguyen, H. T (2013). The sedimentary, magmatic and tectonic evolution of the southwestern South China Sea revealed by seismic stratigraphic analysis. Mar. Geophysical Research. DOI 10.1007/s11001-013-9171-y.

Lowers, H. A., Breit, G. N., Foster, A. L., Whitney, J., Yount, J., Uddin, M. N., and Muneem, A. A. (2007). Arsenic incorporation into authigenic pyrite, Bengal Basin sediment, Bangladesh. *Geochimica Cosmochimcia Acta*, 71, 2699–2717.

Marchand, P. (2006). Integrated Database Information System (IDIS) Basin Kit V1.0 (CD–ROM). Battaramulla, Sri Lanka.

McArthur, J. M., Ravenscroft, P., Banerjee, D. M., Milsom, J., Hudson-Edwards, K. A., Sengupta, S., Bristow, C., Sarkar, A., Tonkin, S., and Purohit, R. (2008). How paleosols influence groundwater flow and arsenic pollution: A model from the Bengal Basin and its worldwide implication. *Water Resources Research*, 44, DOI 10.1029/2007WR006552.

McArthur, J. M., Ravenscroft, P., Safiulla, S., and Thirlwall, M. F. (2001). Arsenic in groundwater: testing pollution mechanisms for sedimentary aquifers in Bangladesh. *Water Resources Research*, 37, 109–117.

Michael, H. A., and Voss, C. I. (2008). Evaluation of the sustainability of deep groundwater as an arsenic-safe resource in the Bengal Basin. *Proceedings of the National Academy of Sciences of the United States of America*, 105, 8531–8536.

Mukherjee, A., Fryar, A. E., Scanlon, B. R., Bhattacharya, P., and Bhattacharya, A. (2011). Elevated arsenic in deeper groundwater of the western Bengal basin, India: Extent and controls from regional to local scale. *Applied Geochemistry*, 26, 600–613.

Murray, M. R., and Dorobek, S. L. (2004). Sediment Supply , Tectonic Subsidence, and Basin-Filling Patterns Across the Southwestern South China Sea During Pliocene to Recent Time. In Continent-Ocean Interactions Within East Asian Marginal Seas, Geophysical Monograph Series, vol. 149, Clift, P., Kuhnt, W., Wang, P., Hayes, D., Eds.; AGU, Washington, D.C., pp 235-254.

Neumann, R. B., Ashfaque, K. N., Badruzzaman, A. B. M., Ashraf Ali, M., Shoemaker, J. K., and Harvey, C. F. (2009). Anthropogenic influences on groundwater arsenic concentrations in Bangladesh. *Nature Geoscience*, DOI 10.1038/NGEO685.

Nguyen, K. P., and Itoi, R. (2009) Source and release mechanism of arsenic in aquifers of the Mekong Delta, Vietnam. *Journal of Contaminant Hydrology*, 103, 58–69.

Nickson, R. T., McArthur, J. M., Ravenscroft, P., Burgess, W. G., and Ahmed, K. M. (2000). Mechanism of arsenic release to groundwater, Bangladesh and West Bengal. *Applied Geochemi*stry, 15, 403–413.

O'Day, P. A, Vlassopoulos, D., Root, R., and Rivera, N. (2004). The influence of sulfur and iron on dissolved arsenic concentrations in the shallow subsurface under changing redox conditions. *Proceedings of the National Academy of Sciences of the United States of America*, 101(38), 13703–8. doi:10.1073/pnas.0402775101.

Papacostas, N. C., Bostick, B. C., Quicksall, A. N., Landis, J. D., and Sampson, M. (2008). Geomorphic controls on groundwater arsenic distribution in the Mekong River Delta, Cambodia. *Geology*, 36(11), 891. doi:10.1130/G24791A.1.

Polizzotto, M. L., Kocar, B. D., Benner, S. G., Sampson, M., and Fendorf, S. (2008). Near-surface wetland sediments as a source of arsenic release to ground water in Asia. *Nature*, 454(7203), 505–508. doi:10.1038/nature07093.

Postma, D., Larsen, F., Nguyen, T. T., Pham, T. K. T., Jakobsen, R., Pham, Q. N., Tran, V. L., Pham, H. V., and Murray, A. S. (2012). Groundwater arsenic concentrations in Vietnam controlled by sediment age. *Nature Geoscience* 2012, DOI 10.1038/ngeo1540.

Postma, D., Larsen, F., Minh Hue, N. T., Duc, M. T., Viet, P. H., Nhan, P. Q., and Jessen, S. (2007) Arsenic in groundwater of the Red River floodplain, Vietnam: Controlling geochemical processes and reactive transport modeling. *Geochimica Cosmochimica Acta*, 71, 5054–5071.

Radloff, K. A., Zheng, Y., Michael, H. A., Stute, M., Bostick, B. C., Mihajlov, I., Bounds, M., Huq, M. R., Choudhury, I., Rahman, M. W., Schlosser, P., Ahmed, K. M., and van Geen, A. (2011). Arsenic migration to deep groundwater in Bangladesh influenced by adsorption and water demand. *Nature Geoscience*, 4, 793–798.

Raftery, A. E. (1995). Bayesian Model Selection in Social Research. *Sociological Methodology*, 25, 11–163.

Raftery, A., Hoeting, J., Volinsky, C., Painter, I., and Yeung, K. Y. (2012). BMA: Bayesian Model Averaging. R package version 3.15.3.2.

Robinson, M. M., Chandler, M. A., and Dowsett, H. J. (2008). Pliocene role in assessing future climate impacts. *Eos Transactions, AGU*, 89(49), 501.

Rodriguez-Lado, L., Sun, G., Berg, M., Zhang, Q., Xue, H., Zheng, Q., and Johnson, C. A. (2013). Groundwater Arsenic Contamination Throughout China. *Science*, 341(6148), 866–868. doi:10.1126/science.1237484.

Stanger, G., Truong, T. V., Ngoc, K. S. L. T. M., Luyen, T. V., and Thanh, T. T. (2005). Arsenic in groundwaters of the Lower Mekong. *Environmental Geochemistry and Health*, 27, 341–357.

Stollenwerk, K. G., Breit, G. N., Welch, A. H., Yount, J. C., Whitney, J. W., Foster, A. L., Uddin, M. N., Majumder, R. K., and Ahmed, N. (2007). Arsenic attenuation by oxidized aquifer sediments in Bangladesh. *Science of the Total Environment*, 379, 133–150.

Swartz, C. H., Blute, N. K., Badruzzman, B., Ali, A., Brabander, D., Jay, J., Besancon, J., Islam, S., Hemond, H. F., and Harvey, C. F. (2004). Mobility of arsenic in a Bangladesh aquifer: Inferences from geochemical profiles, leaching data, and mineralogical characterization. *Geochimica Cosmochimica Acta*, 68, 4539–4557.

van Geen, A., Zheng, Y., Versteeg, R., Stute, M., Horneman, A., Dhar, R., Steckler, M., Gelman, A., Small, C., Ahsan, H., Graziano, J. H., Hussain, I., and Ahmed, K. M. (2003) Spatial variability of arsenic in 6000 tube wells in a 25 $km^2$ area of Bangladesh. *Water Resources Research*, 39, DOI 10.1029/2002WR001617.

Winkel, L., Berg, M., Amini, M., Hug, S. J., and Annette Johnson, C. (2008). Predicting groundwater arsenic contamination in Southeast Asia from surface parameters. *Nature Geoscience*, 1(8), 536–542. doi:10.1038/ngeo254.

Winkel, L. H., Pham, T. K. T., Vi, M. L., Stengel, C., Amini, M., Nguyen, T. H., Pham, H. V., and Berg, M. (2011). Arsenic pollution of groundwater in Vietnam exacerbated by deep aquifer exploitation for more than a century. *Proceedings of the National Academy of Sciences of the United States of America*, 108, 1246–1251.

# 3 Release of arsenic to deep groundwater in the Mekong Delta, Vietnam, linked to pumping-induced land subsidence

## 3.1 Abstract

Deep aquifers in South and Southeast Asia are increasingly exploited as presumed sources of pathogen- and arsenic-free water, though little is known of the processes that may compromise their long-term viability. We analyze a large area (>1000 $km^2$) of the Mekong Delta, Vietnam, in which arsenic is found pervasively in deep, Pliocene-Miocene age aquifers, where nearly 900 wells at depths of 200-500 m are contaminated. There, intensive groundwater extraction is causing land subsidence of up to 3 cm/yr as measured using satellite-based radar images from 2007-2010 and consistent with transient 3D aquifer simulations showing similar subsidence rates and total subsidence of up to 27 cm since 1988. We propose a previously unrecognized mechanism in which deep groundwater extraction is causing interbedded clays to compact and expel water containing dissolved arsenic or arsenic-mobilizing solutes (e.g., dissolved organic carbon, competing ions) to deep aquifers over decades. The implication for the broader Mekong Delta region, and potentially others like it across Asia, is that deep, untreated groundwater will not necessarily remain a safe source of drinking water.

## 3.2 Introduction

Arsenic in groundwater poses a massive and growing human health threat throughout South and Southeast Asia. An estimated 100 million people (Ravenscroft and Brammer, 2009) are chronically exposed to arsenic, a potent carcinogen also linked to a variety of other health risks in adults and children (Smith et al., 2000), through consumption of naturally-contaminated groundwater. Despite widespread awareness of this crisis, groundwater exploitation continues to rise, with demand increasingly being met by deep wells (>150m). Deep wells typically exhibit low arsenic concentrations and have been promoted as an alternative to those tapping contaminated shallow groundwater. "Dig deep to avoid arsenic" (Downey, 2008) has been touted as a safe answer to the provisioning of drinking water in Bangladesh, despite a lack of evidence that deep aquifers indeed remain uncontaminated under prescribed (Radloff et al., 2011; Michael and Voss, 2008) or unregulated pumping. In fact, recent studies indicate that arsenic occurrence may be on the rise where deep aquifers are intensively pumped in parts of Bangladesh, West Bengal, India and the Red River Delta, in northern Vietnam (Mukherjee et al., 2011; Winkel et al., 2011; Burgess et al., 2010). In some cases, isolated deep arsenic contamination may be caused by downward leakage through well bores. However, in the Mekong Delta, in southern Vietnam, deep aquifers show pervasive arsenic contamination that may be directly linked to groundwater exploitation via a causal mechanism not previously considered and described presently.

Arsenic occurs naturally in sediments throughout the depth profile of the major river basins of South and Southeast Asia. Solid-phase arsenic is primarily released to

groundwater during the microbially-mediated reductive dissolution of ferric(hydr)oxides found in buried river-borne sediments. Dissolution is controlled by a suite of physicochemical conditions that vary widely within and among hydrogeologic units (Smedley and Kinniburgh, 2002), largely as a result of variability in depositional and paleoclimatic conditions during their formation. Across basins, dissolved arsenic concentrations tend to be highest in the shallow (<100m) subsurface (Fendorf et al., 2010), where the reactivity of host minerals and the organic carbon needed to dissolve them is also greatest (Postma et al., 2012; Kocar et al., 2008). As a result, considerable attention has been paid to contamination mechanisms in Holocene units (up to ~0.011 Ma in age), where affected wells are most commonly found, and to older Pleistocene units (~0.011-2.6 Ma), where they are usually more rare (Mukherjee et al., 2011; Winkel et al., 2011; Burgess et al., 2010; Zheng et al., 2005). Little is known of arsenic occurrence in older Pliocene-Miocene age (~2.6-23 Ma) aquifers or in the thick sequences of interbedded confining clays (i.e., aquitards), which are known to mobilize high levels of dissolved arsenic in near-surface Holocene clays (Kocar et al., 2008).

Here, we focus on the Mekong Delta, Vietnam, where heavily-exploited Pliocene-Miocene age aquifers are extensively contaminated at depths of 200-500m. A recent nationwide survey of arsenic in wells conducted from 2002-2008 by the Department of Water Resources Management, Vietnam includes 42,921 observations in the Delta alone (Figure 3.1). While prior synoptic studies in the Delta have focused on near-river areas, where the highest population densities and arsenic concentrations are found (Hoang et al., 2010; Nguyen and Itoi, 2009; Berg et al., 2007; Buschmann et

al., 2007; Stanger et al., 2005), wells in this new survey were sampled in proportion to their abundance in all populated areas, providing unprecedented spatial coverage. Our analysis uses 1) the richness of these observations along with 2) simulation of the spatio-temporally explicit flow and pumping history of the multi-aquifer system and 3) validation of pumping-induced compaction by radar remote sensing of land subsidence. This complementary suite of methods allows us to reveal a new human-influenced contamination mechanism in deep aquifers.

## 3.3 Results

In the Mekong Delta, groundwater is widely pumped from seven major aquifers ranging from Holocene to Miocene age. The delineation of aquifers and their ages used here is based on the work of the Division for Geological Mapping for the South (DGMS) of Vietnam, which employed a suite of standard techniques including mud logging of drill cuttings, radiometric dating, analysis of microfossils and geophysical surveys to describe the >1000m-deep, fault-blocked basin underlying the Delta and the complex stratigraphy of its fill. On the Vietnamese side of the Delta, numerous productive, sandy aquifers are separated by and embedded with similarly thick and laterally extensive sequences of significantly less permeable clays. The confining nature of these clays is indicated by distinctly separable hydraulic heads in nested monitoring wells. Well nests, or sets of wells in which each measures the hydraulic head in one of 4-6 aquifers at the same location, are well-distributed throughout the Delta. They allow for examination of both horizontal and vertical hydraulic gradients, and they indicate that several aquifers are experiencing widespread head declines (see Supporting Information (SI)). Pumping wells, in use

since the early 1900s, have become increasingly more common since the early 1980s. Today these wells are widely used for a variety of domestic, agricultural, and industrial purposes. Throughout much of the Delta, deep aquifers are the most heavily-exploited.

Arsenic occurrence in the Mekong Delta exhibits some classic characteristics observed in many other South and Southeast Asian river basins (Figure 3.1A). Dissolved concentrations are highest (max: 1470 µg/L) in the shallow subsurface (<100m), in close proximity (<5km) to the main river and its distributaries, and drop off sharply with distance. Wells with concentrations up to 1000 µg/L, two orders of magnitude greater than the 10 µg/L WHO drinking water standard, are often less than 100m away from others with no detectable arsenic. Pervasive arsenic is found in several extensive hot-spot regions.

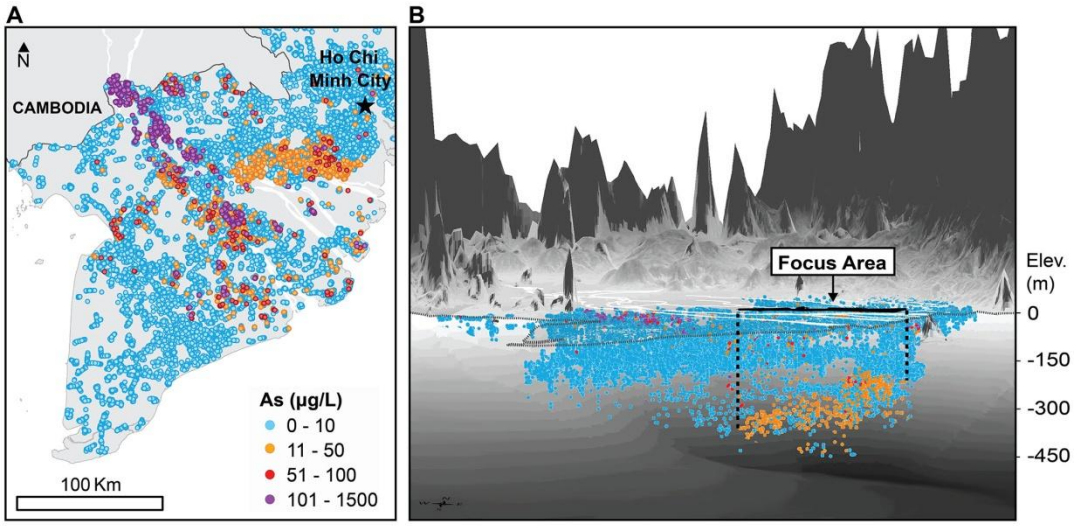


**Figure 3.1** Groundwater arsenic concentrations in the Mekong Delta, Vietnam. **A.** Plan view. **B.** North-looking perspective (vertical exaggeration: 150x), highlighting the focus area of this work. Topography and bedrock surface shown above and below zero elevation (mean sea level), respectively. Coastline is lightly dashed.

The most prominent arsenic hot-spot region is located ~50 km southwest of Ho Chi Minh City (HCMC) and is over 1000 km$^2$ in extent. This "focus area" contains 1059 wells with arsenic exceeding 10 µg/L (Figure 3.1A-B). Based on stratigraphic cross-sections and the evident partitioning of these wells by depth (Figure 3.1B), we divide wells in the focus area into two sets: those in shallow Holocene-Pleistocene aquifers (Figure 3.2C) and those tapping the deep Pliocene-Miocene aquifers (Fig. 3.2D). The deep set (170-500m) contains the majority (84%) of arsenic-contaminated wells.

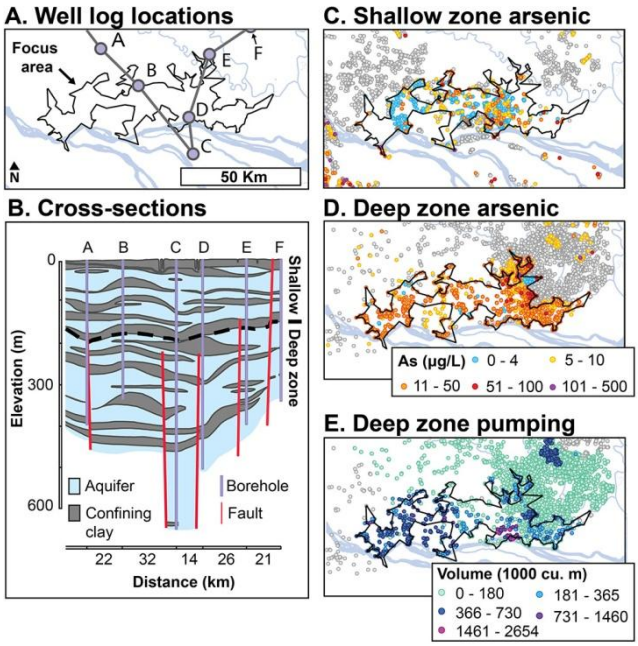


**Figure 3.2 A**. Locations of bores in cross-sections in the vicinity of the focus area. B. Cross-sections illustrating complex stratigraphy and distinction between shallow and deep zones of focus area. C-D. Arsenic concentrations in wells of the shallow and deep zones. Wells with As < 5µg/L outside the focus area are shown in gray. E. Pumping intensity of wells in the deep zone estimated by multiplying the age of each well by the 2007 unit pumping rate (total pumping rate for each district and aquifer divided by the total number of wells in each district's DWRM wells). Wells in districts for which pumping data are unavailable are shown in gray.

The Mekong Delta focus area shows far more deep, contaminated wells than other major arsenic-affected regions of South and Southeast Asia. Prior surveys from Nepal, India, Bangladesh, and Vietnam's Red River Delta (compiled in Fendorf et al., 2010) indicate that the fraction of contaminated wells diminishes with depth (Figure 3.3). In those areas, wells were rarely found with arsenic in excess of 10 µg/L at

depths greater than 200 m. Deep wells, however, tend to be less well represented in surveys, in terms of both total quantity and spatial coverage. As such, our understanding of the extent and mechanisms of deep arsenic contamination has remained incomplete.

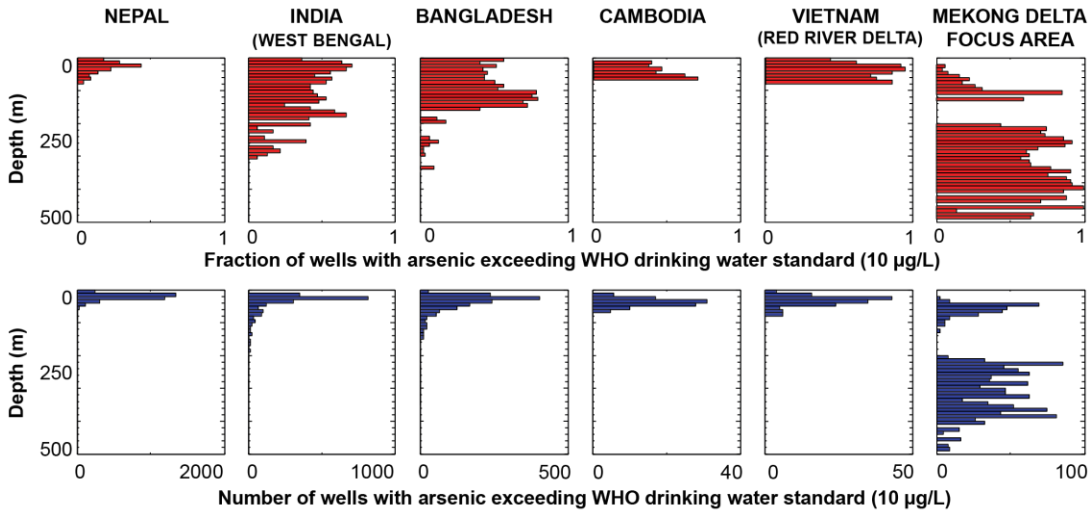


**Figure 3.3** Depth profile of groundwater arsenic occurrence in surveys of major affected areas in South and Southeast Asia.

Evidence suggests that deep contamination in the Mekong Delta focus area is unlikely to have been caused by the only presently-acknowledged mechanism: pumping-induced vertical migration of arsenic or dissolved organic carbon (DOC), which can trigger arsenic release, from the surface or shallow subsurface (Mukherjee et al., 2011; Winkel et al., 2011; Neumann et al., 2009; Polizzotto et al., 2005; Harvey et al., 2002). The number of wells above 10 µg/L in the deep zone is 7 times greater than in the shallow zone. The mean concentration in the shallow zone is significantly less than the deep (4 vs. 20 µg/L, respectively). There are no clusters of overlying shallow wells with concentrations exceeding contaminated wells at depth. Moreover,

vertical velocities through the layered system are estimated, using the hydraulic head record and thicknesses of sand and clay in all 1020 one-$km^2$ locations within the focus area, to be less than 0.2 m/yr. Given that the mean distance between contaminated wells in the shallow and deep zones is 100m, and considering a generous 28 years of travel time since the onset of increasing well installations, downward transport of dissolved arsenic between zones has not likely occurred over any significant area. Short-circuiting through leaky bores cannot account for the regional-scale contamination of deep wells in the focus area given the distribution of the concentration data just described and sound well sealing practices described in documentation from the Division for Water Resources Planning and Investigation for the South of Vietnam (DWRPIS).

Although downward transport of contaminants from the near-surface can be excluded, deep pumping since the mid-90s has caused hydraulic heads in the deepest Pliocene-Miocene age aquifers to decline by several meters. Such head declines induce compaction, as water that previously supported the mineral structure is removed by pumping. Pumping-induced compaction is most pronounced in clays, far more compressible than sands, which are effectively squeezed during persistent over-exploitation of adjacent aquifers. Water expelled from compressible clays, including formations at depths of 100s of meters, has met a large portion of pumping demand in confined aquifer systems around the world, as evidenced by resulting land subsidence (Poland, 1984). During compaction due to pumping, dissolved arsenic and any other, potentially toxic, solutes stored in deep interbedded clays would be expelled into adjacent aquifers. Expelled solutes from clay could also include DOC (McMahon et

al., 1991) or competing ions that could promote arsenic dissolution or desorption within the aquifers.

According to the clay-compaction release mechanism, high densities of arsenic-contaminated wells should correspond to areas of significant cumulative pumping. Indeed, pumping rates among the 1365 wells in the deep zone of the focus area are much greater and the median age of wells is twice that of those within the 10 km surrounding buffer. Deep wells in this buffer (1218 total) largely have been installed since 1996 (see SI) and do not show arsenic (only 4 wells with arsenic >10 μg/L). This implies that prior to significant pumping lasting a decade or more, deep aquifers are not pervasively contaminated through in-situ processes or by solute diffusion out of interbedded clays. Rather, there is a likely ~10-year time lag before contaminant arrival at pumping wells, consistent with the requisite travel time between compacting clays and these wells.

We compute compaction rates within aquifers and confining beds of the focus area and surrounding region using 3D transient aquifer simulation. We recreate the spatially-explicit pumping history in each of the seven major aquifers according to 2007 pumping data from the DWRPIS. We assign typical low permeability values for interbedded clays along with high storage property values, which are known to be 1-2 orders of magnitude greater for clay than sand. The model is calibrated to fit the historical trends in hydraulic head data in all aquifers measured from 1996-2008 in nested monitoring wells across the region. Observed head declines in these wells of up to 74 cm/yr in the Delta and 230 cm/yr in HCMC are well reproduced by our model

(see SI). Our simulations indicate land subsidence rates in the focus area of 1.1-2.4 cm/yr, as pumping demand is met largely by water released from compacting clay storage. Simulated total subsidence is greater within the focus area (max: 27 cm) compared with adjacent areas owing to the greater pumping intensity of wells within it (Figure 3.2E). Pumping in HCMC, more than 50 km away, is not responsible for subsidence in the focus area. Measured hydraulic heads, InSAR-based subsidence estimates, and aquifer simulation all indicate that the effect of HCMC pumping is local.

Pumping-induced clay compaction is measurable as land subsidence. We measure land subsidence rates using interferometric synthetic aperture radar (InSAR) data collected by the PALSAR instrument aboard the ALOS satellite, since no ground-based measurement record is available. Two PALSAR tiles cover our study area and images of them were acquired over the period 2007-2010 every 2-12 months. We form interferograms from all pairs of scenes that span a 1-yr interval, selected to minimize seasonal effects, and average them to reduce atmospheric errors. Based on InSAR, subsidence is occurring at a rate of 1-3 cm/yr (~1.2-3.6 in the vertical assuming no horizontal deformation) relative to a coherent reference area near the Cambodian border and is highest in localized (1-3 km) subsidence bowls centered on many of the regions' small cities (Figure 3.4). Estimated errors in rates are spatially variable, ranging from ± 0.5-1 cm/yr (SI). Comparison of land subsidence rates based on InSAR and based on aquifer system simulation is shown in Figure 3.4.

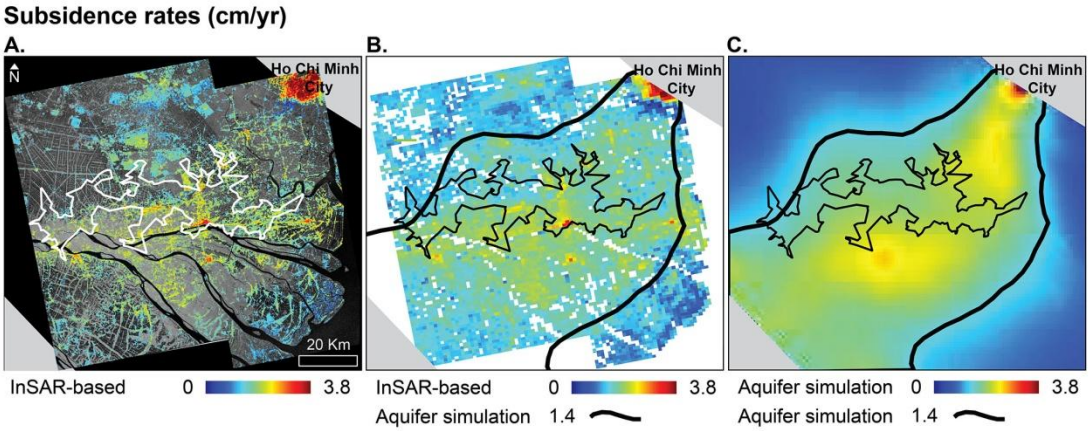


**Figure 3.4** **A.** 2007-2010 InSAR-based line of sight land subsidence rate with superimposed focus area outline (white). Areas of low correlation are excluded. Data from the Alaska Satellite Facility © JAXA, METI (2011). **B.** Comparison of subsidence rates derived from InSAR and aquifer simulation. **C.** Subsidence rates derived from aquifer simulation only. InSAR-based rates shown in B were upscaled to ~1km resolution using the median of values from the finer grid in A to facilitate comparison with the aquifer simulation results. Northeast and southwest corner areas fall outside of the aquifer simulation domain and are indicated in light gray.

Subsidence measured with InSAR is seen throughout the focus area and further extends to the north and south of it where either 1) we do not have arsenic measurements, or 2) wells have generally been pumping for less than 10 years. In the latter case, it appears that the onset of pumping-induced subsidence has begun, and arsenic transport to well screens may be in progress. Subsidence in HCMC is also evident. HCMC is, however, located outside of the Mekong floodplain such that provenance here differs from the Himalayan sediments responsible for most arsenic in wells of the Delta proper. Wells in the HCMC area are, not surprisingly, largely uncontaminated anywhere in the depth profile and it appears that the city's excessive pumping, while inducing subsidence, is therefore not causing release of arsenic from a deep source. Additional factors complicating the relationship between observed subsidence and arsenic occurrence may be related to the network of regional faults,

local depositional conditions and sulfide attenuation (Buschmann and Berg, 2009; Lowers et al., 2007).

The paleoclimatic record supports the occurrence of dissolved arsenic in deep clays. Holocene clays are known to maintain high concentrations of dissolved arsenic over millennia (Benner et al., 2008; Kocar et al., 2008). Modern climate features, notably tropical temperatures and precipitation, and high sea-levels, are conducive to sustaining the biogeochemical conditions that are favorable to arsenic dissolution within Holocene clays. The Pleistocene was marked by frequent glaciations that substantially lowered global sea-levels. In the Mekong Delta, dramatic changes occurred in vegetation types, flooding patterns, hydraulic gradients and mineral weathering (Bird et al., 2005; Heaney, 1991). Evidence of these changes is seen in the abundance of ferric (hydr)oxides that give Pleistocene sands in Bangladesh their oft-noted brown or orange color (Burgess et al., 2010; Fendorf et al., 2010; Zheng et al., 2005; Swartz et al., 2004; van Geen et al., 2003). These oxidized deposits have a higher capacity for arsenic sorption (Radloff et al., 2011; Stollenwerk et al., 2007; Harvey et al., 2002) and are associated with aquifers that are low in dissolved arsenic, which are found at greater depths in the Bengal Basin owing to higher sedimentation rates. In contrast to the Pleistocene in the Mekong Delta region, temperatures during the Pliocene-Miocene epochs were likely similar or elevated relative to the Holocene (Robinson et al., 2008; Heaney, 1991), suggesting biogeochemical conditions may also have been like those responsible for mobilizing arsenic in shallow clay today.

Through our analysis, we put forth a new conceptual model that describes the vertical distribution of arsenic seen in the Mekong Delta in terms of its historical development (Figure 3.5). From Miocene times to the present, fresh clays rich in arsenic and organic carbon were broadly deposited. Upon burial, solid-phase arsenic provided a persistent source that contaminated pore waters trapped in thick clay units. Over millions of years of deposition, dissolved arsenic concentrations in the pore fluids of more permeable aquifer sands were drawn to low levels by advection, mixing, and dilution. Concurrently, clays lost some of their original solute load to diffusion through the limited connected pore network. Slow diffusion out of occluded pores and slow dissolution and desorption of the persistent solid-phase arsenic supply (Kocar et al., 2008; Tufano et al., 2008), however, maintained a continuous dissolved arsenic load in deep clays, as found elsewhere in much older aquitards (>70 million years old (Yan et al., 2000)). When low-arsenic, deep aquifers were over-pumped during recent decades, clay compaction began, leading to water containing arsenic and possibly other, arsenic-mobilizing solutes being squeezed out of dead-flow storage in confining clays to adjacent aquifers, a process taking a decade or more.

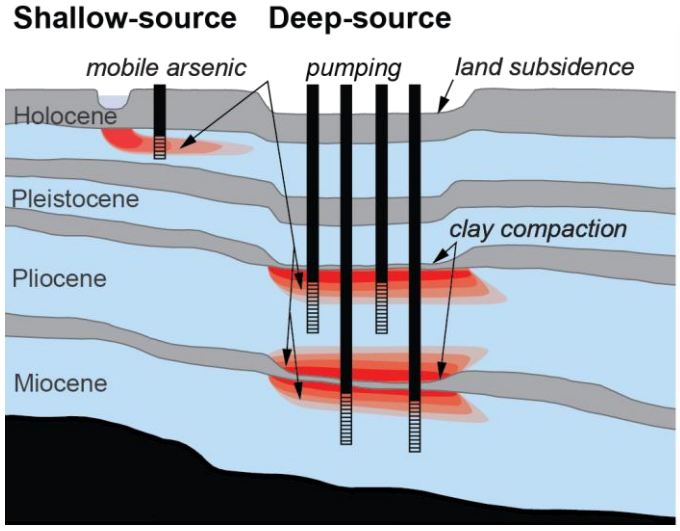


**Figure 3.5** Conceptual model for depth distribution of arsenic in groundwater.

The implication of these findings for the Mekong Delta region, and potentially other arsenic-prone aquifer systems like it, is that deep untreated groundwater is not a safe long-term water source. Deep wells that test clean upon installation, as do those bordering the focus area, may not remain arsenic-free over time as pumping promotes compaction and release of arsenic or arsenic-mobilizing solutes from deep clays. The potential for a deep source of arsenic, resulting from this unrecognized clay expulsion mechanism, should be considered as deep groundwater resources are further developed in these settings. In other confined aquifer systems around the world, solute release from compacting clays could also impact groundwater quality in as yet unknown ways.

Demand for deep groundwater is created by limited freshwater availability, avoiding arsenic contaminated shallow groundwater and non-potable surface water. However, deep groundwater exploitation in the Mekong Delta presents new potential hazards: land subsidence, saline intrusion, and human-induced arsenic contamination. Management of water resources in the complex, deltaic aquifer systems of South and Southeast Asia should seek to minimize human exposure to all relevant threats including, but not limited to, those due to arsenic. To reduce the impacts of arsenic contamination from deep groundwater extraction, water managers should consider a suite of measures. These include first understanding the nature and extent of deep groundwater arsenic, limiting intensive extraction, treating or blending extracted groundwater to meet health standards, and possibly screening pumping wells over intervals of deep aquifers that are distant from confining clays, among other water management strategies aimed at health-risk reduction.

## 3.4 Materials and Methods

Here we provide a summary of the data and methods used in the paper. Greater detail is provided in the Supporting Information (SI).

Arsenic data were acquired from the Department of Water Resources Management (DWRM) in Hanoi, Vietnam. Samples were collected according to national standard TCVN 4556-88 and analyzed in certified laboratories (Vietnam Laboratory Accreditation Scheme, VILAS) by hydride-generation atomic absorption spectroscopy (ISO 11969:1996). In the Mekong Delta, 50,532 wells were surveyed, of which 42,921 were considered, excluding samples with no recorded depth and very shallow ($\leq$10m), potentially open wells that may be exposed to surface conditions. Along with arsenic concentration measurements, depth and the GPS coordinates of each well, the year of installation was generally reported (202 missing values). Missing year of installation values were ignored in analyses involving well ages.

Ancillary hydrogeologic data were acquired from the DWRM and the Department of Water Resources Planning and Investigation for the South (DWRPIS) of Vietnam, Ho Chi Minh City, Vietnam. These include: 1) 10 stratigraphic cross-sections compiled from 81 well logs at ~20 km spacing including mapped geologic faults, originally interpreted by the Division for Geological Mapping for the South of Vietnam, 2) pumping rates in 22 districts, specific to the 6 major pumped aquifers (excluding the Holocene aquifer), from a 2007 survey of 5,282 wells, classified by purpose of water use, 3) transient hydraulic head data from 45 nested monitoring

wells, measured monthly over the period 1996-2008, and 4) hydraulic head maps for the years 1987 (Nguyen, 1987) and 2004 (provided by DWRM).

The 3D extents of the major aquifer and confining units were determined based on the well logs and cross-sections. Clay pods embedded within aquifers appear to be discontinuous and were ignored in the interpolation of the major hydrogeologic unit boundaries and subsequent regional groundwater and subsidence simulations. Each data point in the DWRM survey was assigned to an aquifer according to its latitude, longitude and well screen elevation, taken as the well's recorded depth relative to the STRM 90m DEM.

Estimates of vertical flow between zones of the focus area were made for all 1km$^2$ cells within it. We considered the shortest reasonable distance through which shallow contamination could have been transported to depth: the middle of the Upper Pleistocene aquifer (the most shallow of three Pleistocene aquifers), where the bulk of shallow zone wells are found, to the top of the deep zone (i.e., the top of the Upper Pliocene aquifer). For each cell of the focus area, the effective hydraulic conductivity ($K_{effective}$) over this minimum transport distance was calculated using the harmonic mean of the (n) layer conductivities, scaled by their thicknesses ($b$) as follows:

$$K_{effective} = \frac{\sum_{1}^{n} b_n}{\sum_{1}^{n} \frac{b_n}{K_n}} \qquad \textit{Eq. 3.1}$$

where *n* is the number of layers. Hydraulic conductivity values for each layer type were initially chosen from well construction specification materials acquired from the DWRPIS (for aquifer type) and literature values (for confining unit type) and updated after calibrating the groundwater flow model (described below). Velocity, *v*, in each cell was calculated by Darcy's law for flow through porous media:

$$v = -\frac{K_{effective} I}{\theta} \qquad \textit{Eq. 3.2}$$

where $K_{effective}$ is the effective hydraulic conductivity defined above, $I$ is the vertical hydraulic gradient component and $\theta$ is the effective porosity, taken as the mean of literature values for the two materials, weighted by their relative thicknesses. The average gradient between the Upper Pleistocene and Upper Pliocene aquifers was calculated over two periods determined by data availability: 1987-1997 and 1997-2005. All parameters for the vertical flow calculations are provided in the SI.

Groundwater flow simulation was conducted using the US Geological Survey's vetted software MODFLOW-2005. The Interbed Storage (IBS1) package for MODFLOW was used to simulate compaction and land subsidence according to:

$$\Delta b = S_s b \Delta h \qquad \textit{Eq. 3.3}$$

where $S_s$ is specific storage, $b$ is thickness, and $\Delta h$ is the temporal change in local hydraulic head values. Details of the model discretization, boundary conditions, assignment of pumping conditions, and calibration to monitoring well data in the seven major aquifers considered are provided in the SI.

Radar imagery was acquired by the Alaska Satellite Facility (ASF) from the Japanese Aerospace Exploration Agency (JAXA) for UPASS proposal ID: 589. Data were collected by the PALSAR instrument, a phased array L-band synthetic aperture radar (23.6 cm wavelength) carried on the ALOS satellite, which has a 46 day repeat period. A total of 39 images covering the 2 tiles were analyzed. Interferograms were formed using a geodetically accurate, motion-compensating InSAR processor (Zebker et al., 2010). Elevation correction, negligible in this nearly flat landscape, was made using the SRTM 90m DEM. Results were resampled to a final resolution of ~60m**.** Orbital ramps were removed from interferograms by subtraction of a linear phase plane. The average phase was computed on coregistered stacks of all available 1-yr interval interferograms. The stacking procedure was justified by inspection of the nested hydraulic head data, which consistently show linear average annual declines: stationary subsidence rates are expected.

InSAR-based subsidence rates were retained only for areas in the landscape with high correlation (a measure of radar signal quality), namely developed areas that are elevated above the floodplain. Errors were estimated by taking the standard deviation of the stacked phase in 400-pixel windows and range from ± 0.5-1.0 cm, with lowest errors in highly urbanized, radar bright areas (see SI). All subsidence rates and error estimates are reported in the satellite's line-of-sight direction, which is approximately equivalent to, if slightly less than, the vertical rate.

**Acknowledgments**

We thank the Department of Water Resources Management, Hanoi, for the arsenic data, the Department of Water Resources Planning and Investigation for the South of Vietnam for hydrogeologic datasets, and ASF, JAXA and NASA for SAR data. We thank Y. Chen and C. Wortham for InSAR processing advice and Professor C. Harvey at MIT for his review. We gratefully acknowledge the UPS Endowment Fund and the Global Freshwater Initiative of the Woods Institute for the Environment at Stanford. This work is being supported by the National Science Foundation under grant EAR-1313518 to Stanford University. Any opinions, findings, and conclusions or recommendations expressed in this material are those of the authors and do not necessarily reflect the views of the National Science Foundation.

## 3.5 Supporting Information

This supplement provides additional details on the materials and methods used to support the results in the manuscript *Release of arsenic to deep groundwater in the Mekong Delta, Vietnam, linked to pumping-induced land subsidence.*

### *3.5.1 Data analysis*

Key statistics for wells in shallow and deep zones (horizons) of the focus area referenced in the manuscript are summarized in Table 3.1.

**All Wells**

| Zone | Number | Mean depth (m) | Median As (µg/L) | Mean As (µg/L) | Max As (µg/L) |
|---|---|---|---|---|---|
| Shallow | 1798 | 51 | 0 | 4 | 300 |
| Deep | 1365 | 309 | 20 | 20 | 500 |

**Wells with As>10 µg/L**

| Zone | Number | Mean depth (m) | Median As (µg/L) | Mean As (µg/L) | Fraction of total wells |
|---|---|---|---|---|---|
| Shallow | 170 | 60 | 25 | 35 | 0.09 |
| Deep | 889 | 316 | 25 | 28 | 0.65 |

**Table 3.1** Summary statistics for wells in the shallow and deep focus area zones. There are 48 wells in focus area with depth $\leq$10m (not considered) with a mean arsenic concentration of 5 µg/L (max: 50 µg/L).

### *3.5.2 Vertical flow calculations*

Vertical flow through the multi-layered aquifer system within the focus area was calculated using Darcy's Law for flow through porous media as discussed in the Materials and Methods section of the manuscript. The distributions of parameters and velocity estimates referenced to in the manuscript are summarized in Table 3.2.

| **Parameters and vertical flow estimates** | **Units** | **Min** | **Median** | **Max** |
|---|---|---|---|---|
| Total clay thickness | *(m)* | 12 | 39 | 74 |
| Total sand thickness | *(m)* | 39 | 61 | 73 |
| Effective vertical hydraulic conductivity ($K_{effective}$) | *(m/yr)* | 0.61 | 0.77 | 2.0 |
| Effective porosity ($\theta_{effective}$) | *[-]* | 0.15 | 0.17 | 0.22 |
| Hydraulic gradient: 1987 – 1997 | *[-]* | -0.0013 | 0.0016 | 0.0054 |
| Hydraulic gradient: 1997 – 2005 | *[-]* | -0.017 | -0.0086 | -0.0034 |
| Vertical downward velocity: 1987 – 1997 | *(m/yr)* | -0.038 | 0.0071 | 0.010 |
| Vertical downward velocity: 1997 – 2005 | *(m/yr)* | 0.014 | 0.039 | 0.16 |
| Vertical transport distance: 1987 – 2005 | *(m)* | -0.06 | 0.24 | 1.34 |
| Fraction of total distance traveled: 1987- 2005 | *[-]* | -0.00043 | .0024 | 0.017 |

**Table 3.2:** Range of parameters used in the calculation of vertical flow between zones of the focus area. Positive gradients indicate a driving force for (upward) flow towards the surface, positive velocities indicate flow towards the deep zone. Total distance between zones refers to the distance between the middle of the Upper Pleistocene aquifer and the top of the Upper Pliocene aquifer (total distance ranges from 71m to 147m), as described in the manuscript.

It is important to note that these vertical flow calculations apply only to flow through the entire system of aquifers and confining units (aquitards) between focus area zones. The above results cannot be used to assess vertical velocities within a given aquifer, for example between a confining layer and the screen of a pumping well below. Within an aquifer, a pumping well induces largely horizontal flow, with very

high vertical rates in its immediate vicinity (a region of 10s of meters depending on pumping rate). In contrast, the slow vertical flow rates in the system as a whole are largely determined by the configuration of confining units.

Expedited flow through leaky well bores does not have regional significance. Well construction documentation provided by the Department of Water Resources Planning and Investigation for the South of Vietnam (DWRPIS) details the back-filling of well bores with bentonite clay, a practice which provides excellent sealing and prevention of short-circuiting flow through the bore from overlying units. Deep wells are drilled at increased expense to provide either higher quality water (at the time of installation) or improved yield, thus the practice of adequate sealing is likely well followed. While the presence of some leaky bores in the focus area cannot be ruled out, neither can they explain pervasive contamination over this large region, given the diminished contaminant burden of the shallow zone compared with the deep (see Figure 3.2 of main text and Table 3.1).

### *3.5.3 Simulation of the aquifer - clay confining bed system mechanics*

Spatially and temporally-explicit accounting of the compaction process requires numerical modeling. Aquifer simulation was conducted using the US Geological Survey's vetted software MODFLOW-2005. The Interbed Storage (IBS1) package for MODFLOW was used to simulate compaction and land subsidence according to Eq. 3.3 (see main text for details). A schematic representation of the model and locations of monitoring wells used to calibrate it is shown in Figure 3.6.

To represent the head distribution that develops within clays during compaction, each confining unit was discretized using 5 vertical cells. The top model layer was assigned a specified head boundary condition set to the average annual head (variable over space but constant over time) of the semi-confined Holocene aquifer, in accordance with data indicating heads are generally constant over time in this aquifer. All lateral and bottom boundaries were modeled with a zero gradient boundary condition representing no-flow based on interpretation of the bedrock geometry, the locations of faults and symmetry flow boundaries. The diagonal boundaries in Figure 3.6, *Right* are symmetry boundaries, the remainder were positioned as termination strips after testing that specified heads applied to them produced negligible fluxes. Although no monitoring well nests are located in the focus area, head data at the 10 available nests show substantial head changes over time due to pumping, as shown presently.

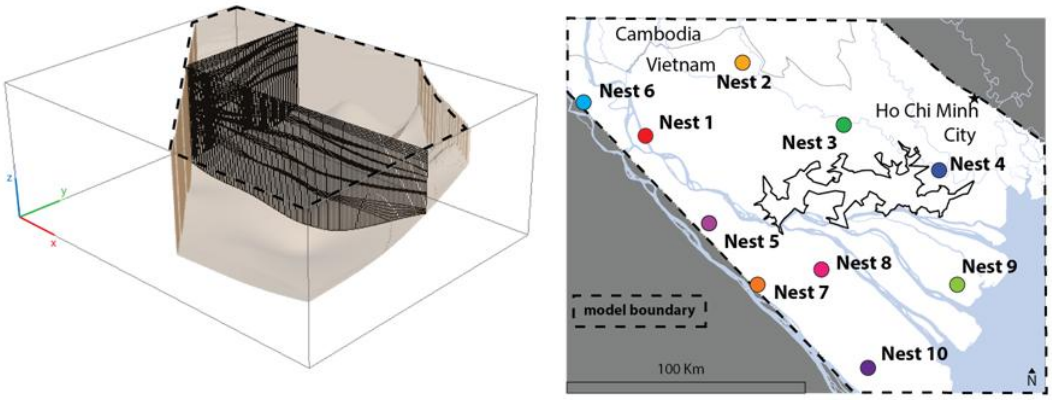


**Figure 3.6** Active domain of groundwater flow model with typical cross-sections (left) and locations of monitoring well nests (right). The outline of the focus area is shown in black.

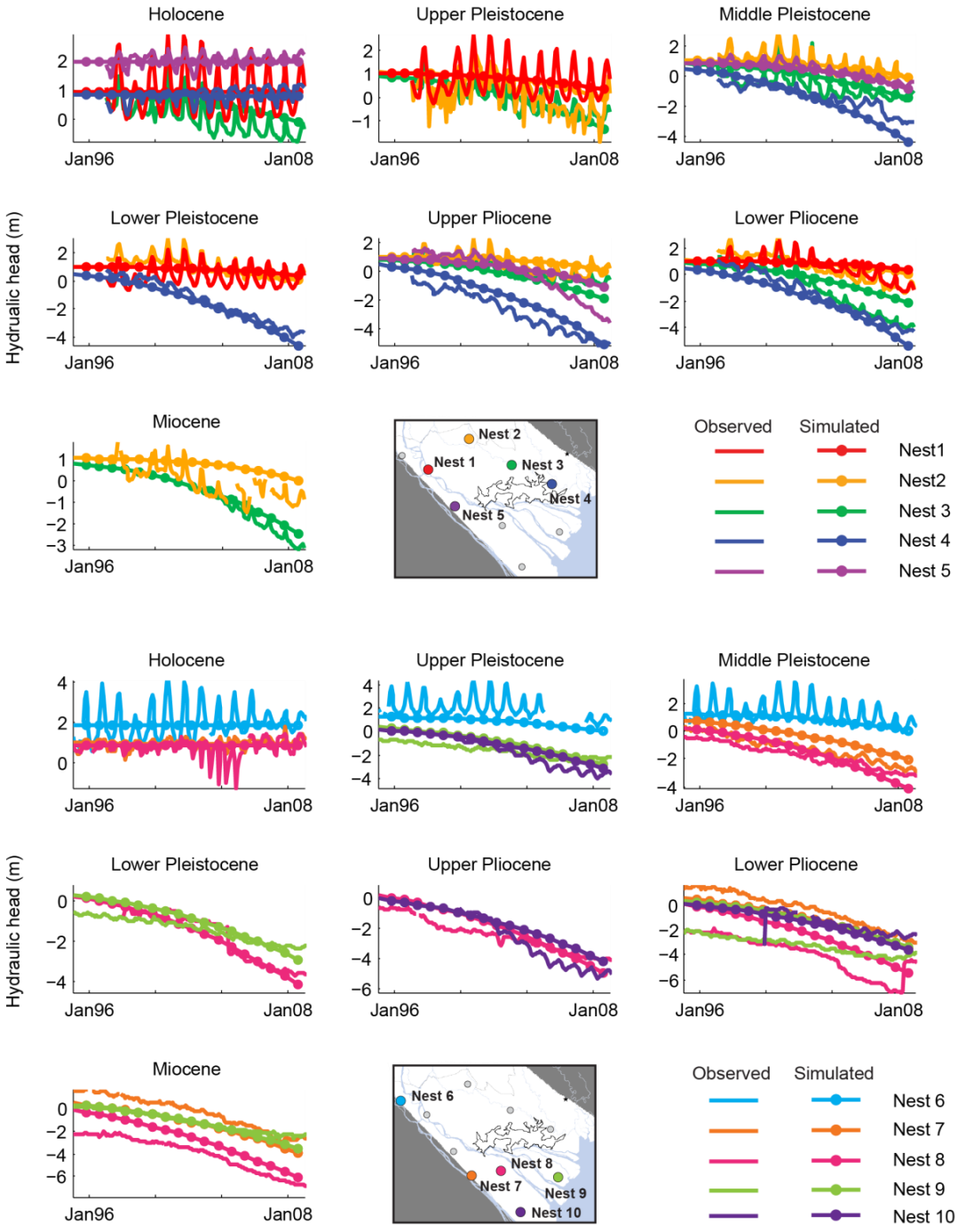


**Figure 3.7** Observed and simulated hydraulic heads for monitoring wells in the Mekong Delta. For clarity, graphs are displayed separately for well nests 1-5 and 6-10.

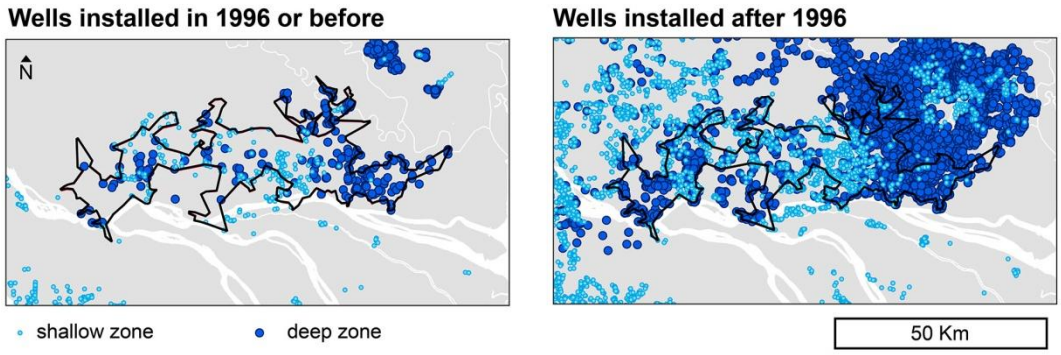


**Figure 3.8** Well installations over time in shallow and deep zones within and around the focus area.

Five parameters were used to fit the model (Table 3.3), derived from literature values and well construction information from the DWRPIS, which specifies that Mekong Delta wells are designed for aquifer conductivities ranging from 2-70 m/d. Both aquifers and confining units were each assumed to be homogeneous, respectively, and assigned the same hydraulic conductivities for aquifer and confining layers except for one near-surface clay layer given a lower hydraulic conductivity. This less permeable layer was used, in conjunction with the surficial specified head boundary, to maintain the stable heads in the Holocene aquifer while allowing Upper Pleistocene aquifer heads to drop in accordance with head data (see Figure 3.7). Aquifers were assigned a hydraulic conductivity anisotropy ratio of 10:1 (horizontal : vertical hydraulic conductivity). Specific storage values were assigned as constants across hydraulic layer type: one value for aquifers and another for confining units. These two storage parameters were calibrated to fit the transient nested head data. All parameters are within the range of typical literature values for regional systems.

| Parameter Number | Description | Units | Value |
|---|---|---|---|
| 1 | Confining layer hydraulic conductivity | *m/d* | $8.64 \times 10^{-4}$ |
| 2 | Low permeable layer hydraulic | *m/d* | $8.64 \times 10^{-6}$ |
| 3 | Aquifer layer horizontal hydraulic | *m/d* | 20 |
| 4 | Confining bed specific storage | $m^{-1}$ | $2 \times 10^{-4}$ |
| 5 | Aquifer layer specific storage | $m^{-1}$ | $2 \times 10^{-5}$ |

**Table 3.3** Groundwater flow model parameter values

The model was run to establish an initial steady state followed by ten 2-yr transient stress periods representing the interval 1988 – 2008. Pumping was assigned as follows: for districts where 2007 pumping data were available in the DWRPIS survey, these district/aquifer-specific rates were distributed according to the locations of wells in the DWRM's arsenic survey. Each model cell where DWRM wells were found was given the district/aquifer-specific unit pumping rate, initiated in the well installation year.

In many districts towards the Southeast of the model domain, there are no deep wells in the DWRM survey, though hydraulic head data indicate significant declines that cannot be reproduced by pumping only in districts where wells are found. Many of these same districts do not have shallow wells either, suggesting some districts were wholly unreported in the DWRM survey. In these cases, the average number of wells found in each aquifer of reporting districts was used, and well locations and installation years were distributed within the districts.

The DWRPIS survey recorded negligible extraction rates in the shallow Holocene and Pleistocene aquifers in the overwhelming majority of districts, despite

the abundance of wells measured in the DWRM arsenic survey in these same areas. Shallow wells from the DWRM survey that mapped to DWRPIS district/aquifer-specific unit rates of zero were assigned a nominal rate of 10 $m^3$/d (compared with 20-404 $m^3$/d, mean of 63 $m^3$/d, for the unit rate where non-zero pumping rates were recorded).

For districts where pumping data were not available, relationships between 2004 population density (GSO, 2006) and total district pumping rate were used to estimate rates:

For low population density districts (<1500 persons/sq km), the district groundwater extraction rate (DGER, $m^3$/d):

$$DGER = 25.258 \times Population\_Density_{2004} \quad (r^2 = 0.58)$$

Else, for high population districts:

$$DGER = 12372 \times e^{(0.0004 * Population\_Density2004)} \quad (r^2 = 0.92)$$

Rates for districts without pumping data were further adjusted to conform to trends in monitoring well data. This multi-faceted approach of assigning pumping to wells is used to realistically represent the observed effects of increased pumping over 3D space and time.

The model was calibrated to fit 1) the general trends in hydraulic head data across the region and among aquifers and 2) InSAR-derived subsidence rates. Comparisons between observed and simulated heads in the Delta, based on data from

the DWRPIS, are shown in Figure 3.7, separated into two plots for no other reason than improved display of the numerous plotted points. The observed annual average maximum drawdown is 6.62 m below sea level. The absolute discrepancy between annual average observed and simulated heads for all wells is 0.60 m (mean), 0.47 m (median), and for the subset of wells in the deep Pliocene-Miocene aquifers it is 0.86 m (mean), 0.72 m (median).

The match for HCMC is based on total drawdown and rates of head decline reported in 2004 aquifer-specific maps provided by the DWRM. This match, not shown, is considered an approximation that is independently supported by the InSAR-based subsidence rates. In HCMC, drawdown is much greater (21.7 m below sea level) than in the Delta. Hydraulic heads in HCMC were reproduced to within 20% (mean) and 7% (median), but compared to the Delta the absolute deviation was larger, 1.79 m (mean), 1.12 m (median). Measured hydraulic heads, InSAR-based subsidence estimates, and aquifer simulation all indicate that HCMC pumping does not affect subsidence in the focus area. Comparisons between InSAR-derived subsidence rates and those simulated with the aquifer model are shown in the manuscript.

### *3.5.4 InSAR-based land subsidence estimates*

Interferograms were formed from the scenes listed in Table 3.4. The average phase was computed on coregistered stacks of all available 1-yr interval interferograms. The choice of anniversary-length interferograms limited the effects of seasonal variability in scattering properties of the surface and subsidence rates. Use of

a single year interval was found to minimize the effects of temporal decorrelation and maximize the subsidence signal and number of total pairs that could be formed with available data. Interferograms were stacked (i.e., averaged) to minimize the influence of atmospheric effects, which can cause phase delays in the return signal that cannot be accurately quantified without independent ground-based GPS measurements. Stacking reduces noise by the square root of the number of interferograms in the stack. The stacking procedure was justified by inspection of the nested hydraulic head data, which consistently show linear average annual declines: stationary subsidence rates are expected.

| **Stack 1: Western Scene** | | **Stack 2: Eastern Scene** | |
|---|---|---|---|
| *Image 1* | *Image 2* | *Image 1* | *Image 2* |
| 7-Feb-07 | 10-Feb-08 | 21-Jan-07 | 24-Jan-08 |
| 10-Aug-07 | 12-Aug-08 | 24-Jan-08 | 26-Jan-09 |
| 25-Sep-07 | 27-Sep-08 | 11-Dec-08 | 14-Dec-09 |
| 10-Nov-07 | 12-Nov-08 | 26-Jan-09 | 29-Jan-10 |
| 10-Feb-08 | 12-Feb-09 | 13-Jun-09 | 16-Jun-10 |
| 27-Jun-08 | 30-Jun-09 | | |
| 12-Aug-08 | 15-Aug-09 | | |
| 12-Nov-08 | 15-Nov-09 | | |
| 28-Dec-08 | 31-Dec-09 | | |
| 12-Feb-09 | 15-Feb-10 | | |
| 15-Aug-09 | 18-Aug-10 | | |
| 15-Nov-09 | 18-Nov-10 | | |

**Table 3.4** Collection dates of data used in InSAR stacks

InSAR-based subsidence rates were retained only for areas in the landscape returning high quality signal, namely developed areas that are elevated above the

floodplain. As such, they are not influenced by changes in flood-controlled sedimentation rates that may have occurred. Reliable signal was defined by visual inspection of changes in the interferometric correlation across the scene. In rural areas, paddy fields were found to have similarly low phase correlation as open water, rendering subsidence measurements meaningless. In contrast, the extensive network of built up towns, levees, roadways and cities returned signal with substantially higher correlation. A threshold value for the average correlation of stacked interferograms of 0.15 was found to readily distinguish low-correlation agricultural areas from the built-up network. Subsidence estimates were only retained for pixels exceeding the correlation threshold. Errors were estimated by taking the standard deviation of the stacked phase in 400-pixel windows and range from ± 0.5-1.0cm, with lowest errors in highly urbanized, radar bright areas. All subsidence rates and error estimates are reported are in the satellite's line-of-sight direction, which is approximately equivalent to, if slightly less than, the vertical rate.

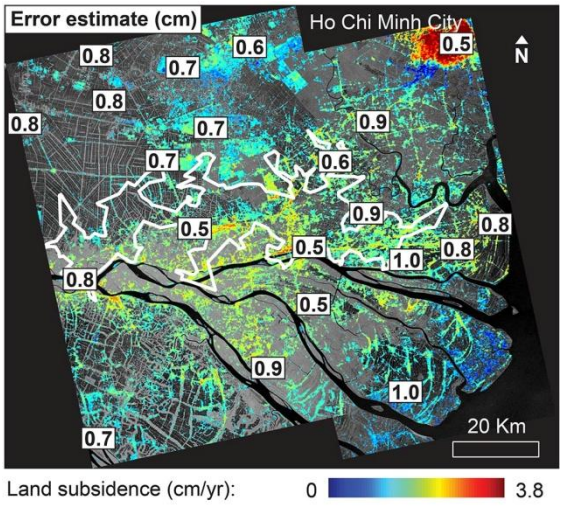


**Figure 3.9**. Error estimates for InSAR stacks superimposed on land subsidence map shown in main text (Fig. 3.4 A). Values are the standard deviation of the stacked interferometric phase in 400-pixel windows, over which the labels are placed.

## References


Benner, S. G., Polizzotto, M. L., Kocar, B. D., Ganguly, S., Phan, K., Ouch, K., Sampson, M., and Fendorf, S. (2008). Groundwater flow in an arsenic-contaminated aquifer, Mekong Delta, Cambodia. *Applied Geochemistry*, 23(11), 3072–3087.

Berg, M., Stengel, C., Trang, P. T.K., Pham, H.V., Sampson, ML, Leng, M., Samreth, S. and Fredericks, D. (2007). Magnitude of arsenic pollution in the Mekong and Red River Deltas—Cambodia and Vietnam. *Science of the Total Environment*, 372(2-3), 413–425.

Bird, M. I., Taylor, D., and Hunt, C. (2005). Palaeoenvironments of insular Southeast Asia during the Last Glacial Period: a savanna corridor in Sundaland? *Quaternary Science Reviews*, 24(20-21), 2228–2242.

Burgess, W. G., Hoque, M. A., Michael, H. A., Voss, C. I., Breit, G. N., and Ahmed, K. M. (2010). Vulnerability of deep groundwater in the Bengal Aquifer System to contamination by arsenic. *Nature Geoscience*, 3, 83–87. doi:10.1038/ngeo750.

Buschmann, J. and Berg, M. (2009). Impact of sulfate reduction on the scale of arsenic contamination in groundwater of the Mekong, Bengal and Red River deltas. *Applied Geochemistry*, 24, 1278–1286.

Buschmann, J., Berg, M., Stengel, C., and Sampson, M. L. (2007). Arsenic and manganese contamination of drinking water resources in Cambodia: coincidence of risk areas with low relief topography. *Environmental science & technology*, 41(7), 2146–2152.

Downey, P. (2008). Dig deep to avoid arsenic. *In This Issue: Proceedings of the National Academy of Sciences*, 105(25), 8483–8802.

Fendorf, S., Michael, H. A., and van Geen, A. (2010). Spatial and Temporal Variations of Groundwater Arsenic in South and Southeast Asia. *Science*, 328(5982), 1123–1127. doi:10.1126/science.1172974.

General Statistics Office (2006). Socio-Economic Statistical Data of 671 Districts, Towns and Cities Under the Authority of Provinces In Vietnam. Hanoi, Vietnam.

Harvey, C. F., Swartz, C.H., Badruzzaman, A.B.M., Keon-Blute, N., Yu, W., Ali, M.A., Jay, J., Beckie, R., Niedan, V., Brabander, D., Oates, P., Ashfaque, K.N., Islam, S. Hemond, H.F., and Ahmed, M.F. (2002). Arsenic Mobility and Groundwater Extraction in Bangladesh. *Science*, 298(5598), 1602–1606. doi:10.1126/science.1076978.

Heaney, L. R. (1991). A synopsis of climatic and vegetational change in Southeast Asia. *Climatic Change*, 19(1), 53–61.

Hoang, T. H., Bang, S., Kim, K. W., Nguyen, M. H., and Dang, D. M. (2010). Arsenic in groundwater and sediment in the Mekong River delta, Vietnam. *Environmental Pollution*, 158(8), 2648–2658.

Kocar, B. D., Polizzotto, M. L., Benner, S. G., Ying, S. C., Ung, M., Ouch, K., Samreth, S., Suy, B., Phan, K., Sampson, M. and Fendorf, S. (2008). Integrated biogeochemical and hydrologic processes driving arsenic release from shallow sediments to groundwaters of the Mekong delta. *Applied Geochemistry*, 23(11), 3059–3071.

Lowers, H. A., Breit, G. N., Foster, A. L., Whitney, J., Yount, J., Uddin, M. N., and Muneem, A. A. (2007). Arsenic incorporation into authigenic pyrite, Bengal Basin sediment, Bangladesh. *Geochimica et cosmochimica acta*, 71(11), 2699–2717.

McMahon, P. B. and Chapelle, F. H. (1991). Microbial production of organic acids in aquitard sediments and its role in aquifer geochemistry. *Nature*, 349(17), 233–235.

Michael, H. A. and Voss, C. I. (2008). Evaluation of the sustainability of deep groundwater as an arsenic-safe resource in the Bengal Basin. *Proceedings of the National Academy of Sciences*, 105(25), 8531–8536.

Mukherjee, A., Fryar, A. E., Scanlon, B. R., Bhattacharya, P., and Bhattacharya, A. (2011). Elevated arsenic in deeper groundwater of the western Bengal basin, India: Extent and controls from regional to local scale. *Applied Geochemistry*, 26(4), 600–613.

Neumann, R. B., Ashfaque, K. N., Badruzzaman, A. B. M., Ashraf Ali, M., Shoemaker, J. K., and Harvey, C. F. (2009). Anthropogenic influences on groundwater arsenic concentrations in Bangladesh. *Nature Geoscience*. doi:10.1038/ngeo685.

Nguyen, K. P. and Itoi, R. (2009). Source and release mechanism of arsenic in aquifers of the Mekong Delta, Vietnam. *Journal of Contaminant Hydrology*, 103(1-2), 58–69. doi:10.1016/j.jconhyd.2008.09.005.

Nguyen, V. C. (1987). Hydrogeological map of Vietnam. *General Department of Geology.* Hanoi.

Poland. (1984). *Guidebook to studies of land subsidence due to ground-water withdrawal* (Vol. 40). UNESCO.

Polizzotto, M. L., Harvey, C. F., Sutton, S. R., and Fendorf, S. (2005). Processes conducive to the release and transport of arsenic into aquifers of Bangladesh. *Proceedings of the National Academy of Sciences*, 102(52), 18819-18823.

Postma, D., Larsen, F., Thai, N. T., Trang, P. T. K., Jakobsen, R., Nhan, P. Q., Tran, V.L., Pham, H.V. and Murray, A. S. (2012). Groundwater arsenic concentrations in Vietnam controlled by sediment age. *Nature Geoscience*. doi:10.1038/ngeo1540.

Radloff, K. A., Zheng, Y., Michael, H. A., Stute, M., Bostick, B. C., Mihajlov, I., Bounds, M., Huq, M. R., Choudhury, I., Rahman, M. W. Schlosser, P., Ahmed, K. M., and van Geen, A. (2011). Arsenic migration to deep groundwater in Bangladesh influenced by adsorption and water demand. *Nature Geoscience*, 4(11), 793–798. doi:10.1038/ngeo1283.

Ravenscroft P, Brammer H, and Richards K. (2009) *Arsenic Pollution: A Global Synthesis.* (RGS-IBG Book Series, Wiley-Blackwell Chichester, U.K.

Robinson, M. M., Chandler, M. A., and Dowsett, H. J. (2008). Pliocene role in assessing future climate impacts. *Eos Trans. AGU*, 89(49), 501-503.

Smedley, P. and Kinniburgh, D. (2002). A review of the source, behaviour and distribution of arsenic in natural waters. *Applied Geochemistry*, 17(5), 517–568. doi:10.1016/S0883-2927(02)00018-5.

Smith, A. H., Lingas, E. O., and Rahman, M. (2000). Contamination of drinking-water by arsenic in Bangladesh: a public health emergency. *Bulletin of the World Health Organization*, 78, 1093–1103.

Stanger, G., To, T.V., Ngoc, K. S. L. T. M., Luyen, T. V., and Thanh, T. T. (2005). Arsenic in groundwaters of the Lower Mekong. *Environmental Geochemistry and Health*, 27(4), 341–357. doi:10.1007/s10653-005-3991-x.

Stollenwerk, K. G., Breit, G. N., Welch, A. H., Yount, J. C., Whitney, J. W., Foster, A. L., Uddin, M. N., Majumder, R. K., and Ahmed, N. (2007). Arsenic attenuation by oxidized aquifer sediments in Bangladesh. *Science of the Total Environment*, 379(2-3), 133–150.

Swartz, C. H., Blute, N. K., Badruzzman, B., Ali, A., Brabander, D., Jay, J., Besancon, J., Islam, S., Hemond, H. F., and Harvey, C. F. (2004). Mobility of arsenic in a Bangladesh aquifer: Inferences from geochemical profiles, leaching data, and mineralogical characterization. *Geochimica et Cosmochimica Acta*, 68(22), 4539–4557.

Tufano, K. J., Reyes, C., Saltikov, C. W., and Fendorf, S. (2008). Reductive Processes Controlling Arsenic Retention: Revealing the Relative Importance of Iron and Arsenic Reduction. *Environmental Science & Technology*, 42(22), 8283–8289. doi:10.1021/es801059s.

van Geen, A., Zheng, Y., Versteeg, R., Stute, M., Horneman, A., Dhar, R., Steckler, M., Gelman, A., Small, C., Ahsan, H., Graziano, J.H., Hussain, I., and Ahmed, K.M. (2003). Spatial variability of arsenic in 6000 tube wells in a 25 km2 area of Bangladesh. *Water Resources Research*, 39(5), 1140. doi:10.1029/2002WR001617.

Winkel, L. H., Pham T.K.T., Vi., M.L., Stengel, C., Amini, M., Nguyen, T.H., Pham, H.V., and Berg, M. (2011). Arsenic pollution of groundwater in Vietnam exacerbated by deep aquifer exploitation for more than a century. *Proceedings of the National Academy of Sciences*, 108(4), 1246–1251.

Yan, X. P., Kerrich, R., and Hendry, M. J. (2000). Distribution of arsenic (III), arsenic (V) and total inorganic arsenic in porewaters from a thick till and clay-rich aquitard sequence, Saskatchewan, Canada. *Geochimica et Cosmochimica Acta*, 64(15), 2637–2648.

Zebker, H. A., Hensley, S., Shanker, P., and Wortham, C. (2010). Geodetically Accurate InSAR Data Processor. *IEEE Transactions on Geoscience and Remote Sensing*, 48, 4309–4321. doi:10.1109/TGRS.2010.2051333.

Zheng, Y., van Geen, A., Stute, M., Dhar, R., Mo, Z., Cheng, Z., Horneman, A., Gavrieli, I., Simpson, H.J., Versteeg, R., Steckler, M., Grazioli-Venier, A., Goodbred, M.S., Shamsudduha, M., Hoque, M.A., and Ahmed, K.M. (2005). Geochemical and hydrogeological contrasts between shallow and deeper aquifers in two villages of Araihazar, Bangladesh: Implications for deeper aquifers as drinking water sources. *Geochimica et Cosmochimica Acta*, 69(22), 5203–5218. doi:10.1016/j.gca.2005.06.001.

# 4 Pumping-induced regional land subsidence in the Mekong Delta detected using InSAR

## 4.1 Abstract

In the Mekong Delta, Vietnam, the recent rise in groundwater exploitation is causing widespread overdraft. We show that steadily declining hydraulic heads in multiple aquifers has created large regional land subsidence. Pumping-induced subsidence is particularly concerning in the Delta, which lies <2m above sea level and where a dense and largely agrarian population already faces widespread annual flooding and saline surface water intrusion. We present the first estimates of Delta-wide land subsidence based on stacking of 78 interferograms made from ALOS PALSAR acquisitions spanning 2006-2010. Subsidence of ~1-4 cm/yr occurs in large regions (1000s of $km^2$) where measured groundwater overdraft is also occurring. InSAR-based subsidence rates agree with expected rates based on mechanistic calculations of media compaction at monitoring well locations throughout the Delta. Subsidence is most pronounced in urbanized areas. In rural areas, coherent radar signal is preserved, despite the abundance of paddy and water bodies, by the network of levees, roads and otherwise built-up areas. We further demonstrate the successful use of interferometric synthetic aperture radar (InSAR) in a landscape that is especially challenging to study using this method.

## 4.2 Introduction

In the Mekong Delta, shared by Cambodia and Vietnam, groundwater exploitation has increased dramatically in recent decades. Today groundwater is widely used to meet domestic, agricultural, and industrial needs, causing hydraulic heads to steadily decline in many aquifers over extensive regions (DWRPIS, 2010). This trend is likely to continue in future years owing to rising demand for groundwater and ineffectual regulatory systems (Wagner et al., 2012). Over-exploitation of groundwater exposes the Delta's densely settled population of >20 million to a variety of hazards associated with naturally-occurring arsenic contamination (Erban et al., 2013), subsurface saline intrusion (Bear et al., 1999) and land subsidence (Poland, 1984).

Pumping-induced land subsidence has been observed in unconsolidated aquifer systems around the world (reviews include Galloway and Burbey, 2011; Poland, 1984). In regions with extensive confined aquifers, where productive aquifers are capped by much less permeable layers, storage of groundwater within the sediment structure meets a significant portion of pumping demand. Pumping lowers pore-water pressure, increasing the stress borne by the solid media and causing expulsion of water from storage in compressible sediments as they undergo compaction. Sediment compressibility tends to be highest in interbedded clay layers, common in deltaic settings, from which a high proportion of pumped water is withdrawn. The depth of water removed from storage, i.e., the pumped volume in a given area, is equivalent to the amount of land subsidence at the surface. Measurements of land subsidence can

be made locally using ground-based methods, but remotely-sensed observations are essential for spatially comprehensive analysis over large regions, particularly where ground-based measurements are absent.

Regional deformation of the land surface is often measured remotely using satellite-based synthetic aperture radar (SAR) imagery processed by interferometry, or InSAR. InSAR has been used to study many types of surface deformation including ice flows, tectonic slip, volcanic activities and land subsidence due to the extraction groundwater and oil (Chaussard et al., 2013; Chatterjee et al., 2006; Buckley et al., 2003; Colesanti et al., 2003; Bawden et al., 2001; Hoffmann et al., 2001; Amelung et al., 1999; Fielding et al., 1998; Galloway et al., 1998). Studies use a variety of available satellite data, from SAR instruments imaging at various wavelengths ($\lambda$), to examine processes that occur over different time periods and landscapes. To quantify recent land subsidence in the agriculture-dominated Mekong Delta, the L-Band PALSAR instrument ($\lambda$ = 23.6 cm) aboard ALOS-1 (2006-2011) offers the best data product.

This study is the first to estimate land subsidence rates throughout the Mekong Delta using InSAR and relate them to rates of groundwater overdraft and aquifer system properties. The Delta is an especially challenging region to study by InSAR due to widespread crop cover and annual flooding that interfere with back-scattering of radar signal. We estimate annual average rates of subsidence for a majority of the Delta (including both Cambodia and Vietnam) where data are available over the 2006-2010 period using interferograms formed from ALOS-1 PALSAR acquisitions. We

show that spatial patterns of InSAR-based subsidence rates are consistent with patterns of measured lowering of hydraulic heads (i.e., drawdown) and agree well with hydrogeologically-based rates from spatially-explicit mechanistic calculations of expected subsidence at monitoring wells. Our results indicate that over-exploitation of groundwater is inducing widespread subsidence of the land surface. This is likely to compromise groundwater quality, create flood risks, and produce hazards to infrastructure due to differential surface deformation.

## 4.3 Background

### *4.3.1 The aquifer system*

The aquifer system underlying the Mekong Delta consists of unconsolidated alluvial sediments filling a deep, tectonic trough. The basin trough is deepest along a northwest-trending axis aligned with the modern Bassac River, a major distributary of the Mekong, beneath which depth to bedrock can exceed 800m. It tilts along this same axis, deepening from the Delta's apex at Phnom Penh in central Cambodia in the direction of the South China Sea. The basin fill contains at least seven distinct sand and gravel

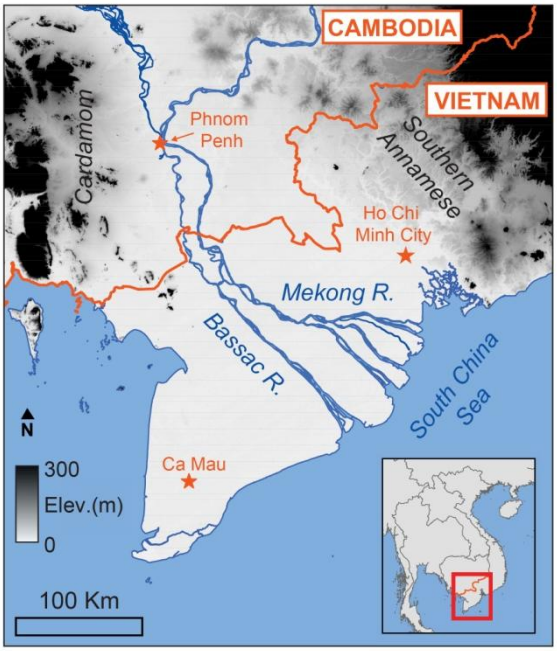


**Figure 4.1** Location map showing Mekong Delta and surrounding region, highlighting major geographic features referenced in the text.

aquifers interbedded with thick and laterally continuous confining clays. Sequences range in thickness from <1 to >180m and date to at least the Miocene epoch. Layer thicknesses taper in the directions of the Cardamom and Southern Annamese mountain ranges bounding the Delta to the northwest and northeast, respectively. They terminate at unmapped offshore locations in the seaward southern margins (DWRPIS, 2011).

### *4.3.2 Groundwater exploitation over space and time*

Groundwater has been used in the Mekong Delta since it was settled more than two thousand years ago, but the nature of that use has changed considerably in the past century. While surface water is abundant during the wet season of the annual monsoon, it is scarce during the prolonged dry season that follows. Dry season household water supplies have long been supplemented or even sustained by dug, or open wells. Open wells tap the shallow subsurface, most are <3m deep, and are particularly important in areas distant from the main river network or proximate to the coast, where seasonal saline incursion compromises surface waterways. Tube wells, which can access much greater depths, were introduced in the early 1900s. By the early 1960s, tube wells had reached depths of up to 568m in southern Vietnam (Anderson, 1978). Well installations and volumetric extraction rates on the Vietnamese side of the Delta have increased significantly following the country's reunification in 1975 and market-liberalizing economic reforms of 1986 (DWRPIS, 2010; DWRM, 2008; White, 2002). Since the mid 1990s, hydraulic heads have been

steadily declining in monitoring wells throughout the Delta, indicating widespread groundwater overdraft.

Seven major aquifers are now extensively and intensively exploited for water supply. The shallow Holocene-Pleistocene aquifers (4 total) are tapped by the largest number of wells, estimated at >1 million, but deeper Pliocene-Miocene units are subject to high volumetric rates of extraction (Wagner et al., 2012). The two most significant pumping centers are located at Ho Chi Minh City (HCMC), on the Delta's northeastern margin, and Ca Mau in the southwestern peninsula of the same name. Some extraction wells in the greater HCMC region began experiencing saline intrusion as early as the 1960s (Anderson, 1978), though the city continues to extract groundwater at a rate of at least 700 $m^3$/d (Wagner et al., 2012). The Ca Mau area has over 100,000 wells with a cumulative capacity of nearly 400,000 $m^3$/d (MONRE, 2013). An extensive region of groundwater head decline runs between these two major pumping centers, induced by aquifer exploitation in many smaller cities, towns and densely populated rural areas. At any given location, the magnitude of head decline varies among aquifers but is often highest in deeper units (DWRPIS, 2010).

### *4.3.3 Principles of compaction and subsidence*

The structure of an unconsolidated aquifer system is supported by both the granular matrix and the pore fluid pressure. Pore pressure is reduced during excessive pumping, shifting support for the overburden to the granular matrix. The shift of support causes overlying units to effectively squeeze compressible layers, resulting in their compaction. The magnitude of vertical compaction in a layer, expressed as a

change in layer thickness, is directly proportional to the layer's compressibility and the change in hydraulic head it undergoes, as:

$$\Delta b = S_s b \Delta h \qquad \textit{Eq. 4.1}$$

where $b$ is the layer thickness, $h$ is hydraulic head, $\Delta$ represents a change in either variable over some time period, and $S_s$ is the layer's specific storage ($1/L$), a metric related to compressibility that expresses the volume of water released from storage per unit volume per unit decline in hydraulic head. The decline in hydraulic head is referred to as drawdown. We later refer to storativity [-], defined for a hydrogeologic layer as the product of its specific storage ($S_s$) and thickness ($b$). Summation of vertical compaction of all compressible layers gives the total amount of land-surface subsidence.

### *4.3.4 Principles of measuring subsidence using InSAR*

SAR instruments emit radar waves of a specified wavelength and receive the portion of their signal that is back-scattered by the Earth's surface in view. Two coregistered SAR images acquired on different dates are used to form an interferogram, which encodes a wrapped (on the interval $-\pi$ to $\pi$) phase difference. The phase difference ($\Delta\Phi$) reported by an interferogram is composed of several components, including a deformation term:

$$\Delta\Phi = \Delta\Phi_{def} + \Delta\Phi_{topo} + \Delta\Phi_{atm} + \Delta\Phi_{n} \qquad \textit{Eq. 4.2}$$

where the right-hand side terms are associated with surface deformation ($\Delta\Phi_{def}$), topography ($\Delta\Phi_{topo}$), atmospheric effects ($\Delta\Phi_{atm}$) and noise ($\Delta\Phi_{n}$). The phase

difference due to deformation, $\Delta\Phi_{def}$, is determined after accounting for the additional terms and related to the magnitude of surface deformation in the sensor's line-of-sight (LOS), $\Delta d$, by:

$$\Delta d = \frac{\lambda \Delta \Phi_{\text{def}}}{4\pi} \qquad \textit{Eq. 4.3}$$

where λ is the wavelength. LOS-measured deformation has vertical and horizontal components determined by the look angle of the side-looking sensor. The look angle for the instrument used in this work, ALOS-1's PALSAR, was ~34°, such that vertical rates may be up to ~20% greater than the LOS rates.

The main challenge of interpreting interferograms derives from variable back-scattering properties of the landscape that reduce signal coherence over space and time. Coherence is commonly quantified by estimating the complex correlation among neighboring resolution elements, analogous to pixels, hereafter referred to as the correlation. Correlation (with magnitude 0 to 1) may be low-valued throughout much of a given landscape. A threshold correlation value, determined on a case-by-case basis, is often used to suppress low-quality resolution elements during the final estimation of deformation rates (Reeves et al., 2011; Lyons and Sandwell, 2003).

## 4.4 Data and methods

### *4.4.1 Description of SAR acquisitions*

We obtained a total of 259 ALOS-1 PALSAR acquisitions of the Mekong Delta for this study. These data were acquired in Fine Beam Single (FBS) and Fine

Beam Double (FBD) polarization modes and belong to 9 scenes covering most of the Delta. Each of the 9 scenes shares some degree of overlap (up to ~40 km along-track and ~10km across-track) with neighboring scenes. Scenes that mainly cover offshore areas were not regularly imaged. ALOS-1 had a repeat period of 46 days, but because image acquisition depends on satellite tasking, even fully onshore scenes are not available with such regularity. The average effective repeat period, accounting for when images were acquired by PALSAR, is ~90 days for this set of scenes. From all available images, we culled a subset to meet the criteria, the rationale for which is discussed below, that a sizeable number of anniversary pairs (+3 days, due to repeat period) could be formed for a given scene. A total of 121 acquisitions were retained in this subset for further processing.

### *4.4.2 InSAR processing*

The core analysis method used was interferometric stacking. The procedure determines the average phase of a stack of coregistered interferograms, reducing atmospheric errors by a factor of the square root of the number of interferograms in the stack (Strozzi et al., 2001). Stacking is appropriate in this case because linear annual average subsidence rates are expected based on linear annual average trends in drawdown. However, although drawdown tends to increase linearly over annual periods, hydraulic heads oscillate seasonally. To minimize the influence of seasonal oscillations, we consider only anniversary interferograms. Such interferograms should capture a similar amount of deformation in each, since the drawdown rate is

approximately constant over same-month annual intervals. For improved subsidence estimates, we stack all single-year anniversary interferograms in a given scene.

Interferograms were formed using a motion-compensating processor (Zebker et al., 2010) in a series of steps. First, all acquisitions for a given scene were co-registered (geographically aligned) to a common master. Images acquired in FBD mode were resampled to the higher resolution of the FBS images. Elevation correction, negligible in this exceedingly low-relief landscape, was done using the SRTM 90m DEM. Next, all interferograms were visually examined for orbital ramps. Orbital ramps were removed using a linear phase plane. Interferograms with nonlinear ramps were discarded. A total of 78 interferograms were ultimately retained, with 5-12 (mean = 9) in each of the 9 stacks. Finally, stacks of interferograms were averaged and multi-looked (spatially-averaged in complex form, here using a 4x4 window). The phase component of each interferogram was median-filtered (5x5 window) before mosaicing. Unwrapping, the process of adding appropriate integer multiples of $2\pi$ to the wrapped phase, was not necessary as subsidence rates across the Delta are < 11.8 cm/yr (i.e., $(\lambda/2)/\Delta t$). Pixels with average correlation $\leq 0.15$, determined as a threshold that readily distinguished low-coherence paddy and open water from the radar-bright built-up network, were masked prior to mosaicing and are not shown in our figures.

### *4.4.3 Analysis of spatially-explicit drawdown rates*

Hydraulic heads data from 106 nested monitoring wells throughout the Vietnamese Delta were measured monthly over the period 1995-2010 by the Division of Water Resources Planning and Investigation for the South (DWRPIS) of Vietnam. Most, though typically not all, of the seven major exploited aquifers were monitored in each of the 19 well-distributed nests. Of these nests, 15 overlap with the spatial and temporal coverage of the PALSAR imagery. Wells that are isolated, i.e., do not belong to nests, or that duplicate measurements by monitoring the same aquifer in a nearby (<5 km) location, were also not considered (25 total).

We calculated the rate of drawdown in each well using linear regression of the hydraulic head observations over the 2006-2010 period coinciding with the PALSAR record. Spurious periods of measurement, found in 10 well records, were excluded from regression-fitting and 3 wells were not monitored over the period of interest. Drawdown rates were calculated as the slope of the best-fit linear regression equation for each remaining well (78 total). Rates for

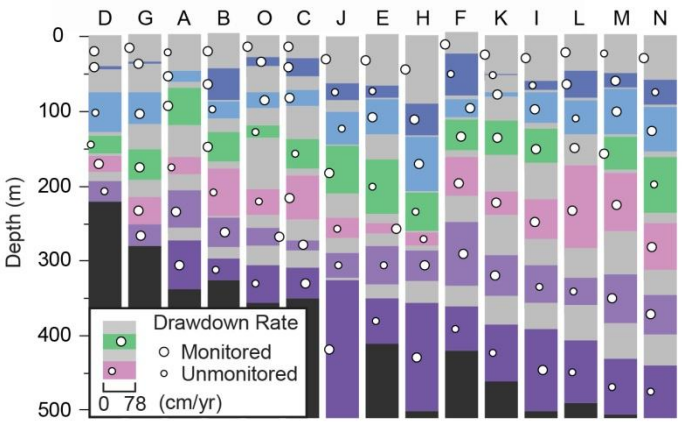


**Figure 4.2** Drawdown rates during the 2006-2010 period by aquifer (colored) and well nest. The position of the circles along the width of each column indicates the magnitude of the drawdown rate. Larger circles indicate locations where monitoring data are available, while drawdown rates for unmonitored locations were interpolated and indicated using smaller circles. Confining clays shown in light gray, bedrock in dark gray.

unmonitored aquifers in a nest were interpolated from neighboring nest data for the same aquifer. Fig. 4.2 displays the stratigraphy at each well nest and the complete set of drawdown rates, including known and interpolated values, for nests where InSAR coverage is available.

### *4.4.4 Estimate of spatially-explicit system storage*

Storativity is unknown and variable throughout the 3D aquifer system, depending on the variable thickness and compressibility of hydrogeologic units throughout it. Thicknesses for each unit at each location in the monitoring-well network were extracted from DWRPIS well logs. Bores are found at >50 well-distributed locations, many co-located with sites in the monitoring well network. Seven of the monitoring well nests do not have co-located well logs, but a logged bore can be found within 7 km. Most well logs include the depth to bedrock, the lower boundary on the aquifer system; however, several indicate a trough of unknown depth underlying the main river network in the central Delta. In the central bedrock trough we interpolated between the nearest measured bedrock elevation measurements to estimate an effective thickness (i.e., the thickness influenced by pumping) for the deepest aquifer. Specific storage values for the uppermost units were assumed laterally constant ($5.5 \times 10^{-4}$/m for confining clays and $5.5 \times 10^{-5}$/m for aquifer sands), but decreased with depth according to an exponential function (Ingebritsen et al., 2006) due to naturally occurring consolidation since deposition. Specific storage values in the deepest layers are half that of the near-surface values.

### *4.4.5 Synthesis*

We compare InSAR-based subsidence rates with spatially-explicit hydrogeologically-based rates. InSAR-based subsidence rates were estimated using 0.5 km-radius circles, or windows, of pixels centered on each monitoring nest. LOS rates were converted to approximate vertical rates by scaling by $\cos(\theta)^{-1}$, where $\theta$ is the 34° sensor look angle. Representative rates for each window were determined using all high-correlation (>0.15) pixels by averaging the mean value of a 25-pixel sub-window centered on the nest with the overall window mean. This window-weighting procedure allows for inclusion of sufficient numbers of high-correlation pixels while weighting the pixels nearest to the well nest where drawdown rates were compared. Errors were estimated as the window-weighted standard deviation. Hydrogeologically-based rates were determined based on *Eq. 4.1*, which estimates compaction in clays and sands due to drawdown in each aquifer at all 15 monitoring nest locations with overlapping InSAR coverage. Estimated compaction rates were summed over all layers underlying a nest location, based on drawdown in up to six aquifers, excluding the semi-confined Holocene. The Holocene aquifer is locally connected to surface water bodies and drawdown is not observed in it at monitored locations. This summation provides the estimate of hydrogeologically-based subsidence rates at the surface at each nest. The agreement between rates determined by these two approaches is discussed presently.

## 4.5 Results

### *4.5.1 Spatio-temporal patterns in InSAR signal quality*

The Mekong Delta is, in principle, an exceedingly difficult landscape to image using SAR. Signal quality is greatly affected by spatio-temporally variable surface conditions. Scattering properties change in the large portion of the Delta that is dedicated to paddy, alternately inundated or vegetated during one of up to three rice-cropping seasons. Much of the region is radar-dark during multi-month annual flooding driven by the Southeast Asian monsoon. In addition to these climatically-driven effects, the changing atmospheric water vapor mass further imposes spatially and temporally-variable radar phase delays, referred to generally as atmospheric effects (Zebker et al., 1997).

Interestingly, the same characteristics that obscure the SAR signal in much of the landscape have shaped Delta development in ways that also make it amenable to InSAR. Widespread, repeated inundation and agriculture-based land use has driven demand for dry land and dry-season irrigation supplies, leading to the development of an extensive canal and levee network. This network, along with natural levees lining the main river system, concentrates human settlements and associated stable surfaces (e.g., buildings, roads, and packed clay levees), creating radar-bright areas throughout the Delta. The brightest areas correspond to major cities, located at the network intersections, which are also marked by high relative interferometric correlation, indicating high signal quality. Not only are these areas characterized by high InSAR correlation, but measurements made on the network of development, elevated above

the floodplain, are not affected by sedimentation, which could counteract subsidence at potentially time-variable rates. Human modifications to the built-up land surface may confound InSAR interpretation locally. At the regional scale, however, the network of development renders InSAR measurements reliable.

The spatially-variable quality of radar signal throughout the landscape described above is illustrated in Fig. 4.3. The average amplitude, or magnitude, of returned radar signal is shown in gray-scale in Fig. 4.3A and the average phase correlation is shown in Fig. 4.3B. Both values are maximum in the brightest areas of the respective images.

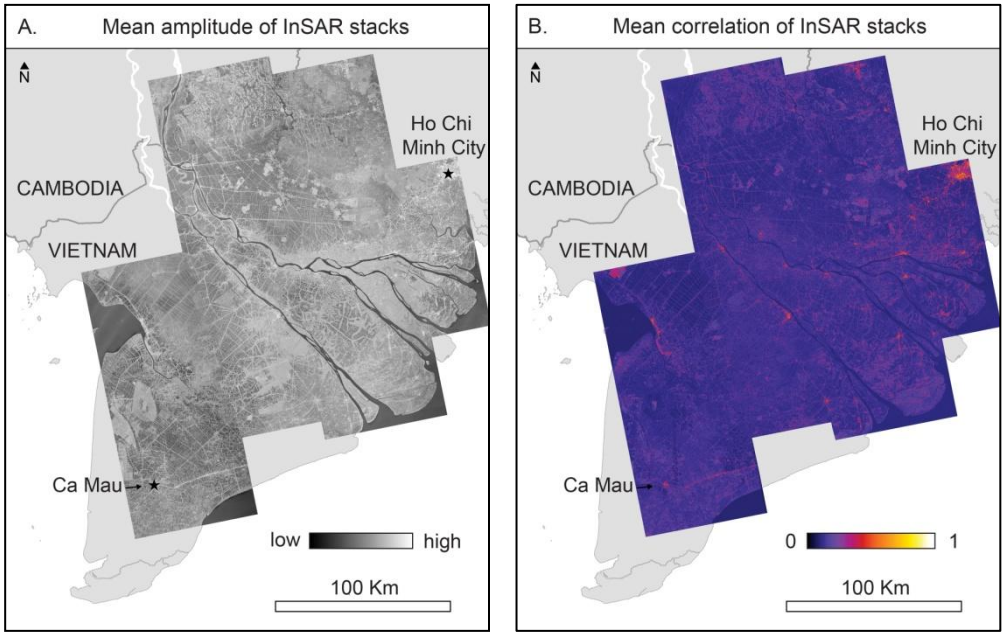


**Figure 4.3 A.** Radar-brightness of landscape expressed as mean amplitude of stacks. **B.** Mean correlation of stacks, an indicator of spatially-variable InSAR signal quality. Data © JAXA, METI 2011.

### *4.5.2 Comparison between patterns in InSAR-based subsidence and drawdown*

InSAR-based subsidence rates throughout the Mekong Delta are shown in Fig. 4.4 (colored overlay). The most conspicuous feature is a large subsidence bowl centered on Ho Chi Minh City (HCMC) in the northeast corner, where the highest rates are observed over the largest continuous area. Similarly high rates are observed in smaller areas centered on many of the Delta's major cities (e.g., Ca Mau, Can Tho, and My Tho). Between these localized high subsidence areas, a widespread region of lower-rate subsidence, which appears yellow in color, extends along a generally southwest-northeast axis aligned with numerous urban areas and industrial corridors connecting the major pumping centers at HCMC and Ca Mau.

Similar patterns are observed in regional drawdown. Monitoring wells indicate deep cones of depression, exceeding 20 m, at HCMC and Ca Mau and widespread regional drawdown in a ~100 km-wide swath between them. Embedded in this regional depression are smaller cones of significant magnitude (7-9 m below zero). The magnitude of drawdown diminishes in wells with increasing proximity to the

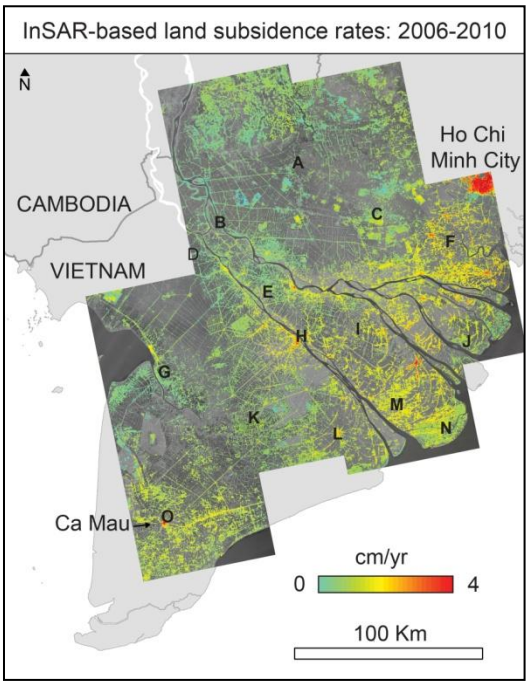


**Figure 4.4** InSAR-based subsidence rates in the Mekong Delta with locations of monitoring nests. Data © JAXA, METI 2011.

international border, owing to minimal volumetric extraction in Cambodia, reduced development density in the Plain of Reeds, and bedrock outcropping in the northwestern corner of the Delta. Rates of hydraulic head decline range from 9 – 78 cm/yr (mean: 24 cm/yr) in Delta monitoring wells (see Fig. 4.2). The spatial patterns in maximum drawdown rates among wells at each nest are shown in Fig 4.5.

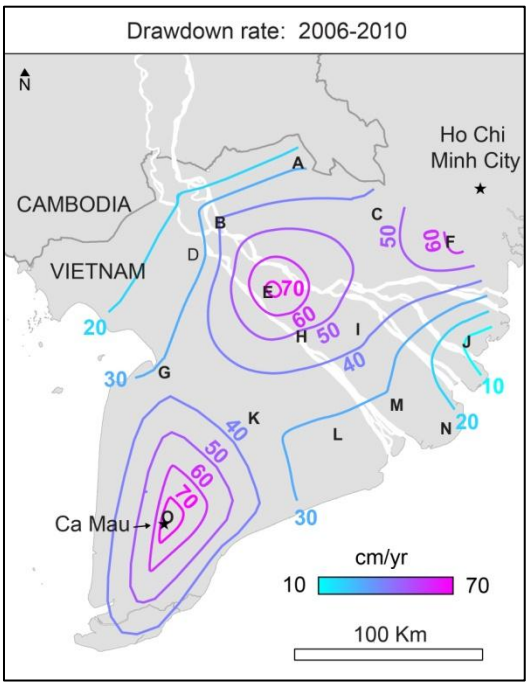


**Figure 4.5** Maximum drawdown rates among all aquifers at each well nest.

### *4.5.3 Comparison between InSAR and hydrogeologically-based subsidence rates*

InSAR-based estimates agree well with hydrogeologically-based subsidence rates that account both for spatially-explicit variability in physical properties and conditions in the subsurface (Fig. 4.6). The two rates are clearly correlated; the least-squares fit between the two estimates has a trendline whose slope is near one with a correlation coefficient, $r^2$, of 0.52. The relationship passes through the origin and extends to ~3 cm/yr. The RMS error between rates estimated by the two approaches is 0.5 cm/yr, with 10 of the 15 points falling within 0.5 cm/y of the best-fit relation. InSAR estimated errors alone range from 0.5-1 cm/yr.

Deviations between the two estimates derive from several potential sources of error. In addition to errors introduced in the InSAR-based estimates, others result from incomplete knowledge of 1) drawdown rates in all aquifers, 2) the degree of connectivity between them, and 3) variable specific storage within and among hydrogeologic units. The overall agreement between estimates, however, suggests that our methods of estimating unknown parameters are capturing major differences in conditions among well nest locations.

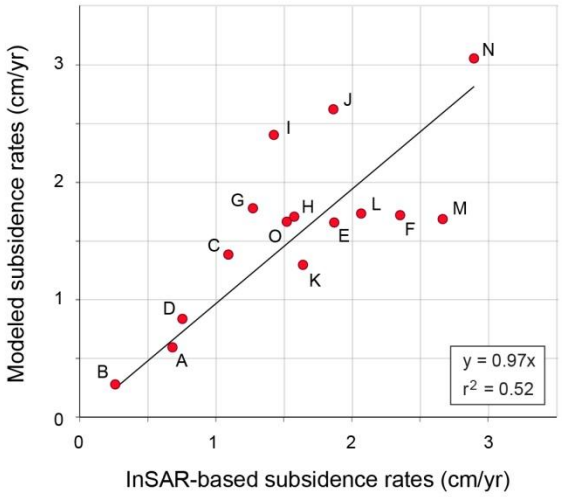


**Figure 4.6** Comparison between InSAR and hydrogeologically-based (modeled) subsidence rates.

## 4.6 Discussion

### *4.6.1 Pumping-induced subsidence in the Mekong Delta*

InSAR-based subsidence patterns in the Mekong Delta are consistent with observed patterns in groundwater exploitation. Groundwater extraction is focused most intensively in the Delta's urban and industrial areas, driven in large part by pollution of surface waterways and high-valued uses for groundwater (Wagner et al., 2012; Dang, 2008; White, 2002). The positive relationship between settlement density and drawdown rates is also evident in the InSAR-based subsidence rates. Subsidence rates are highest in many of the Delta's urban areas, and generally diminish in the

directions of more rural regions. Groundwater extraction rates also appear to be considerably lower in more rural areas, according to lower drawdown rates in monitoring wells. Lower rates of drawdown in rural areas imply low volumetric extraction rates despite high rural domestic reliance on groundwater (White, 2002), suggesting that the dense canal network satisfies much of the current agricultural water demand. However, in addition to this observed urban-rural trend, a seaward-landward trend is also evident: pumping rates appear to be higher in most coastal rural areas compared to inland rural regions. This trend may be related to pumping of groundwater used to freshen brackish aquaculture ponds in areas prone to saline incursion in surface water bodies (Dang, 2008).

The general agreement between drawdown and InSAR-based subsidence patterns is mechanistically linked upon accounting for the spatially-variable properties of the aquifer system. The hydrogeologically-based subsidence estimates consider head declines in the context of local aquifer-confining bed storage properties. These system properties are spatially-explicit in 3D; they account for the conditions in each aquifer at each monitoring well nest along with layer thicknesses from co-located well-logs. The hydrogeologically-based subsidence estimates account for variable storativity throughout the subsurface, making a more accurate link between drawdown in each aquifer and expected subsidence.

The magnitude of InSAR-based subsidence rates is also consistent with observations from comparable systems. Subsidence rates measured using ALOS-1 PALSAR in Indonesia and India, where intensive groundwater extraction is also

occurring, range from 0.5 to more than 20 cm/yr (Chaussard et al., 2013; Chatterjee et al., 2006). In nearby Bangkok, located on perhaps the most analogous aquifer system, a combination of ground-based methods estimate that subsidence has a ratio to pumping of 1:10 (Phien-Wej et al., 2006). A similar ratio may apply in the Mekong Delta, where drawdown rates are on the order of tens of centimeters per year while InSAR-based subsidence rates range from ~1-4 cm/yr. A substantial fraction of the Delta's pumped demand appears to be sourced by storage lost during compaction of the aquifer system, as has been observed by these and other methods around the world.

### *4.6.2 Considerations*

The scale and scope of this work necessitates a set of simplifying assumptions and indirect methods for minimizing errors. Common sources of measurement error associated with InSAR processing, most significantly atmospheric effects and temporally-variable surface scattering properties, were minimized by our methods but remain difficult to quantify. Nonetheless, the final mosaic of InSAR-based subsidence rates reveals consistent patterns across space and stacks of interferograms that were processed in parallel. The spatial consistency of the InSAR results both within and among stacks, and over large scales (order 10s of km) lends additional support for their reliability. Verifying the magnitude of InSAR-based rates using a hydrogeologically-based approach requires assumptions about the system storage capacity and the influence of drawdown throughout the complex aquifer system. However, the overall consistency between subsidence rates derived from these

independent procedures and execution of methods, despite multiple potential sources of error, supports their overall validity.

## 4.7 Conclusions

Unregulated groundwater extraction appears to be causing widespread land subsidence in the Mekong Delta. Although subsidence rates may be low in magnitude, they are significant in this low-relief landscape prone to widespread annual flooding: modest deformation can change flooding conditions over large areas. Extensive subsidence further indicates that excessive exploitation is occurring that may have other unintended consequences for groundwater quality. Over-pumping may induce saline intrusion and/or exacerbate arsenic contamination in antecedently high-quality fossil groundwater reserves (Erban et al., 2013; Mukherjee et al., 2011; Winkel et al., 2011).

InSAR serves as a valuable tool for monitoring subsidence rates in the Delta, despite many challenges in successfully applying the method. The scale and comprehensiveness of InSAR measurements are unmatched by any other presently available technique. Even if ground-based measurements were available, it would be exceedingly difficult to observe the extensive, low-rate subsidence detected by InSAR. The imaging capability of the L-band ALOS-1 PALSAR mission is, in large part, responsible for the quality of these estimates. The network of development amid an otherwise heavily vegetated and seasonally flooded landscape provides a fairly stable surface from which reliable subsidence estimates can be made.

Relatively simple accounting for hydrogeologic conditions throughout the aquifer system leads to good agreement between expected and observed subsidence rates. Absent ground-based data, our spatially-explicit estimates of subsurface compaction from a mechanistic equation based on available drawdown and stratigraphic data can serve as a useful and independent means of validating InSAR-based observations. These dual estimation approaches are the only presently available ones for use in the Delta and serve as a guide for ground-based monitoring and future management of the aquifer system.

**Acknowledgments**

We wish to thank the Department of Water Resources Planning and Investigation for the South of Vietnam (DWRPIS), the Japanese Aerospace Exploration Agency (JAXA), Japanese Ministry of Economy, Trade and Industry (METI) and the Alaska Science Facility (ASF) for providing data used in this work. We gratefully acknowledge the UPS Endowment Fund and the Global Freshwater Initiative of the Woods Institute for the Environment at Stanford. This work is supported by the National Science Foundation under grant EAR-1313518 to Stanford University. Any opinions, findings, and conclusions or recommendations expressed in this material are those of the authors and do not necessarily reflect the views of the National Science Foundation.

## References


Amelung, F., Galloway, D. L., Bell, J. W., Zebker, H. A., and Laczniak, R. J. (1999). Sensing the ups and downs of Las Vegas: InSAR reveals structural control of land subsidence and aquifer-system deformation. *Geology*, 27(6), 483–486.

Anderson, H. R. (1978). Hydrogeologic Reconnaissance of the Mekong Delta in South Vietnam and Cambodia. US Government Printing Office.

Bawden, G. W., Thatcher, W., Stein, R. S., Hudnut, K. W., and Peltzer, G. (2001). Tectonic contraction across Los Angeles after removal of groundwater pumping effects. *Nature*, 412(6849), 812–5. doi:10.1038/35090558.

Bear, Jacob, Cheng, H-D, Sorek, S., Ouazar, D., and Herrera, I. (1999). Seawater intrusion in coastal aquifers : concepts, methods, and practices. Dordrecht, Netherlands: Kluwer Academic.

Buckley, S. M. (2003). Land subsidence in Houston, Texas, measured by radar interferometry and constrained by extensometers. *Journal of Geophysical Research*, 108(B11), 2542. doi:10.1029/2002JB001848.

Chatterjee, R., Fruneau, B., Rudant, J., Roy, P., Frison, P. L., Lakhera, R., Dadhwal, V., and Saha, R. (2006). Subsidence of Kolkata (Calcutta) city, India during the 1990s as observed from space by Differential Synthetic Aperture Radar Interferometry (D-InSAR) technique. *Remote sensing of environment*, 102(1-2), 176–185.

Chaussard, E., Amelung, F., Abidin, H., and Hong, S.-H. (2013). Sinking cities in Indonesia: ALOS PALSAR detects rapid subsidence due to groundwater and gas extraction. *Remote Sensing of Environment*, 128, 150–161. doi:10.1016/j.rse.2012.10.015.

Colesanti, C., Ferretti, a., Novali, F., Prati, C., and Rocca, F. (2003). Sar monitoring of progressive and seasonal ground deformation using the permanent scatterers technique. *IEEE Transactions on Geoscience and Remote Sensing*, 41(7), 1685–1701. doi:10.1109/TGRS.2003.813278.

Dang, D. P. (2008). General on Groundwater Resources. Department of Water Resources Management, Vietnam, Water Sector Review Project ADB-TA-4903 VIE. Hanoi.

Department of Water Resources Management. (2008). Nationwide survey of arsenic in wells. Vietnam.

Department of Water Resources Planning and Investigation for the South of Vietnam. (2010). Monitoring of groundwater levels in the Mekong Delta. *Unpublished*. Ho Chi Minh City.

Department of Water Resources Planning and Investigation for the South of Vietnam. (2011). Well logs and geologic cross-sections in the Cuu Long (Mekong) River Delta. *Unpublished*. Ho Chi Minh City.

Erban, L. E., Gorelick, S. M., Zebker, H. A., and Fendorf, S. (2013). Release of arsenic to deep groundwater in the Mekong Delta, Vietnam, linked to pumping-induced land subsidence. *Proceedings of the National Academy of Sciences of the United States of America*. doi:10.1073/pnas.1300503110.

Fielding, E. J., Blom, R. G., and Goldstein, R. M. (1998). Rapid subsidence over oil fields measured by SAR. *Geophysical Research Letters*, 25(17), 3215–3218.

Galloway, D. L., and Burbey, T. J. (2011). Review: Regional land subsidence accompanying groundwater extraction. *Hydrogeology Journal*, 19(8), 1459–1486. doi:10.1007/s10040-011-0775-5.

Galloway, D., Hudnut, K., Ingebritsen, S., Phillips, S., Peltzer, G., Rogez, F., and Rosen, P. (1998). Detection of aquifer system compaction and land subsidence using interferometric synthetic aperture radar, Antelope Valley, Mojave Desert, California. *Water Resources Research*, 34(10), 2573–2585.

Hoffmann, J., Zebker, H. A., Galloway, D. L., and Amelung, F. (2001). Seasonal subsidence and rebound in Las Vegas Valley, Nevada, observed by Synthetic Aperture Radar Interferometry. *Water Resources Research*, 37(6), 1551–1566. doi:10.1029/2000WR900404.

Ingebritsen, SE, Sanford, WE, and Neuzil, C. (2006). Groundwater in Geologic Processes. (2nd ed.). Cambridge: Cambridge University Press.

Lyons, S., and Sandwell, D. (2003). Fault creep along the southern San Andreas from interferometric synthetic aperture radar, permanent scatterers, and stacking. *Journal of Geophysical Research*, 108(B1), 2047. doi:10.1029/2002JB001831.

Ministry of Natural Resources and Environment, Vietnam. (2013). Land subsidence in Ca Mau Peninsula.http://www.monre.gov.vn/v35/default.aspx?tabid=675&CateID=57&ID=128134&Code=5YBS128134.

Mukherjee, A., Fryar, A. E., Scanlon, B. R., Bhattacharya, P., and Bhattacharya, A. (2011). Elevated arsenic in deeper groundwater of the western Bengal basin, India: Extent and controls from regional to local scale. *Applied Geochemistry*, 26(4), 600–613.

Phien-Wej, N., Giao, P. H., and Nutalaya, P. (2006). Land subsidence in Bangkok, Thailand. *Engineering geology*, 82(4), 187–201.

Poland, J.F (Ed.) (1984). Guidebook to studies of land subsidence due to ground-water withdrawal (Vol. 40). UNESCO.

Reeves, J. A., Knight, R., Zebker, H. A., Schreüder, W. A., Shanker Agram, P., and Lauknes, T. R. (2011). High quality InSAR data linked to seasonal change in hydraulic head for an agricultural area in the San Luis Valley, Colorado. *Water Resources Research*, 47(12). doi:10.1029/2010WR010312.

Strozzi, T., Wegmuller, U., Tosi, L., Bitelli, G., and Spreckels, V. (2001). Land subsidence monitoring with differential SAR interferometry. *Photogrammetric engineering and remote sensing*, 67(11), 1261–1270.

Wagner, F., Tran, V. B., and Renaud, F. G. (2012). Groundwater Resources in the Mekong Delta: Availability, Utilization and Risks. In F. G. Renaud and C. Kuenzer (Eds.) Dordrecht: Springer Netherlands.

White, I. (2002). Water management in the Mekong Delta: changes, conflicts and opportunities. *UNESCO International Hydrological Program Technical Documents in Hydrology No. 61*. Paris.

Winkel, L. H., Pham T.K.T., Vi., M.L., Stengel, C., Amini, M., Nguyen, T.H., Pham, H.V., and Berg, M. (2011). Arsenic pollution of groundwater in Vietnam exacerbated by deep aquifer exploitation for more than a century. *Proceedings of the National Academy of Sciences of the United States of America*, 108(4), 1246–1251.

Zebker, H. A., Hensley, S., Shanker, P., and Wortham, C. (2010). Geodetically Accurate InSAR Data Processor. *IEEE Transactions on Geoscience and Remote Sensing*, 48, 4309–4321. doi:10.1109/TGRS.2010.2051333.

Zebker, H. A., Rosen, P. A., and Hensley, S. (1997). Atmospheric effects in interferometric synthetic aperture radar surface deformation and topographic maps. J*ournal of Geophysical Research*, 102(B4), 7547–7563. doi:10.1029/96JB03804.

# 5 Summary and future directions

## 5.1 Overview of findings

The preceding chapters discussed new understanding of the nature of groundwater arsenic occurrence in the heavily-pumped Mekong Delta. The Delta's deep multi-aquifer system is widely, though non-uniformly, contaminated with arsenic. Regional-scale trends in arsenic occurrence are strongly related to the distance of a well to the Mekong river system or coastline, its depth and the pumping intensity of the region where it is found. Local-scale heterogeneity in arsenic concentrations is nonetheless apparent, confounding the ability of statistical models based on regional-scale trends to predict outcomes at individual wells, with which users are concerned. The importance of scale in the collection and interpretation of data, elucidation of controlling processes and relevance to groundwater management decisions cannot be overstated. This concluding chapter is concerned with reconciling differences in our understanding of arsenic occurrence at different scales, highlighting remaining gaps based on the lessons of this and other work, and identifying the implications of this work for long-term human use of groundwater when arsenic is a potential hazard.

A major discovery of this work is that arsenic contamination may be generated at depth by pumping-induced compaction of confining clays. The potential for solutes stored in confining clays to be released during compaction, a consequence of over-exploitation, and to subsequently induce or stimulate contamination in deep aquifers

was previously unappreciated. Now it becomes possible to specify under which sets of conditions this process may manifest. The overriding limitation for such prediction, however, is knowledge of spatially-variable subsurface physico-chemical properties. Biogeochemical conditions in deep, buried clays may only be inferred, at present, from near-surface observations in limited locations. The physical properties of confining units and aquifers, namely permeability, specific storage, and compressibility, are similarly variable and largely unknown. Even the most rigorous of available techniques for characterizing these properties are currently unable to comprehensively describe the subsurface.

Future investigations may be informed by the lessons learned during this dissertation. It began with consideration of arsenic concentrations measured in wells and analysis of spatial contamination patterns, evolved to develop conceptual and numerical aquifer system models, based on ancillary ground-based measurements, that were aimed at explaining well observations, and expanded to include analysis of remotely-sensed data to independently confirm modeling results. Each step required assumptions and scale-dependent considerations that might prove helpful for the development of future studies.

## 5.2 Guidance for future research

### *5.2.1 Primary data collection*

The most spatially comprehensive access to information about subsurface conditions in the aquifer systems of Southeast Asia is offered by existing well data.

Both within and across basins, existing wells have afforded the largest datasets on arsenic occurrence and in some cases, other chemical indicators. Past well surveys provide some of the most valuable information for designing future studies.

Surveys of arsenic concentrations in existing wells typically include a single measurement for each well, along with a few other common kinds of ancillary information. Often the wells' GPS coordinates and depths are reported. In the Mekong Delta dataset used in this work, the well installation year was also given and provided a critical piece of ancillary information. Surveys conducted for scientific purposes tend to also include information about additional chemical constituents or indicators, e.g., sulfate, nitrate, trace elements, conductivity, DOC, pH, or ORP, which allows for more robust consideration of the arsenic measurements. Future well surveys would do well to include as many of the above parameters as is feasible. Based on the findings of Chapters 2-3, it would be desirable to know additional well specifications (i.e., beyond location, depth and installation year) like screen length and pumping rate history.

Past surveys have largely focused on describing the natural distribution of dissolved arsenic in affected systems, as anthropogenic controls on arsenic contamination were only recently recognized. In light of new scientific results and increasing reliance on groundwater for high-volume purposes in many of the arsenic-prone basins of Southeast Asia, future surveys of well contamination would be best coupled with knowledge of aquifer-specific pumping rates and hydraulic heads. Coupling may be loose, as in this work, where temporally-overlapping datasets were

gathered from multiple sources. Collection or compilation of these ancillary hydrogeologic data should, however, be prioritized during any campaigns designed to understand arsenic contamination in heavily-exploited regions.

Long-term monitoring of selected wells in heavily-exploited regions would be particularly useful for understanding contamination events that evolve over time. Ideally such efforts would be accompanied by detailed interpretation of local stratigraphy. The optimal location for a paired well log is in the same bore as the monitoring well. However, when pre-existing wells are monitored, this well-log information will typically not be available. Absent a same-location log, well logs from within 1km may be useful, as depositional environments should not vary appreciably over this distance. Well logs from greater distances will have less relevance for describing conditions at the monitoring well. Knowledge of local physical conditions is especially important because the capture radius of individual wells on a multi-decadal timescale is 10s to 100s of meters, depending on its pumping rate (see Appendix A). Well logs should include, at a minimum, 1) the depth to each major transition between layers, 2) a description of the physical properties of the layer material (e.g., fine/coarse sand, gravel, plastic or stiff clay) and a 3) a description of the layer color(s), from which redox conditions might be interpreted. Recovery of intact cores from logged bores would be additionally useful for determining layer compressibility and solid and pore fluid geochemistry, but such samples are acquired at much greater effort and expense. Measurements of land subsidence by differential GPS at monitoring well locations would also help support these efforts.

Despite the value of land subsidence measurements for understanding the aquifer system response to pumping and interpreting well survey data, they are rarely available. Ground-based subsidence measurements are fundamentally limited by local initiatives to collect them. They therefore tend to be spatially and temporally limited, usually collected in urban areas already known to be sinking. Space-based imagery, from which subsidence rates were determined by InSAR for this work, captures most areas of the world with relatively high frequency. Remotely-sensed subsidence rates providing unmatched spatial and temporal coverage, though associated errors cannot be independently assessed without ground-based measurements. Owing to the increasing availability of satellite data, studies of regional subsidence are becoming more common. Better quantification of subsidence, using either land or space-based data, would complement investigations and planning efforts in the arsenic-prone, deltaic regions of South and Southeast Asia in different ways. In addition to contributing to arsenic-related research, information on land subsidence rates is independently valuable for flood forecasting, agricultural management, and protection of infrastructure, among other regional management activities.

### *5.2.2 Modeling*

Interpretation of primary data collected during well surveys or other campaigns usually relies on statistical or numerical modeling. The following section discusses some of the major limitations to each approach as they have been historically applied in this and other related work.

Statistical modeling of arsenic observations are frequently subject to one or more of four major limitations: 1) no consideration for well depth, 2) absent or poorly specified hypotheses for relationships between a contamination outcomes and explanatory variables, 3) lack of ancillary data specific to each well and 4) no consideration of dynamic environmental conditions that give rise to modeled outcomes. Well depth is a key variable in deep, layered systems, in which arsenic occurrence shows considerable vertical structure. Accounting for depth both of well measurements and in ancillary datasets that may help explain them (e.g., a secondary dataset on groundwater salinity) should be done whenever possible. A hypothesis-driven approach to variable and model selection is fundamental when large-n datasets, subject to misleadingly high statistical significance, are used. Lack of ancillary data like chemical parameters, well pumping histories or local physical conditions for each well in an arsenic survey is certainly the most challenging limitation to overcome. With such additional information, however, it would likely be possible to refine statistical models for better performance at the scale of individual wells. Dynamic, process-based models are needed to understand the mechanisms underlying contamination; statistical models do not elucidate them, but can only indicate the relative importance of known mechanisms for explaining observations or highlight knowledge gaps.

Physical modeling of arsenic-affected groundwater systems at the regional-scale has, prior to the work presented in Chapter 2, not considered transient hydraulic behavior in response to pumping, and the implications for changes in storage. Changes in storage within confined regions of these systems, however, largely

determine the sources of water available to wells. Different water sources are in turn associated with different chemical compositions, with consequences for pumped water quality. Moreover, changes in storage due to groundwater exploitation have consequences for land subsidence and associated increases in flooding, and also for infrastructure damage. Future modeling efforts would do well to consider the physical dynamics of these complex systems.

### *5.2.3 InSAR as a reconnaissance tool*

InSAR offers a valuable early tool reconnaissance tool for detection of pumping-induced disturbance of the subsurface and consequent subsidence of the land surface. InSAR-based studies are advantageous, compared with strictly ground-based efforts, in terms of data availability and the relative speed with which information can be extracted from existing satellite imagery. They further provide spatial coverage that is impractical to achieve in field campaigns. Although not all areas of a landscape return usable radar signal, as back-scattering properties vary among them, InSAR-based subsidence measurements range over scales unmatched by any other available method.

As a technique for reconnaissance of potential arsenic hotspots, InSAR-based studies must, however, be coincident with or followed-up by ground-truthing of hydrogeologic conditions and well sampling. The product of InSAR-based reconnaissance analysis is therefore the identification of areas that are subsiding and may be at risk of compaction-induced arsenic contamination if other necessary requisite conditions are also present, not to definitely identify them.

## 5.3 Guidance for water resources management in arsenic-prone regions

This work clearly shows that over-exploitation of groundwater in the Mekong Delta is not only ill-advised because it leads to the already well-known problems of increased pumping lift, saline intrusion, and land subsidence, but also because it exacerbates the spread of arsenic contamination. Pumping in excess of natural recharge rates, leading to long-term drawdown of groundwater levels, should be avoided in order to avoid these numerous and cascading negative consequences for development and human welfare.

Limiting groundwater pumping to responsible levels, however, requires careful consideration for site-specific circumstances related to both natural and socio-economic environments. In the Bengal Basin, one proposed management scheme involves restricting high-volume irrigation pumping to shallow aquifers, while reserving cleaner deep aquifers for low-volume domestic supply (Michael and Voss, 2008). This approach may minimize the potential for human-induced contamination of deep aquifers, but may not avoid some of the other concerns associated with aquifer overdraft while also incurring other costs: irrigation with arsenic-rich shallow groundwater can lead to uptake of arsenic in crops and reduced rice yields (e.g., Dittmar et al., 2010; Abedin et al., 2002). Rice yields are especially important in this densely populated area where food security is especially vulnerable. In the Mekong Delta, groundwater pumping for irrigation is much less significant and population densities are much lower. The exploited groundwater system consists of thinner aquifers, representing older paleo-periods, such that the physico-chemical system

response to pumping differs compared with the Bengal Basin. As a result, potential groundwater management schemes for the Delta are subject to a different set of constraints. In the Delta context, improving the capacity to store and treat surface water supplies may go a long way to alleviate pressure on groundwater resources, much of which is focused in the population centers.

A broader view includes full consideration for the portfolio of water supply options in these settings. The makeup of an optimal portfolio will differ throughout each region as a consequence of multi-faceted constraints imposed by spatio-temporally variable physical conditions, source qualities, and purposes of use. Rainwater capture offers perhaps the most convenient and safest source in many locations for the duration of the year when it is available. With sufficient storage and protection or treatment, it could potentially provide sufficient drinking water supplies throughout the year. Surface water is also subject to seasonal changes in availability, but should not be overlooked as an important supply for agriculture and aquaculture, both of which support household nutrition and income-generation. Depending on its quality, surface water may also be easier to treat for other uses than arsenic-contaminated shallow groundwater. Use of shallow groundwater should not be wholly discouraged, as use for washing and bathing supports household welfare without incurring the risks of direct arsenic ingestion. Shallow wells used under the guidance of testing and labeling for arsenic may help satisfy dry-season demand in areas where rain or surface water sources cannot be safely secured. Deep, fossil groundwater should be used sparingly for direct human consumption or other low-volume, high-value purposes, only where quality can be ensured.

Indeed, long-term responsible management of water resources in any of the arsenic-prone regions of South and Southeast Asia must take a comprehensive view, rather than focusing on singular or narrowly-specified "solutions." The advent of tubewells in the region came as a dichotomous response to surface water pollution: groundwater accessed via wells was incentivized over microbiologically-inferior surface water. More recently, the discourse has encouraged deep groundwater over shallow arsenic-contaminated groundwater. In reality, a suite of water sources with varying qualities suited to different purposes is available, while heavy dependence on a particular one comes with its own risks. Minimizing these diverse risks to human well-being overall depends on adjusting the way this portfolio is exercised.

## References

Abedin, MD. J., Cresser, M. S., Meharg, A. A., Feldmann, J., and Cotter-Howells, J. (2002). Arsenic accumulation and metabolism in rice (*Oryza sativa L.*). *Environmental science & technology*, 36, 962-968.

Dittmar, J., Voegelin, A., Maurer, F., Roberts, L. C., Hug, S. J., Saha, G. C., Ali, M. A., Badruzzaman, B. M., and Kretzschmar, R. (2010). Arsenic in soil and irrigation water affects arsenic uptake by rice: complementary insights from field and pot studies. *Environmental science & technology*, 44, 8842-8848.

Michael, H. A., and Voss, C. I. (2008). Evaluation of the sustainability of deep groundwater as an arsenic-safe resource in the Bengal Basin. *Proceedings of the National Academy of Sciences*, 105(25), 8531–8536.

# Appendix A. Additional transport considerations associated with the compaction-induced arsenic contamination mechanism

In Chapter 2, *Release of arsenic to deep groundwater in the Mekong Delta, Vietnam, linked to pumping-induced land subsidence,* a new mechanism for deep arsenic contamination was proposed and supported by ground-based and remote sensing observations along with regional-scale hydromechanical modeling. The analysis described the current distribution of groundwater arsenic in the focus area and generalized flow conditions over space and time for the aquifer system within it, but did not explicitly consider contaminant transport. Additional efforts were made to understand transport considerations at the scale of individual wells that could result in spatially and temporally variable contaminant concentrations in the presence of larger-scale subsidence throughout over-exploited regions.

The dissolved arsenic measured in pumping wells in subsiding regions largely depends on 1) the arsenic concentration in different sources of water that are drawn into pumping wells, 2) the attenuation capacity of aquifer sediments in the capture envelopes of the wells, and 3) the size and shape of the wells' capture envelopes as determined by aquifer anisotropy and pumping rates. Though information is incomplete at the scale of individual wells in this work, scoping calculations and simulations were conducted to quantify the effects of variability in these factors.

## A.1 Arsenic concentrations of water sources

Over the multi-decal timescale considered here, pumped water derives from two sources: 1) the aquifer in which the well is screened and 2) adjacent or interbedded clays. Arsenic concentrations measured in a well reflect a mixture of these two sources.

### *A.1.1 Background arsenic concentrations in the aquifer*

The arsenic survey data collected by the Vietnamese Department of Water Resources Management (DWRM) indicate negligible natural background arsenic concentrations in the deep aquifers. Outside of the heavily-pumped focus area, wells in Pliocene-Miocene age aquifers are rarely contaminated: 1.4% exceeds 10 µg/L and the mean concentration in this group is 1.7 µg/L (median is 0 µg/L). While these deep aquifers may have contained significant dissolved arsenic burdens immediately after they were deposited, like shallow aquifers do today, adequate advective flushing over their long history appears to have drawn concentrations to the near-zero average.

In addition to advective flushing, diffusion of arsenic or arsenic-mobilizing solutes out of confining clays over the depositional period could also play a role in determining concentrations in the aquifer. However, it is highly unlikely that diffusion resulted in the generally low-concentrations and widespread contamination of deep wells in the focus area, for two reasons. First, if diffusion were an important contamination process, it should similarly affect wells in deep aquifers outside of the focus area, but near-zero average concentrations indicate this is not the case. Second,

historic flow conditions do not support downward diffusion from confining clays to underlying aquifers. Prior to 1987, confined aquifers were under positive pressure and subject to an upward vertical gradient component (Nguyen, 1987), such that flow through confining clays would have been directed towards the ground surface. Diffusion out of clay layers in the downward direction, towards wells that are typically screened closer to the overlying aquitard, would have been offset by this counter flow.

### *A.1.2 Arsenic concentrations in compacting clays*

Upon pumping of an aquifer, water is derived in large part from adjacent compacting clay layers. The porewater concentrations of arsenic and arsenic-mobilizing solutes in deep confining clays of the Mekong Delta are not explicitly known, but available evidence suggests they may be high in arsenic-prone regions. Support for high solute concentrations in deep clays derives from a) dissolved arsenic concentrations in shallow clays of the Delta, deposited under similar paleoclimatic conditions, b) dissolved solute concentrations in confining clays in other regions of similar and older age, and c) consideration of the timescales for loss of arsenic from deep clays in the Delta context.

Near-surface Holocene clays in the Mekong Delta support high arsenic concentrations both in pore fluids and conditionally-stable solid phases. Below the seasonal water table, an abundant supply of organic carbon drives the microbially-mediated reductive dissolution of arsenic-rich minerals, generating porewater arsenic. Porewater in near-surface clays has measured *in situ* arsenic concentrations as high as

1000 µg/L (Kocar et al., 2008). Pliocene-Miocene age confining units were likely buried with similar pore water concentrations, given analogous paleoclimatic conditions between that period and the modern one. Arsenic concentrations in deep clays of the Delta likely remain high because unlike the permeable aquifers, clays have not been sufficiently flushed.

Numerous studies confirm that confining clays retain high solute concentrations, relative to adjacent, more permeable aquifers, over relevant geologic timescales. For reference, the beginnings of the Pliocene and Miocene periods date to ~2.5 and 23 million years ago, respectively. In Canada, 71-72 million year-old Cretaceous clays have *in-situ*-measured porewater concentrations of bromide, chloride and arsenic that are 10 to 50-fold greater than in the 80m of overlying till (Hendry et al., 2000; Yan et al., 2000). Cretaceous clays in the Northeast US contain sulfate concentrations 10-100 times higher than in adjacent aquifers and have been blamed as the source of sulfate in wells (Brown and Schoonen, 2004). In the Chalco Basin near Mexico City, porewater measured in Quaternary clays estimated to be ~300,000 years old reveals chloride concentrations of up to 4000 mg/L, levels of 80- to more than 300-times greater than in the underlying aquifer (Ortega-Guerrero et al., 1997). In the Eastern US, porewater measured in a Holocene to Cretaceous-age sequence of aquifers and thick (10s of meters) confining clays shows concentrations of a suite of major cations and chloride consistently spiking in the clay-layers (Pucci et al., 1992). In the same region, aquitards buried to depths of 90m, age unspecified, have consistently elevated levels of formate and acetate relative to the interbedded aquifers (by a factor of ~2-6, McMahon and Chapelle, 1991). Buried clays of similar and

greater age than those we consider maintain elevated dissolved solute loads despite existing gradients for diffusion and advection, irrespective of solute and setting. This strongly suggests that it is plausible that the dissolved arsenic persists in deep clays of the Mekong Delta as in other relevant hydrogeologic environments. Finally, aside from adjacent clays, there appears to be no other likely source of arsenic or arsenic-mobilizing solutes that could be responsible for the pervasive arsenic that is observed in deep aquifers of the Mekong Delta.

The high solute concentrations observed in the confining clays just described may persist, in part, due to extremely slow out-diffusion from within a variety of pore space environments. In their recent review of diffusion through clay containment barriers, Shackelford and Moore identify four types of pore spaces: interconnected voids, non-interconnected or dead-end voids, and inaccessible or occluded voids (Shackelford and Moore, 2013). The size, shape and positioning of these voids, in addition to properties of the mineral surface properties (e.g., charge, sorption capacity) and bulk solution (ionic strength, size of diffusing species) all act to determine a range of diffusion rates controlling transport within a given material. In the interconnected void network, which can be thought of as the "fast lane," the ratio of mineral surface area to pore space volume is minimized and diffusion rates are maximized. Within non-interconnected and inaccessible void spaces that make up the "slow lane," physico-chemical limitations (e.g., constrictions due to pore size and geometry or electrically charged layers) prolong diffusion timescales, which may be infinite for occluded voids.

The timescale for overall diffusion of solute in or out of a low permeability layer can be approximated as:

$$T_d = R_p \frac{\tau w^2}{D_m} \qquad \text{(Crank, 1975)}$$

where $D_m$ is the molecular diffusion coefficient for the solute in water, $R_p$ is the retardation factor due to equilibrium pore-scale mass transfer, $\tau$ is the tortuosity, and $w$ is the half thickness of the layer. Using a diffusion coefficient for arsenic in water of $9 \times 10^{-10}$ $m^2/s$ (Li and Gregory, 1974), a range of tortuosity values set to reproduce the effective diffusion coefficients measured in clay formations of 3-41, corresponding to effective diffusion coefficients of $2.8 \times 10^{-10}$ and $2.2 \times 10^{-11}$ $m^2/s$ (Mazurek et al., 2011), a range of representative half-thicknesses (10m – 25m) and assuming very low-end (conservative) $K_d$ of 6 L/kg (Radloff et al., 2011) and corresponding retardation factor, $R_p$, equal to 30 (using a clay total porosity, $\theta$, for a naturally consolidated clay of 0.4 (Mazurek et al., 2011) and bulk density of 1.9 $g/cm^3$, calculated using a particle density of 2.65 $g/cm^3$ multiplied by (1- $\theta$), the residence time for solutes would be 0.3 to 27 million years (compared, again, with 2-23 million for the age of Plio-Miocene units). The retardation factor may in fact be much higher, as representative $K_d$ values for these clays are not known and the value used was taken from reduced aquifer sands (from Bangladesh) which have similar types of adsorbing minerals, but lower mineral concentrations. This calculation assumes the rate-limiting step is slow diffusion from dead-end voids in the clay, where the mineral surface area to void volume ratio is maximized and retardation occurs. During pumping-induced clay compaction, these

diffusion-limited voids are crushed, expelling previously immobile solutes to the interconnected void network, the fast lane, where surface reactions are less influential.

Finally, a near-perpetual arsenic source in deep confining clays of the Mekong Delta may be maintained by solid-phase hosts. Solid-phase analysis of a deep core (max. depth: 265m) taken from a near-river site in the Delta has shown abundant manganese and iron oxides, specifically identifying goethite and hematite associated with arsenic throughout the depth profile, and noticeably enriched in a deep (194m) clay layer (Nguyen and Itoi, 2009). These minerals have a high capacity for both adsorption and desorption of arsenic, particularly the reduced form (As(III)), and release the majority of their original adsorbed arsenic load to the first ~20 pore volumes of introduced fluid (Tufano et al., 2008). Few, if any, pore volumes of uncontaminated fluid have been in contact with deep clays in the Delta, depending on their age and thickness. The limited extent of flushing of deep clays suggests desorption of arsenic may contribute significantly to pore fluid concentrations.

## A.2 Attenuation capacity of the aquifer sediments

The sorption capacity of aquifer sediments can retard the rate of contaminant transport relative to the rate of groundwater flow. Oxidized, "brown" sands have a significant but limited ability to retard the rate of arsenic transport in slow-flowing groundwater (Radloff et al., 2011; Stollenwerk et al., 2007). The attenuation capacity of reduced aquifer sediments is considerably more limited (Radloff et al., 2011; Harvey et al., 2002). Adsorption experiments on both sediment types are well modeled by Langmuir isotherms (Radloff et al., 2011; Stollenwerk et al., 2007;

Harvey et al., 2002), indicating that at high concentrations, retardation of arsenic by aquifer sands is insignificant, as sorption sited are saturated. Field experiments in reduced sands in Bangladesh suggest that attenuation is limited at groundwater arsenic concentrations >100 µg/L (Harvey et al., 2002).

High-concentrations of arsenic in porewater expelled from clays should be minimally influenced by the attenuation capacity of the aquifer sediments as it is likely low: deep aquifers in the Mekong Delta are reportedly reduced (Nguyen and Itoi, 2009). Additionally, the hydraulics of pumping likely lead to saturation of the limited sorption capacity after an initial period of loading by the first clay-derived arsenic inputs to the aquifer. Water expelled from clays in the capture envelope of a pumping well enters into a horizontally-oriented, piston-like flow path; essentially a plume of clay-sourced water is drawn into the well (see Figures A1-2). At the front of this high-concentration plume, some solute may be adsorbed, filling the sorption sites of sediments. Behind the leading edge of the plume, however, high arsenic concentration groundwater continues to flow, sourced by on-going clay compaction. The hydraulics of pumping allow for minimal dilution along the flow path. Rather, in-well mixing dilutes the plume to the arsenic concentrations observed.

### A.3 Capture envelope of the pumping well

As discussed above, pumping wells extract a mixture of water derived from the aquifers in which they are screened and the adjacent compacting clay. The two sources do not freely mix within the aquifer, except locally at the interface between

them, as transport is governed en route to the pumping well by the physics of groundwater flow, which is dominated by advection. Any significant mixing occurs only within a pumping well as groundwater from the two sources enters the well screen. The size and shape of a well's capture envelope determine the proportions of water derived from each source in this mixture.

This section assesses the expected variability in arsenic concentrations among wells due to variability in the factors controlling the size and shape of their capture envelopes. In these capture envelopes, the proportions of water drawn from aquifer and compacting clay sources results from a variety of characteristics of the pumping wells and the sediments in their immediate lateral vicinity (<500m). Well screen length and position, local aquifer geometry and anisotropy, and the history of pumping rates in a given well and in neighboring wells all influence the concentration of arsenic observed in it over time. These factors undoubtedly influence the variability in arsenic contamination among neighboring wells that is observed in the DWRM survey, but they cannot be modeled at the relevant scale with available data. Nonetheless, the influence of these factors is apparent given that wells in subsiding areas of the Delta show a distribution of arsenic concentrations, some zero.

The relative in-well contribution of water from the aquifer and compacting clay sources depends, in large part, on local pumping rates and histories. At low pumping rates, the magnitude of induced drawdown and consequent compaction is minimal, such that less water is drawn into the aquifer from the release of clay porewater than at higher pumping rates. Higher pumping rates cause more water to be

drawn from the clay source into the pumped aquifer, and solutes in this source arrive at a given well after a lag period. At early times, the capture envelope of a pumping well is filled only with pre-existing (native) aquifer water because water from clays has yet to be expelled and travel to the well. At later times, the capture enveloped includes water that is drawn both from the aquifer and from the adjacent, compacting clays. Over time, the capture envelope of the well contains an increasing proportion of water derived from on-going clay compaction (Figure A1).

The arrival time of clay-sourced solutes, and their representation in the two-source mixture, further depends on 1) the well screen length and position, 2) the geometry and anisotropy of the aquifer, and the 3) configuration of nearby wells, as illustrated in Figure A2. The first two factors effectively act to determine the length of the flow path between the well screen and the compacting clay, with a shorter path hastening solute arrival. Fully screened wells sample from the entire aquifer thickness, drawing water from long and short flow paths. In contrast, partially-penetrating wells, typically screened closer to an overlying confining unit, preferentially draw from areas closer to their screen, where flow paths are shorter. The geometry and anisotropy of the aquifer in the region surrounding the well further determine the shape of the capture envelope. Aquifer thinness and anisotropy both have the effect of condensing the capture envelope in the vertical, shortening the travel distance between the overlying clay layer and the well screen, and expediting the arrival time of compaction-derived solutes.

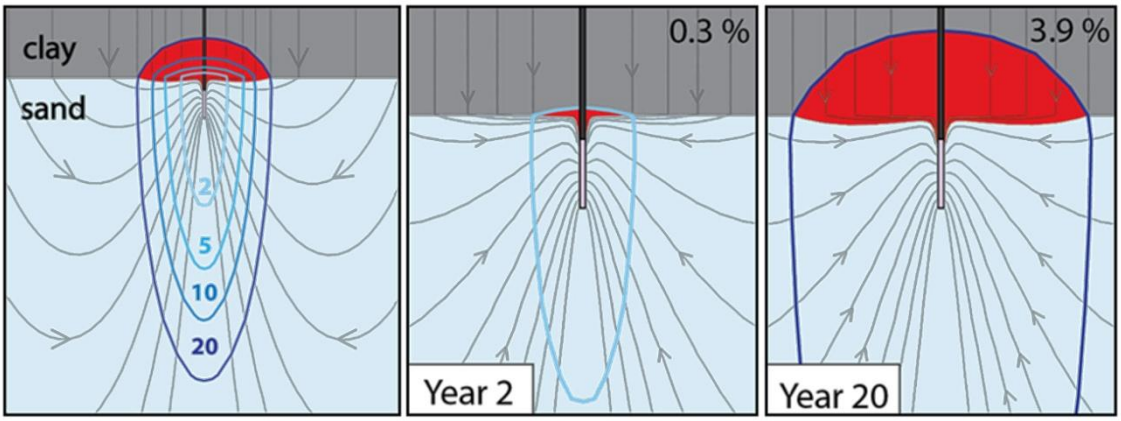


**Figure A1** Evolution in time of the capture envelope of a pumping well below a clay layer undergoing compaction. Water in capture envelope derived from clay storage is shown in red. *Left:* 2, 5, 10, and 20-year contours of the capture envelope, illustrating distances from which pumped water is drawn over these timeframes. *Center and right:* As time passes, water drawn from compacting clay represents a greater proportion of all water in the well's 2-yr capture envelope: water from clay is gradually filling the volume from which the well water is obtained during pumping (percent of water from clay in capture envelope is labeled in upper right. Flowlines in all panels are shown in gray, with arrows on selected ones indicating flow direction. All flow is toward the well. All panels based on results of modeling described below.

The configuration of nearby wells can also impact mixing in the pumped well. First, well crowding restricts the lateral extent of the capture envelopes, inducing greater drawdown, compaction, and expediting the arrival of clay-derived water to the well. Second, variability in the pumping rates of neighboring wells results in differences in the arrival time of clay-derived water among these wells. For example, a single well pumping at a rate that is significantly higher than the rates of others in its vicinity is primarily responsible for the local induced drawdown and resulting clay compaction. This high-rate pumping well, however, draws from a capture envelope that extends laterally further and deeper into the aquifer than nearby low-rate pumping wells. Consequently, the low-rate pumping well receives a greater proportion of its

water from clay-compaction more quickly than the high-rate pumping well (Figure A2).

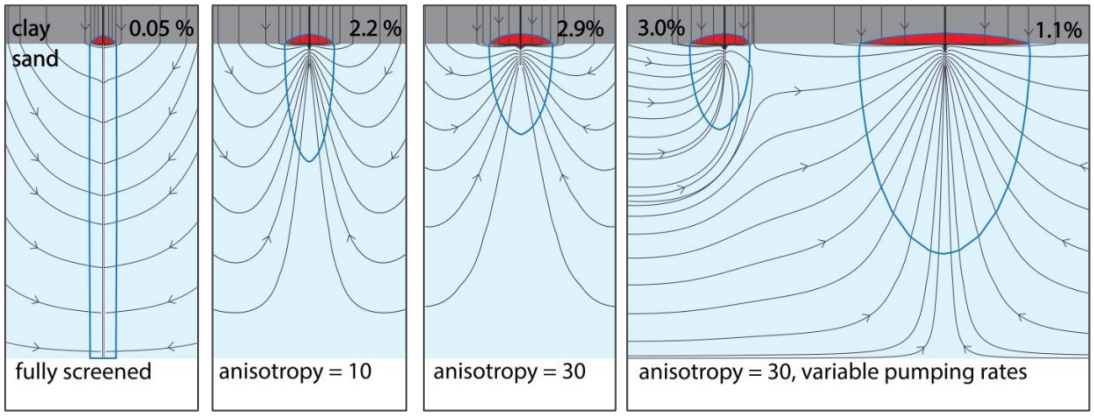


**Figure A2** Factors affecting the travel time of solutes to a pumping well. The 10-year capture envelope is shown in blue, water from clay in red, percent of water from clay in the capture envelope labeled in upper right. Full thickness of modeled clay layer not shown. Flowlines in all panels are shown in gray, with arrows on selected ones indicating flow direction. All flow is toward the well. All panels based on results of modeling described below.

The combination of variable extraction rates, histories, and well configuration causes the concentrations measured in different pumping wells to follow different temporal trajectories. These temporal trajectories were simulated to estimate upper bounds on the proportion of pumping demand met by water from compacting clays for wells of varying age and location in the unevenly-subsiding Mekong Delta. High resolution 3D two-layer models were constructed using the same hydrogeologic parameter values as given in the Supporting Information for Chapter 2 and a representative ratio of aquifer to confining layer thickness (1.5:1). A single well was set to pump at a representative constant-rate (40 $m^3$/d) over a 20-yr period. Lateral model boundaries were adjusted until the specified pumping induced compaction at an average rate, as observed using InSAR: 1.5 cm/yr (compared with ~3 cm/yr maximum

from InSAR in the focus area). The majority of this compaction (~85%) occurred in the confining clay layers, specified to have a representative value of specific storage that is 10x greater than the aquifers. Well screen length and the vertical hydraulic conductivity of the aquifer sands were modified and a second, variable-rate pumping model was constructed in the same manner as the first. In the second model, an additional well was set to pump at 25x the rate of the original well, a multiplier that is consistent with extraction rates of industrial wells based on data provided by the Department or Water Resources Planning and Investigation for the South of Vietnam (DWRPIS). For each modification tested in these models, the 2, 5, 10, and 20-yr capture envelopes were determined and the water budgets enumerating the fluxes derived from storage in the aquifer and confining unit in those envelopes were determined. Results are summarized in Figures A1-3. Figure A3 illustrates how the proportion of water drawn into the well from storage in clay aquitards increases over time, and the mixed in-well arsenic concentration assuming a clay source concentration of 1000µg/L and an aquifer concentration of zero. The in-well concentration ($C_{well}$) is calculated as follows:

$$C_{well} = C_{aquifer} \times \frac{V_{aquifer}}{V_{total}} + C_{aquitard} \times \frac{V_{aquitard}}{V_{total}}$$

where $V$ is the volume pumped over a given time period. For example, a partially-screened well pumping at a typical rate for 10 years in an aquifer with an anisotropy ratio of 10 receives 2.2% of its pumped demand from the compacting clay source. Its expected concentration at 10 years is: 0 µg/L x 0.978 + 1000 µg/L x 0.022 = 22 µg/L, as shown in Figure A3 (upper panel, blue line). Higher in-well concentrations can be

reached under the following conditions: 1) higher clay source concentrations, 2) higher compaction rates, 3) greater anisotropy and 4) longer time horizons.

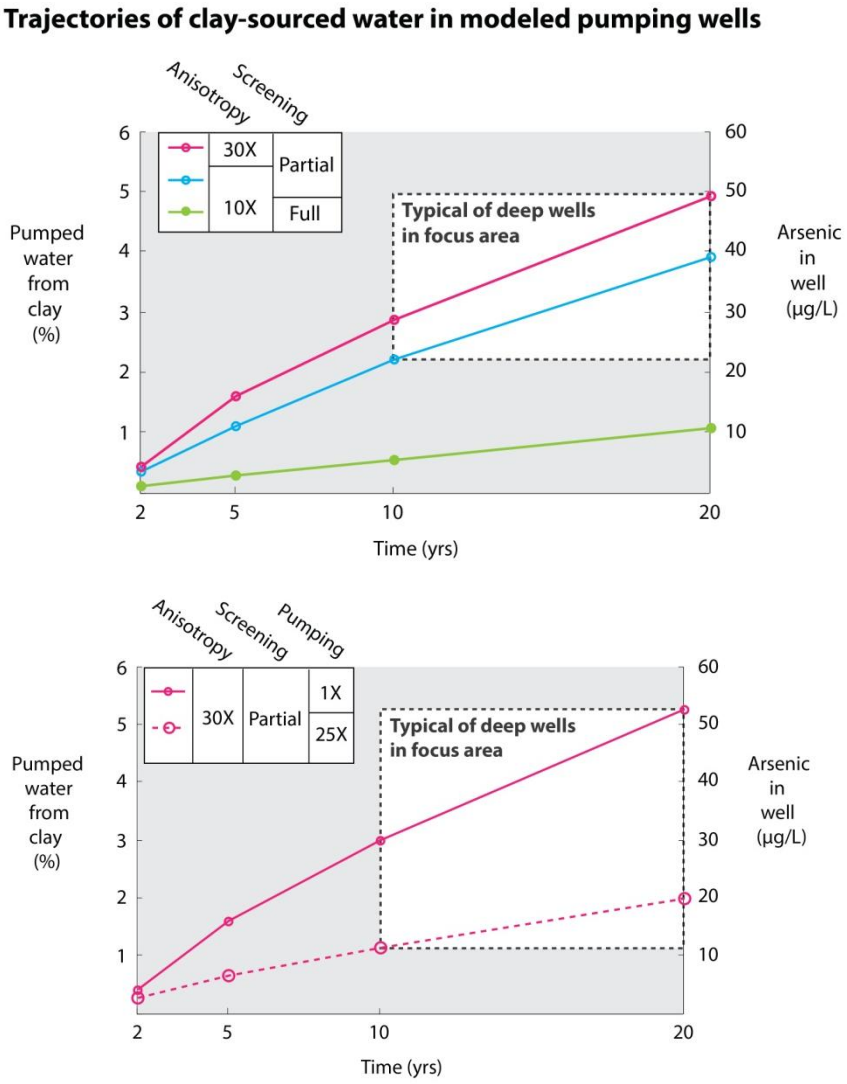


**Figure A3** Simulated temporal concentration trajectories showing the percent of water from clay compaction that mixes with native groundwater in a pumping well and resulting in-well concentrations, assuming 1000 µg/L arsenic concentration for water from clay. Regions of the curve that best represent deep contaminated wells in the focus area are outlined.

The trends in the arsenic data are generally consistent with the temporal concentration trajectory concept: deep wells with elevated arsenic concentrations map well to regions with older wells and higher pumping rates (Figure A4).

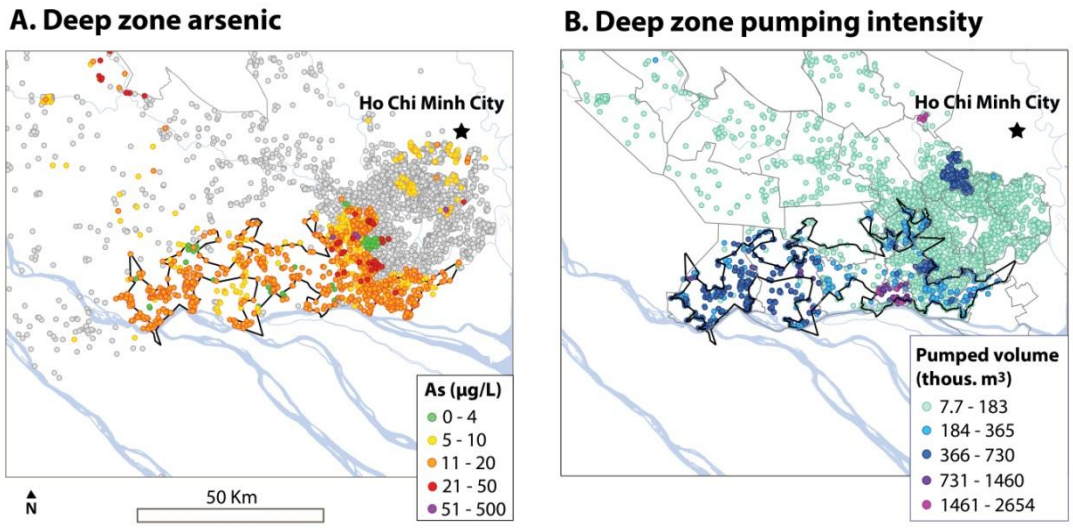


**Figure A4** Arsenic data (**A**) compared with pumping intensity (**B**). Pumped volume is approximated by multiplying the age of each well by the 2007 deep unit pumping rate of the district. Gray outlines in **B** show district boundaries where pumping data are available. Each color change represents a doubling in pumping intensity. Excellent correspondence between arsenic occurrence and pumping intensity suggests that both clay compaction and sustained pumping over time are required to generate new areas of contamination, consistent with the temporal trajectory concept and quantification.

Application of the temporal concentration trajectory concept to individual wells in the DWRM survey is precluded by several confounding factors. First, the precise date of well sampling was not known, and the survey was conducted over the period 2002-2008 countrywide. It was therefore not possible to precisely specify the time point on the concentration trajectory at which arsenic was measured for each well. Second, it was also not possible to specify pumping rates at the scale of individual wells, since extraction data are only specified at for each aquifer within

each district in the DWRPIS survey. A unit pumping rate for wells in each district, calculated as the 2007 rate divided by the number of wells surveyed (in the extraction survey), gives an indication of the variability in pumping intensity among districts, but could not be used to identify the start year or explicit locations of wells that deviate significantly from average pumping rates.

## References


Brown, C. J., and Schoonen, M. A. A. (2004). The origin of high sulfate concentrations in a coastal plain aquifer, Long Island, New York. *Applied Geochemistry*, 19(3), 343–358. doi:10.1016/S0883-2927(03)00154-9.

Crank, J. (1975). The Mathematics of Diffusion. New York: Oxford University Press.

Harvey, C. F., Swartz, C. H., Badruzzaman, A. B. M., Keon-Blute, N., Yu, W. Ali, M. A., Jay, J., Beckie, R., Niedan, V., Brabander, D., Oates, P. M., Ashfaque, K. N., Islam, S., Hemond, H. F., and Ahmed, M. F. (2002). Arsenic Mobility and Groundwater Extraction in Bangladesh. *Science*, 298(5598), 1602–1606. doi:10.1126/science.1076978.

Hendry, M J, Wassenaar, L.I., and Kotzer, T. (2000). Chloride and chlorine isotopes ($^{36}Cl$ and $\delta^{37}Cl$) as tracers of solute migration in a thick, clay-rich aquitard system. *Water Resources Research*, 36(1), 285–296.

Kocar, B. D., Polizzotto, M. L., Benner, S. G., Ying, S. C., Ung, M., Ouch, K., Samreth. S., Suy, B., Phan, K., Sampson, M., and Fendorf, S. (2008). Integrated biogeochemical and hydrologic processes driving arsenic release from shallow sediments to groundwaters of the Mekong delta. *Applied Geochemistry*, 23(11), 3059–3071.

Li, Y-H, and Gregory, S. (1974). Diffusion of ions in sea water and in deep-sea sediments. *Geochimica et Cosmochimica Acta*, 88, 708–714.

Mazurek, M., Alt-Epping, P., Bath, A., Gimmi, T., Waber, N. H., Buschaert, S., Cannière, P. D., De Craen, M., Gautschi, A., Savoye, S., Vinsot, A., Wemaere, I., and Wouters, L. (2011). Natural tracer profiles across argillaceous formations. *Applied Geochemistry*, 26(7), 1035–1064. doi:10.1016/j.apgeochem.2011.03.124.

McMahon, Peter B., Chapelle, F. H. (1991). Microbial production of organic acids in aquitard sediments and its role in aquifer geochemistry. *Nature*, 349(17), 233–235.

Nguyen, K. P., and Itoi, R. (2009). Source and release mechanism of arsenic in aquifers of the Mekong Delta, Vietnam. *Journal of Contaminant Hydrology*, 103(1-2), 58–69. doi:10.1016/j.jconhyd.2008.09.005.

Nguyen, V. C. (1987). Hydrogeological map of Vietnam. General Department of Geology, Vietnam. Hanoi.

Ortega-Guerrero, A., Cherry, J. A., and Aravena, R. (1997). Origin of pore water and salinity in the lacustrine aquitard overlying the regional aquifer of Mexico City. *Journal of Hydrology*, 197(1-4), 47–69.

Pucci, Amleto A, Ehlke, Ted A., and Owens, J. P. (1992). Confining Unit Effects on Water Quality in the New Jersey Coastal Plain. *Groundwater*. 30(3) 415-427.

Radloff, K. A., Zheng, Y., Michael, H. A., Stute, M., Bostick, B. C., Mihajlov, I., Bounds, M., Huq, M. R., Choudhury, I., Rahman, M. W., Schlosser, P., Ahmed, K. M., and van Geen, A. (2011). Arsenic migration to deep groundwater in Bangladesh influenced by adsorption and water demand. *Nature Geoscience*, 4(11), 793–798. doi:10.1038/ngeo1283.

Shackelford, C. D., and Moore, S. M. (2013). Fickian diffusion of radionuclides for engineered containment barriers: Diffusion coefficients, porosities, and complicating issues. *Engineering Geology*, 152(1), 133–147. doi:10.1016/j.enggeo.2012.10.014.

Stollenwerk, K. G., Breit, G. N., Welch, A. H., Yount, J. C., Whitney, J. W., Foster, A. L., Uddin, M. N., Majumder, R. K., and Ahmed, N. (2007). Arsenic attenuation by oxidized aquifer sediments in Bangladesh. *Science of the Total Environment*, 379(2-3), 133–150.

Tufano, K. J., Reyes, C., Saltikov, C. W., and Fendorf, S. (2008). Reductive Processes Controlling Arsenic Retention: Revealing the Relative Importance of Iron and Arsenic Reduction. *Environmental Science & Technology*, 42(22), 8283–8289. doi:10.1021/es801059s.

Yan, X. P., Kerrich, R., and Hendry, M. J. (2000). Distribution of arsenic (III), arsenic (V) and total inorganic arsenic in porewaters from a thick till and clay-rich aquitard sequence, Saskatchewan, Canada. *Geochimica et Cosmochimica Acta*, 64(15), 2637–2648.

# Appendix B. InSAR as a reconnaissance tool for detecting areas of potential compaction-induced arsenic contamination in the Mekong Delta

Chapter 2 used Interferometric Synthetic Aperture Radar (InSAR) to support a proposed new mechanism of arsenic contamination linked to solute expulsion from compacting clays in an intensively-investigated sub-area of the Mekong Delta. The use of InSAR as a reconnaissance tool for detecting other areas that may be at risk of compaction-induced contamination was not addressed. The information upon which to make an assessment, however, is contained in Chapters 1 and 3, which at the Delta scale describe the current distribution of arsenic in wells and rates of land subsidence, respectively. Here the results of these three chapters are re-evaluated in order to consider the applicability of InSAR for early identification of vulnerable areas in the Mekong Delta and potentially other similar systems.

## B.1 Generalized region of land subsidence in the Mekong Delta

To facilitate a direct comparison with observations of arsenic in wells, the InSAR-based results from Chapter 3 are here generalized to show boundaries of the regions of land subsidence. A threshold for delineating the boundaries of subsiding regions of $\geq$1.5 cm/yr was chosen to separate regions of significant subsidence from others where the estimated error of 0.5-1 cm/yr could be more influential. Boundaries are idealized, or smoothed, compared with those contoured directly from the somewhat noisy InSAR data to improve visual display. The precise locations of these boundaries are not important since they are based on a threshold value within a

continuum of subsidence rates. The generalized regions of subsidence are shown in Figure B1.

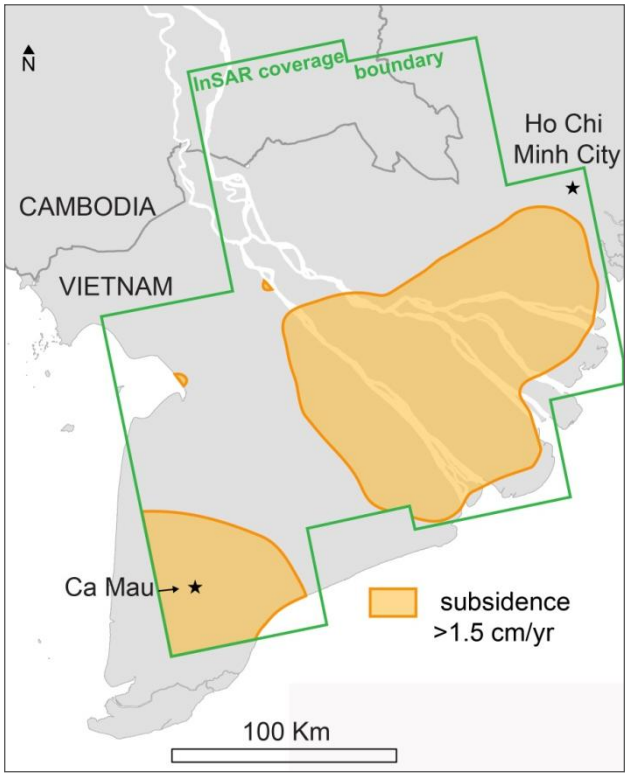


**Figure B1** Generalized regions of InSAR-based subsidence.

## B.2 Correspondence between regions of land subsidence and arsenic incidence

The analysis of well observations conducted in Chapter 1 found that the Mekong Delta region is characterized by regions of high and low arsenic incidence. Incidence regions were delineated according to mapped fault lines that appeared to mark transitions between them, possibly signaling significant changes in depositional conditions across the divides. Within a low-incidence region, arsenic is rarely found in wells of any depth. In the high-incidence region of the central Delta, traversed by

the Mekong and its distributaries, contaminated wells are most commonly found in shallow aquifers, but are also found in the large, deep-aquifer cluster that was the focus of Chapter 2. Across both high and low incidence regions, significant aquifer drawdown and subsidence is observed. That deep arsenic contamination in over-exploited regions of the Delta has only been observed in the high-incidence regions suggests that depositional conditions are ultimately controlling (Chapter 1). Figure B2 shows the correspondence between generalized subsidence and arsenic incidence regions.

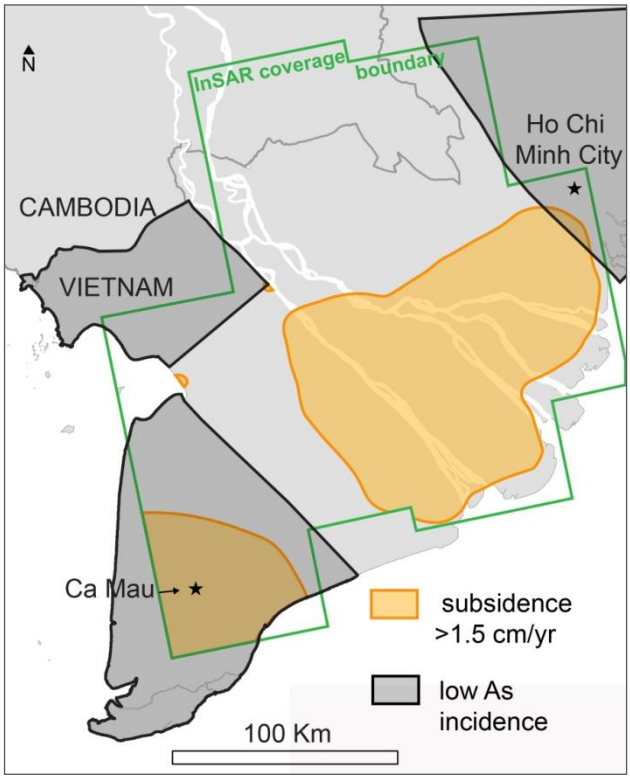


**Figure B2** Generalized area of InSAR-based subsidence with superimposed areas of low arsenic incidence.

## B.3 Potential for compaction-induced arsenic in subsiding regions

Clusters of wells with arsenic in excess of 10 μg/L are depicted in Figure B3. Arsenic clusters were identified using the DBSCAN algorithm as implemented in the "Flexible procedures for clustering" (fpc) package for R. The algorithm identifies networks of neighbors with a specified minimum number of points (minPts) within a given radius, or "reachability distance" (commonly denoted by "eps") of one another. The scan was conducted separately for each aquifer with the criteria that minPts = 5 and eps = 10km. Clusters were combined if found in the same location in adjacent aquifers. Only clusters with more than 10 arsenic-affected wells assigned to them were retained and displayed in Figure B3. Summary statistics for each cluster are given in Table B1.

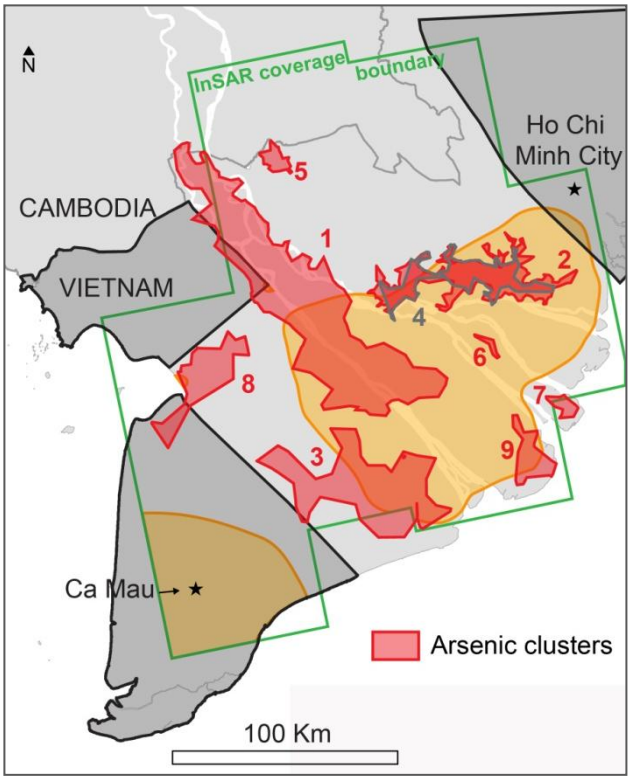


**Figure B3** Arsenic clusters superimposed on regions of subsidence and generally low arsenic incidence.

| Cluster | Number of wells | Mean depth (m) | Range of aquifers | Mean arsenic (µg/L) |
|---|---|---|---|---|
| 1 | 2801 | 50 | qh-qp23 | 205 |
| 2 | 889 | 316 | n22-n13 | 28 |
| 3 | 266 | 90 | qh-qp1 | 60 |
| 4 | 170 | 60 | qh-qp1 | 35 |
| 5 | 137 | 24 | qp3-qp23 | 76 |
| 6 | 57 | 25 | qh | 208 |
| 7 | 38 | 32 | qh-qp23 | 144 |
| 8 | 71 | 79 | qh-qp23 | 42 |
| 9 | 32 | 102 | qp23 | 37 |

**Table B1** Summary statistics for arsenic clusters. Aquifers are identified by Vietnamese classification scheme as in Chapter 1: qh = Holocene, qp3 = Upper Pleistocene, qp2-3 = Middle Pleistocene, qp1 = Lower Pleistocene, n22 = Upper Pliocene, n21 = Lower Pliocene, n13 = Miocene.

The arsenic clusters fall almost exclusively within the region of high arsenic incidence and largely within the region of generalized land subsidence. Clusters are predominantly comprised of wells in shallow aquifers. While compaction-induced contamination of shallow aquifers is possible, it is difficult to isolate arsenic-affected wells resulting from this mechanism from those caused by natural conditions. Shallow clusters caused by strictly natural conditions may potentially be marked by high mean arsenic concentrations (>50 µg/L), for at least two reasons. First, wells in the clusters associated with deep compaction-induced subsidence in Chapter 2, cluster 2, generally have concentrations below 50 µg/L. Second, compaction-induced contamination is subject to in-well mixing (Appendix A) that dilutes concentrations. For these reasons, is unlikely that clusters 1, 6, or 7 have a significant compaction-induced contamination burden. Clusters 5, 7 and 8 are also unlikely to be strongly influenced by this

mechanism because they wells in them are generally shallow and located outside the subsidence regions. More questionable are clusters 3, 4, and 9, which have significant overlap with subsidence regions, and, compared with many of the other clusters, lower mean arsenic concentrations and greater mean depths. Cluster 4 overlies the deep focus area described in Chapter 2, and may result from a convolution of natural and compaction-induced conditions. Accordingly, it appears that there may be some contribution to arsenic clusters from the compaction mechanism, but this contribution remains difficult to discern and quantify.

At the same time, the preceding set of figures also illustrates that arsenic contamination does not occur consistently throughout the regions of subsidence. There are two leading explanations:

1) *Compacting clays are non-uniformly contaminated with arsenic or arsenic-mobilizing solutes.* Though subsidence is evident, indicating subsurface compaction, predominantly in clays, these layers expel water of varying chemical composition. Not all water expelled from clays will induce arsenic contamination.
2) *Compaction commenced recently and contamination has not arrived at pumping wells.* The InSAR-based subsidence shown here depicts recent rates, not total subsidence. Recently-initiated clay compaction would release contaminated water that arrives at pumping wells only after a lag period. Results from the analysis of cluster 2 in Chapter 2 suggest a lag period on the order of 10 years.

## B.4 Considerations for the use of InSAR as an arsenic-detection tool

InSAR is a valuable tool for large-scale, relatively rapid assessment of land subsidence, which has immediate benefits for land and water resources planning and management purposes, as well as for further investigation of compaction-induced arsenic contamination. InSAR-based subsidence maps may be used to identify where compaction is occurring, a first step towards determining whether contamination is also an issue. Subsequent steps would involve 1) mapping high-occurrence arsenic regions to look for overlap, 2) measuring well samples in over-exploited, subsiding regions to confirm groundwater quality and, 3) potentially modeling groundwater flow and transport. Knowledge of pumping rates would greatly enhance the latter effort. In conclusion, although InSAR is not a stand-alone reconnaissance tool for detection of compaction-induced arsenic contamination, it adds a unique contribution to a suite of tools that may be used to monitor arsenic-affected systems and can help delimit the regions having the greatest likelihood of deep groundwater arsenic occurrence.